GEND
014

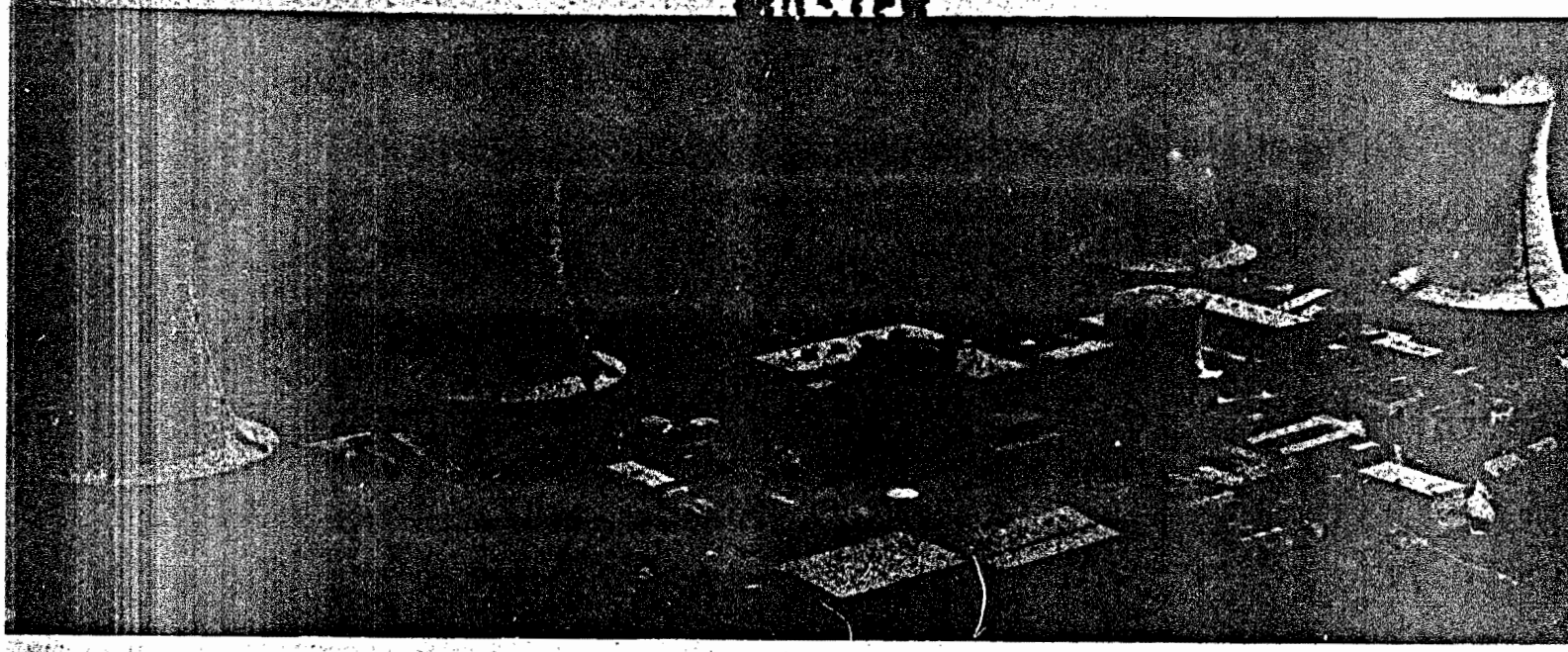

GEND

General Public Utilities • Electric Power Research Institute • U.S. Nuclear Regulatory Commission • U.S. Department of Energy

Examination Results of the Three Mile Island Radiation Detector HP-R-211

Michael B. Murphy
Geoffrey M. Mueller
Frank V. Thome

October 1981

Prepared for the
U.S. Department of Energy
Three Mile Island Operations Office

GEND-014
Distribution Category: UC-78
TMI Supplement

EXAMINATION RESULTS OF THE THREE MILE ISLAND RADIATION DETECTOR HP-R-211

Michael B. Murphy
Geoffrey M. Mueller
Frank V. Thomé

Published October 1981

Sandia National Laboratories
Albuquerque, New Mexico 87185
and
Livermore, California 94550

ABSTRACT

An area radiation detector, HP-R-211, which was removed from the Three Mile Island containment building on August 15, 1980 has been examined. The detector had failed at some time following the accident and indicated erroneous, low radiation levels from that point on. This report discusses the cause of failure, detector radiation measurement characteristics, our attempts to reconstruct the gamma rate history from detector output stripchart recordings, and our estimates of the total gamma radiation dose received by the detector electronics. We have also identified the radioactive contaiminants present on the detector and explored decontamination methods.

Prepared for EG&G Idaho, Inc.
Under Subcontract No. K-9027
and the U.S. Department of Energy
Under Contract No. DE-AC07-76ID01570

ACKNOWLEDGEMENTS

This examination was administered by the Technical Integration Office at Three Mile Island. Willis Bixby, DOE; Harold Burton, EG&G; and Jim Mock, EG&G, were especially helpful in producing this report. A special thanks goes to the support and cooperation offered by General Public Utilities in allowing access to and providing information about the Unit 2 plant. Much of the technical information and consultation was supplied by John Brummer of Metropolitan Edison Company. Others on the Island who were quite helpful were: Bob Rudolph, Pete Wood, and Ed Walker of Bechtel; Lori Hecker of EG&G; Ron Jacobstein a GPU Consultant; John Flint of B&W; Jim Renshaw and Henry Peterson of GPU; and Paul Ruhter of TMI.

At Sandia, Lloyd Bonzon, Paul Yarrington, and Dick Damerow provided technical support. Al Asselmeier provided all of the transistor failure analysis. Billy O'Neal of Sandia and Glen Waterbury of Los Alamos National Laboratories did most of the work in gamma spectra and radiochemical analysis. Lloyd Bonzon was responsible for determining the elastomeric materials total dose. Special thanks goes to Gary Romero of Sandia's Health Physics division in supporting all of the radiological work and assisting in the decontamination.

Special thanks goes to Karl West, Oak Ridge National Laboratory, for his enthusiastic support and helpful suggestions. Mel Mathis and Jim Jones at Technology for Energy, Inc. provided all of the on-site test data in a most helpful manner.

CONTENTS

FIGURES & TABLES

I. INTRODUCTION AND SUMMARY FINDINGS

A. Background

On August 15, 1980, during the second manned entry into the Three Mile Island (TMI) Unit 2 containment building, the first piece of electrical equipment was removed for examination and laboratory testing. The instrument that was removed is an area radiation detector having the TMI-2 equipment tag number HP-R-211. This particular instrument was chosen for examination because of its accessibility, its similarity to other instruments found in the containment building, and the desire to replace it with an operable unit. The detector is a gamma radiation monitor manufactured by Victoreen (Model 857-2) and employs a GM tube to detect events. It had operated continuously during and following the accident; however, it had indicated erroneous, low radiation levels both during the accident and at the time of removal some 506 days later. Extensive in situ electrical measurements were made on the instrument from the TMI-2 control room by General Public Utilities (GPU) and Technology for Energy, Inc.[1] the day before removal. The detector was delivered to Sandia National Laboratories on October 7, 1980 for extensive electrical and radiological examination. The radiation detector was removed as a part of the DOE TMI-2 Instrumentation and Electrical Equipment Examination Program administered by the DOE/EG&G Technical Integration Office (TIO) at Three Mile Island.

B. This Report

This report summarizes the results of the Sandia examination of HP-R-211. The specific areas discussed are:

1. the cause of failure,
2. detector characteristics and gamma doserate history,
3. total gamma dose received,
4. contamination nuclides and activity levels, and
5. decontamination methods and efficiencies.

One problem which we have encountered is that of striking a balance between a completely thorough experimental and theoretical examination and one which addresses the most important areas and obtains results for timely release. We believe this report achieves that balance. In the interest of distributing our results as quickly as practicable, some of our experimental data has been omitted from this report and is contained in laboratory notebooks.[2,3,18] Data felt to be most important in understanding or supporting conclusions are included here. This document is an expansion and update of the preliminary findings reported at the TMI-2 Information and Examination Program International Seminar sponsored by the U. S. Department of Energy and held in Washington DC on November 21 and 22, 1980.[4]

C. Findings and Recommendations

1. The mode of failure of HP-R-211 was confirmed to be a low impedance fault between the collector and emitter leads in transistor Q6 in the detector output circuit. The transistor failed because of catastrophic, non-annealing, punch-through from collector to emitter caused by high voltage breakdown and energy deposition. Substantial evidence indicates that this occurred at least partially when the reactor building sprays were initiated some 10 hours into

the accident. Spray and/or steam apparently entered the connector assembly where the detector and cable mate and caused the 600 volt GM tube power line to short, momentarily, to the signal output line. The connector backshell does not look as though it was properly mated to the connector insert. This, and the orientation in which the detector was mounted provided an entryway for the moisture. To prevent this from occurring in the future, we recommend that Victoreen detectors of this and similar types be mounted with the connector below the housing and that the connector backshells be potted. Even more fundamentally we question the need for having anything other than a sensor inside the containment building. Wherever possible, active electronics should be located outside containment.

2. The repaired, but degraded, detector exhibits a radiation level indication which becomes multivalued when it is exposed to radiation levels in the 10^3 to 10^6 R/H range. Instead of remaining pegged at its maximum 10^4 mR/H indication in this range, the readout begins to decrease at 10^3 R/H, reaches a minimum at approximately 50×10^3 R/H, and then begins to increase thereafter. This characteristic is caused by detector to cable impedance mismatches and is accentuated by long cable lengths and radiation degradation of detector transistors and the GM tube. This could present a hazardous situation in a reactor LOCA wherein radiation degraded detectors may indicate radiation levels to be significantly lower than they actually are. Changes in circuit design and/or the use of more radiation tolerant transistors can correct this problem.

3. We have been unable to reconstruct the time history of containment building gamma radiation using the HP-R-211 stripchart data at this writing. These data have certain characteristics during

the first several days of the accident which we cannot fully explain. Hopefully, the analysis of other detectors and the Dome monitor will provide information to fill in gaps in our understanding of this detector. A separate report will address this subject.

4. Both transistor and elastomeric data indicate that the electronics inside HP-R-211 received a total gamma radiation dose of approximately 2.5×10^5 rads. This level is appreciably below some earlier estimates.

5. The major radionuclides on the outside of the detector were found to be CS-134, CS-137 and SR-90. The concentration of CS-137 was found to be 0.973 $\mu Ci/cm^2$ on the top horizontal surface and 0.103 $\mu Ci/cm^2$ on the side and bottom surfaces. These findings are higher than those obtained using swipes on floors and walls.[17]

6. The approach used to decontaminate the detector outside was to avoid scrubbing and minimize the use of caustic chemicals. We found that as much as 44% of the contaminants were removed simply by handling during shipment and contaminant characterization. Low-pressure water and detergent sprays were ineffectual. Low-pressure steam and mild phosphoric acid washes (Turkel 4512A) were the most efficient. Even so, only about an order of magnitude reduction was achieved using all of the above steps.

II. DESCRIPTION

A. Detector Channel

HP-R-211 (SN 359) is one of six containment building area radiation monitors. It was mounted on a pillar at the 305' elevation near personnel hatch No. 2, as shown in Figure 1. Similar detectors are mounted at the 305' elevation near the equipment hatch (HP-R-212), the 347' elevation near the incore tubes (HP-R-213), and the 347' elevation fuel handling bridges (HP-R-209 and HP-R-210). In addition, an ion chamber monitor housed within a lead shield is located at the 372' elevation above the elevator (HP-R-214, dome monitor). Separate instrumentation cables connect each detector located inside the containment building to ratemeter readout electronic modules located in the TMI-2 control room. There, a multipoint stripchart recorder (HP-UR-1901) records each readout using a sample interval of 1 minute. Figure 2 shows the cable interconnect diagram for HP-R-211. The detector power and signal cable exits the containment building through penetration R507 and eventually connects to a remote readout and alarm located in the anteroom. From there, signals are distributed to the control room, where the ratemeter (readout electronics and power supply) is located, and back into containment to an alarm. It is noteworthy that the HP-UR-1901 stripchart shows traces for only detectors 211, 213, and 214 at the time of reactor trip. The trace for 212 is unreadable.

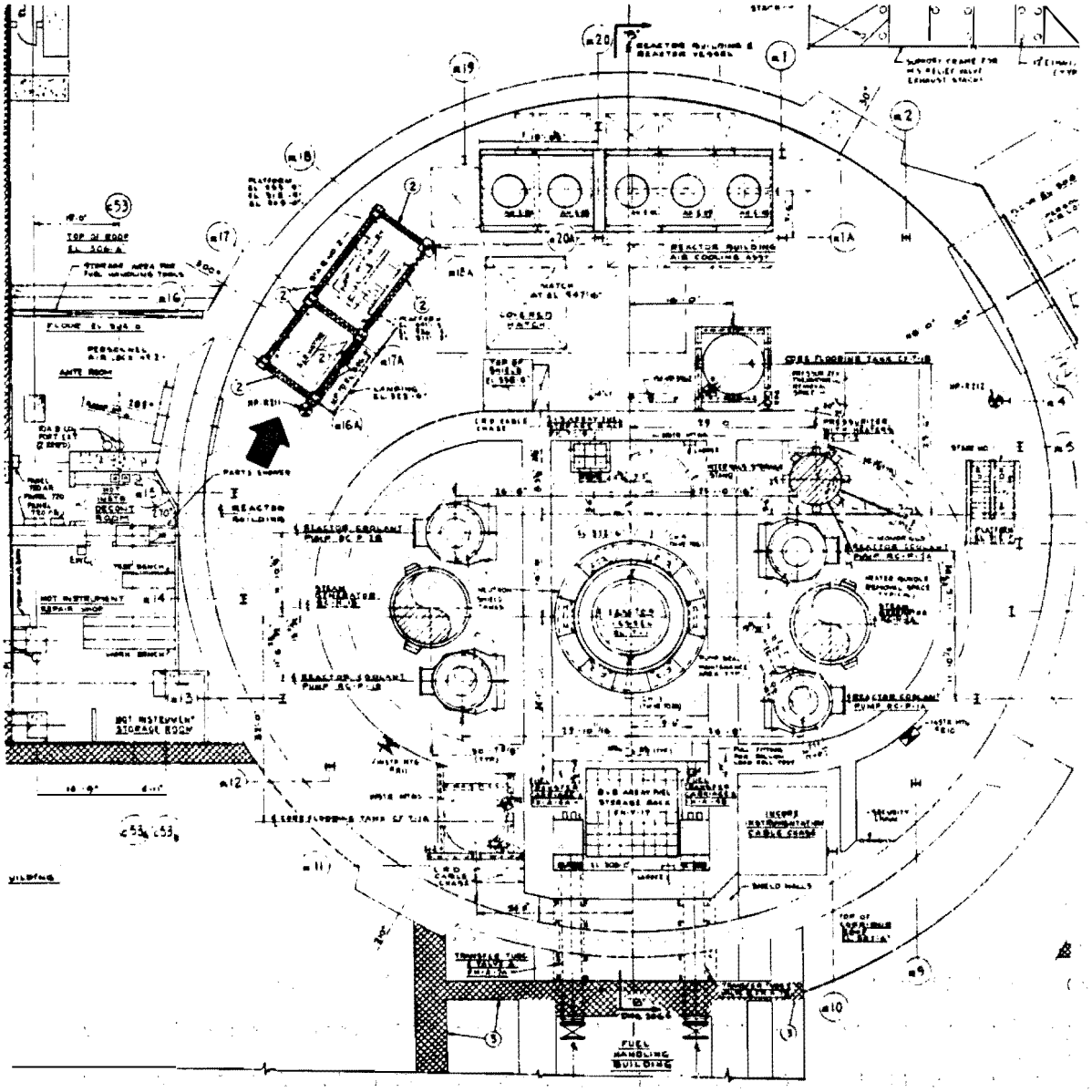

FIGURE 1. TMI Unit 2 305' Plan Layout. Radiation detector HP-R-211 (HP-R211) is located near Personnel Air Lock No. 2.

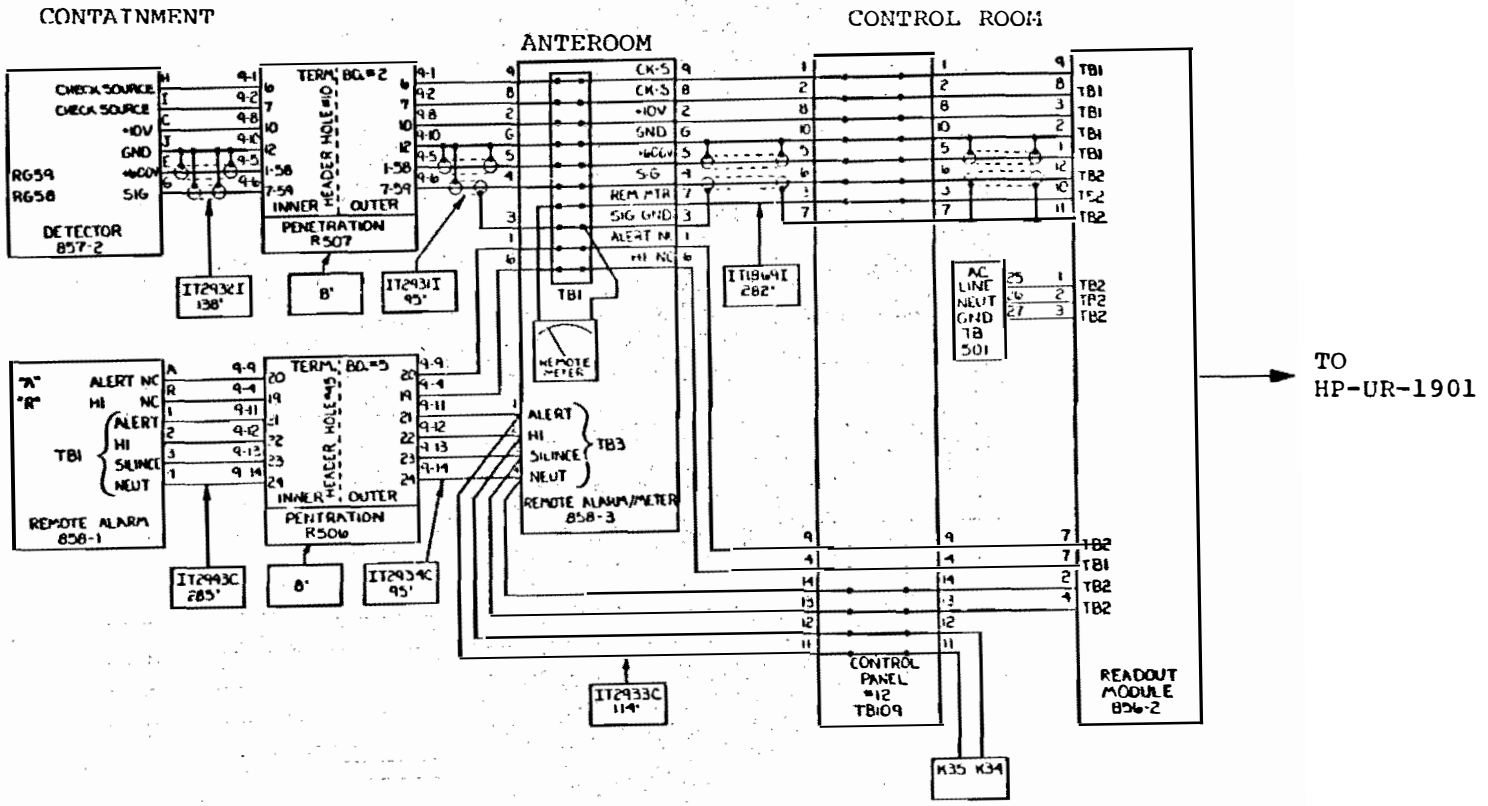

FIGURE 2. Cabling and Interconnect Diagram.
The approximate length in feet of each cable is shown.

B. Removal

Extensive preparations were made prior to removal to minimize the time spent by the GPU staff inside the containment building. This included practice on a full scale mock-up assembled by the TIO staff. The plan was to remove the faulty detector and replace it with a functional one. Unfortunately, during removal (Figures 3 and 4) the cable was detached from the connector backshell at the point where solder connections are made. The result of this was to make it impractical to install the replacement.

C. Detector Description

The Model 857-2[5] detector, shown after removal in Figures 5, 6 and 7, consists of a painted, nominal 5 mm thick aluminum housing, a 64 x 137 mm glass epoxy circuit board with electronics, an O-ring seal, and a waterproof Bendix connector. The detector is connected to the Victoreen Model 856-2 ratemeter (Figure 8) through an estimated 159 m (523 ft.) of cabling. The printed circuit board holds the Geiger-Mueller (GM) tube and signal conditioning electronics. The detector is not loss-of-cooling-accident (LOCA) qualified but does have a good O-ring seal and sturdy housing and is designed to function up to a total accumulated radiation dose of 10^5 rads. This unit was set to indicate radiation rates ranging from 0.1 mR/H to 10^4 mR/H. The ratemeter was adjusted to actuate the alarm at 50 mR/H. A 0.08 μCi Ra-226 check source can be used to indicate operability.

FIGURE 3. Detector Removal. The detector has been removed from the wall slide bracket and the cable is being disconnected.

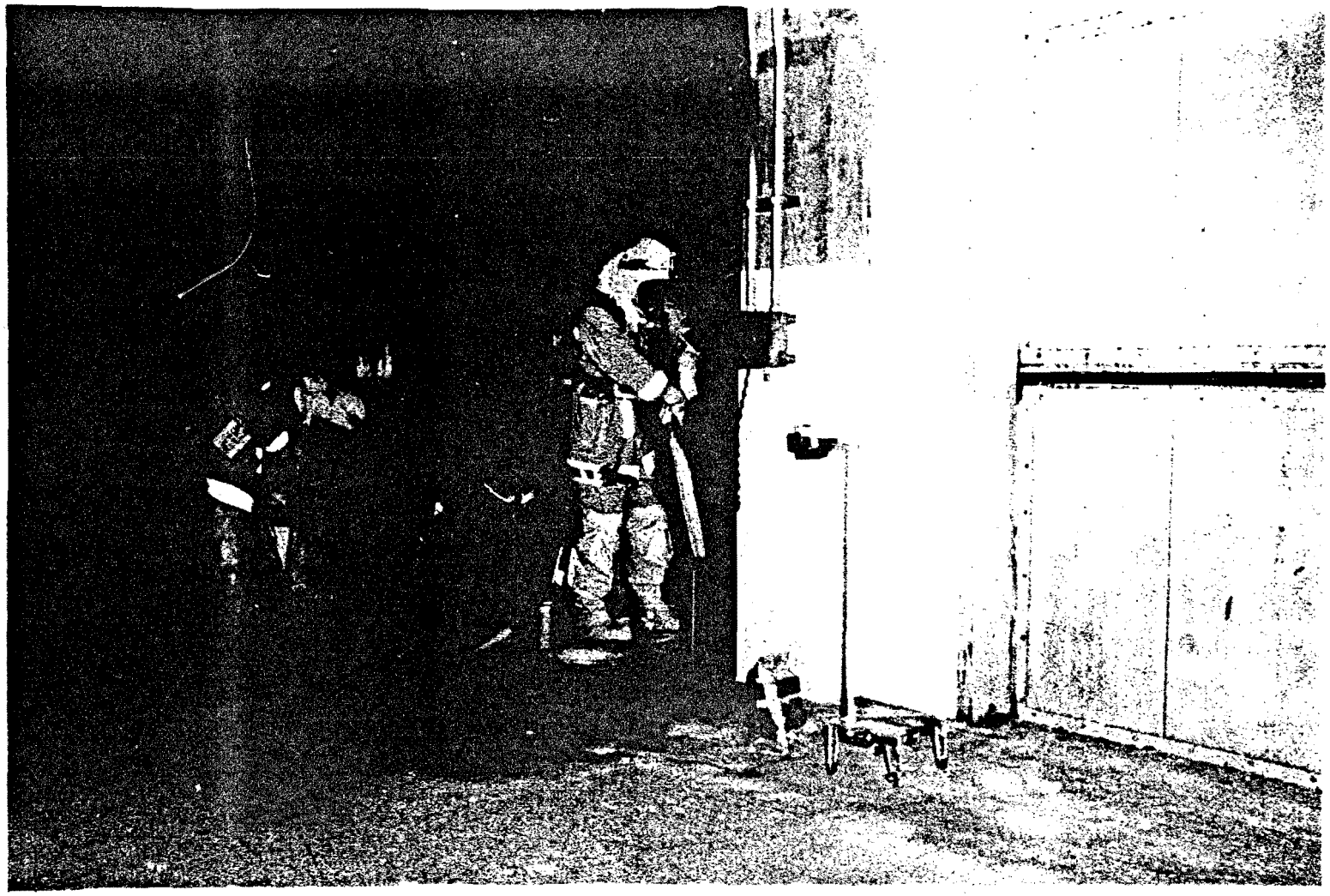

FIGURE 4. Elevator Shaft and Airlock. The detector was located directly in front of the technician in the center of the picture. The personnel airlock entryway is shown.

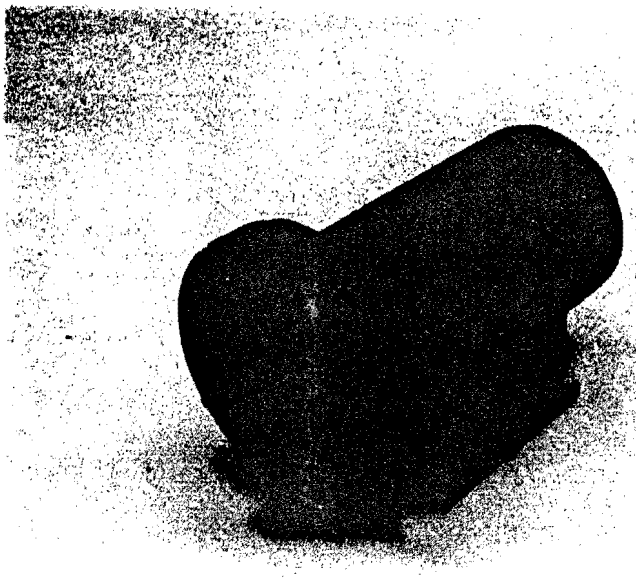

FIGURE 5. Detector Outside Case. The corrosion is apparent on the detector shown approximately as received at Sandia (the nameplate has been removed for isotopic analysis).

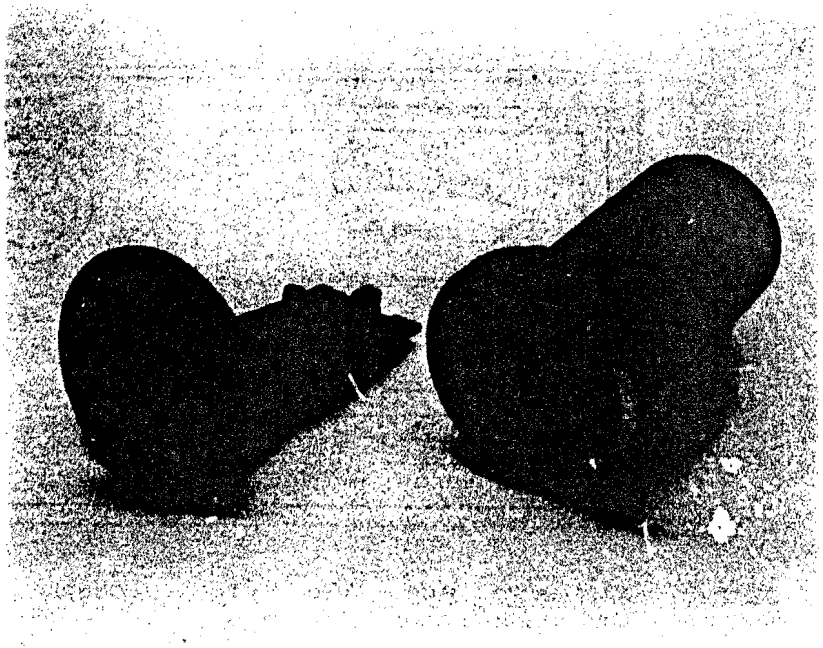

FIGURE 6. Detector Exploded View. The 211 detector circuit board was mounted on a spare front plate for testing. The O-ring seal channel can be seen on the case.

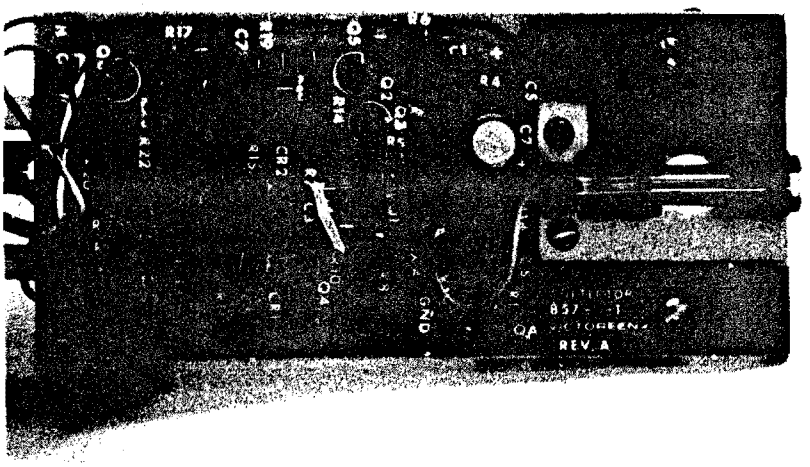

FIGURE 7. HP-R-211 Circuit Board. This picture shows the actual circuit board as removed from the housing. Notice the clean, uncorroded appearance. The GM tube is shown on the right end.

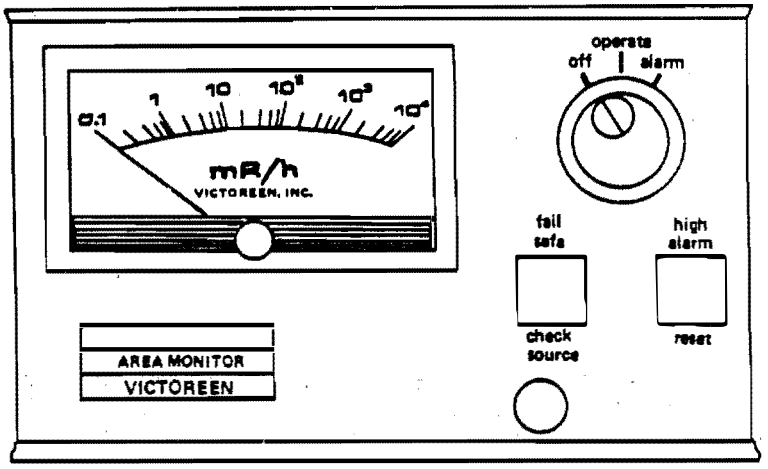

FIGURE 8. Ratemeter Face. The Victoreen channel measures radiation rates of from 0.1 to 10^4 mR/H.

Figure 9 shows a circuit diagram of the detector. The GM tube operates from a 600 volt DC power supply which is current-limited by 2 MΩ resistors both in the detector and in the ratemeter. The signal conditioning electronics of the detector uses a +10 volt DC supply. The Ra-226 check source is switched from behind a lead shield by the application of ground to one of the check source leads at the ratemeter. A DC voltage of 22 volts is used for the driver solenoid. Transistors Q4 and Q5, under normal range operation, form a cross-coupled toggle flip-flop. Each breakdown of the GM tube generates a narrow pulse which is amplified by the Q1 amplifier and routed to the flip-flop. This binary changes state after each pulse. The flip-flop output is buffered by line drivers Q6 and Q7. Thus the detector output is a zero to 10 volt logical signal whose frequency is dependent on the rate of GM pulses. A pulse counter placed on the detector output measures only half the number of actual "event" GM pulses. The Signal Output goes to a log pump circuit in the ratemeter, as shown in Figure 10. A discrete summing amplifier sums all the log pump voltages, amplifies the sum and produces meter and computer outputs. The computer output is a zero to 1V signal which drives the HP-UR-1901 stripchart recorder. The detector is calibrated by first adjusting the +10 and +22 volt sources. The detector is then placed inside a Victoreen field source having three radiation rates (this detector was calibrated with a source of approximately 49, 360, and 1800 mR/H) and "zero" and "gain" pots are alternately adjusted. If the rate that photons arrive at the GM tube exceeds a certain upper limit, the GM tube cannot respond to each individually and tends toward a constant discharge. This high frequency train of pulses or constant discharge current is integrated by C1 in the detector and causes the "antijam" circuit to become functional. Transistor Q3 switches on, and subsequently causes the Q4, Q5 flip-flop to become a freerunning multivibrator, which oscillates at a nearly

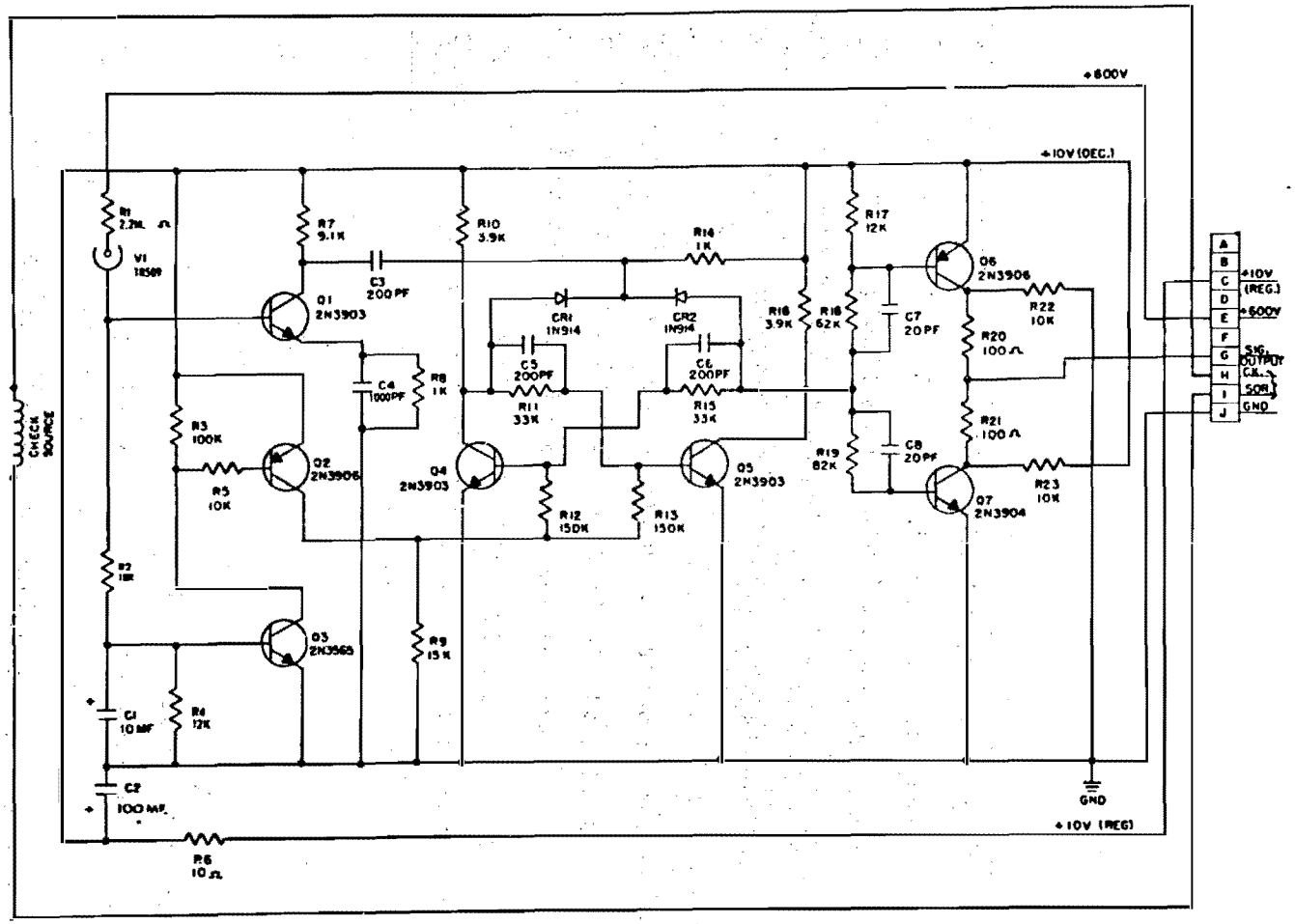

FIGURE 9. Detector Schematic. The GM tube and antijam circuits are on the left, the flip-flop is in the center and the output driver is on the right side of the schematic. Transistor Q6 failed.

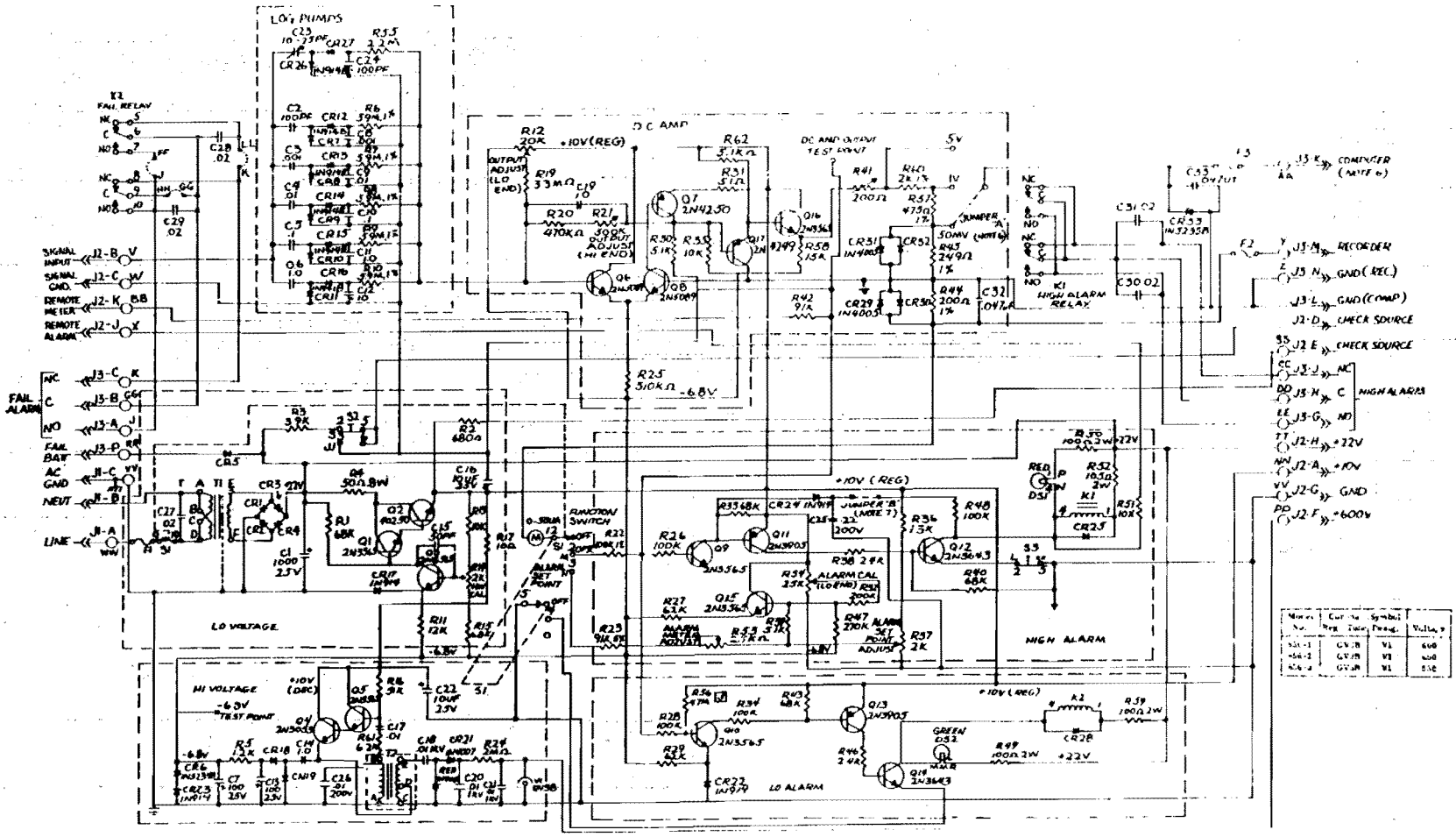

FIGURE 10. Ratemeter Schematic. The detector signal enters the log pump circuit in the upper left. The log pump outputs are then summed and amplified by the differential amplifier. The computer output connection goes to the stripchart recorder. R19 and R21 ("zero" and "gain" adjust) taylor the ratemeter response to each unique detector.

constant 40 kHz. This frequency is high enough to cause the readout meter to peg on the upper limit. This antijam circuit thus should prevent a decrease in the detector output frequency for radiation levels higher than approximately 10^4 mR/H.

D. Specifications

The electrical specifications for the detector are shown in Figure 11.

E. Containment Environment

During the first day of the accident the environment inside containment was one of intense beta and gamma radiation, steam, moderate temperature excursions, a hydrogen burn and the resultant pressure spike, and NaOH/boron spray. No attempt will be made here to quantify these in detail. Generally, the nominal temperature experienced by this detector was probably 54°C (130°F) and peaked at 85°C (185°F).[6] The pressure spike was approximately 1.93×10^5 Pa (28 psi).[6] The building spray was initiated at 1350 Hrs on March 28, some 10 hours after the start of the accident, and lasted for approximately 5 minutes. Other events happening during the first day can be found in reference material.[6,7] High radiation levels and high humidity characterized the building environment over the remainder of the period before removal.

Feature	Specification
Dimensions	3 in. diameter, 7 1/8 in high (7.63 cm, 18.1 cm)
Weight	Approximately 1 lb. (0.45 kg.)
Mounting	Wall Bracket
Radiation detected	Gamma rays
Energy dependence of reading	± 15% from 100 keV to 1.5 MeV
Range of radiation measureable:	
857-10	0.01 to 10^3 mR/hr. (Lo-channel)
857-20	0.1 to 10^4 mR/hr. (Med-channel)
857-30	1.0 to 10^5 mR/hr. (Hi-channel)
Temperature limits	-20 deg. F to 140 deg. F (-29 deg. C to 60 deg. C)
Pressure limits	30 psig.
Detector element life	Exceeds 100 hours at full scale
Electronic exposure life	Approximately 10^5 Rads
Connector required	Bendix #10-72628-18S
Check Source: (Microcuries of radium):	
Det. Model 857-10	0.02
Det. Model 857-20	0.08
Det. Model 857-30	0.16

FIGURE 11. Detector Electrical Characteristics[5] HP-R-211 was a Model 857-2 and had serial number 359.

INTENTIONALLY LEFT BLANK

III. ELECTRICAL/PHYSICAL EXAMINATION AND FAILURE MODE

A. Physical Examination

As shown in Figure 5, the painted aluminum housing of the detector is heavily corroded where pinholes in the paint allowed the underlying aluminum to be attacked. Chemical analyses have been performed on the Victoreen nameplate (top horizontal surface) specifically looking for sodium and boron.[8] Both sodium and boron were found in moderate concentrations (see Table 8). The white granular material on the connector threads was found to be $CaCO_3$ (residue from tap water) by X-ray diffraction analysis. Analysis of the surface around the connector solder pots will be discussed later. These were the only chemical analyses performed with the exception of the radiochemical analyses. The Buna Nitrile O-ring and sealed connecter performed exceptionally well in keeping contaminants out of the inside of the housing. The circuit board is shown in Figure 7 and, under close visual and radiological examination, was found to be clean; no radioactive contamination was found. Except for the corroded housing, no other mechanical defects were observed.

B. Electrical Measurements

Prior to Removal

Before the detector was removed from the containment building, extensive in situ unpowered and powered electrical tests were performed by TEC on the detector channel.[1] These tests showed fairly conclusively that a resistance of approximately 305 ohms existed between the signal output (pin G) and the +10 volt (pin C) detector lines. The observable effect of this shunt resistance was to cause the output signal level to switch between 5.7 and 9.3 volts rather than from 0 to 10 volts. The frequency of the signal looked reasonable (for some, as then unknown, radiation rate).

Unpowered Tests

Similar passive resistance and impedance checks were made on the detector on arrival at Sandia. For comparison, data were also taken on a test detector (Victoreen SN 673), which is the same model as HP-R-211. Table 1 lists the unpowered resistance measurements taken at Sandia and TMI. Probably the only differences in readings are those due to differences in ohmmeters. These tests show a 296 ohm resistance between pins G and C. No other irregularities were observed.

TABLE 1. UNPOWERED 211 MEASUREMENTS

OHMMETER POLARITY/ LINE TO LINE MEAS.		RESISTANCE (OHMS)		
+	-	211 AT TMI	211 AT SANDIA	TEST DETECTOR
+10V	Gnd.	6.47K	5.63K	6.04K
Gnd.	+10V	8.59K	8.50K	11.67K
+10V	Sig.	→ 305	296	7.95K
Sig.	+10V	→ 305	296	5.59K
Gnd.	Sig.	8.62K	8.52K	8.44K
Sig.	Gnd.	6.53K	5.78K	6.98K
+600V	Gnd.	Open	Open	Open
Gnd.	+600V	Open	Open	Open
CS1	CS2	40.2	27.5	24.2
CS2	CS1	40.2	27.5	24.2

Powered Tests

For all powered measurements, whether in the laboratory or at the Co-60 gamma facility, a standard Victoreen Model No. 856-20 ratemeter was used to supply power and process the detector signal output. In addition, a Victoreen Model 857-2 test detector was characterized along with the 211 detector for comparison. There was, however, one problem. In order to obtain accurate ratemeter readings, the ratemeter power supply voltages are normally adjusted to specified limits; then,

using the detector and a known radiation source, the zero offset and gain of the ratemeter are set. Unfortunately, because of GM tube differences, the zero and gain must be adjusted for the particular detector being used. Since this was not possible for 211, because it had failed, only the power supply voltages going to it were adjusted. The zero and gain adjustments were left as set at the factory. Later, when 211 was repaired, a calibration factor was determined. Thus, any ratemeter/detector mismatches could be eliminated; and, as will be shown later, this proved to be a good approach.

Table 2 shows the uncorrected voltage and meter readings obtained when 211 was initially powered. Again, the TMI and test detector data are included for comparison.

TABLE 2. POWERED 211 MEASUREMENTS (DC)

QUANTITY MEASURED		MEASUREMENT		
		211 AT TMI	211 AT SANDIA	TEST DETECTOR
+10V	(V)	9.3	10.04	10.06
→ SIG.	(V)	5.7/9.3	6.7/9.9	0.07/10.0
+600V	(V)	605	598.8	599.1
+22V	(V)	13.66	20.75	21.1
CS 1	(mA)	-	2.44	2.55
Mtr	(mR/H)	1.5	0.2	0.15
Rec	(mV)	-	0.5/1.0	0.35

The effect of the shunt resistance is apparent in the SIG. voltages in the TMI and Sandia measurements (arrow). The conclusion is that all measurements both at TMI and Sandia point to the same failure mode.

C. Failure Mode

Following tests at the Sandia gamma range facility, the detector was opened, node voltages were measured, and the failure was diagnosed. Transistor Q6, a Motorola 2N-3906, was removed and found to exhibit a 163 ohm collector-to-emitter shunt resistance. No other circuit abnormalities were found. Figure 12 shows several of the more important transistor Q6 characteristics as measured on a curve tracer. The collector current characteristics show the presence of an approximate 160 ohm slope on any given base current curve. The transistor gain and the base-emitter junction characteristics are all proper. The presence of this apparent shunt resistance is consistent with the passive tests due to the nominal 100 ohm current-limiting resistor R20 in series with the collector of Q6. The Motorola 2N-3906 is a general purpose 350 mW, epoxy encapsulated PNP transistor which is designed to operate with a maximum collector current of 200 ma. The collector to emitter breakdown voltage is rated at 40 V. The epoxy case was removed by grinding the surface away until the semiconductor chip cavity was exposed; normal solvents were ineffective. The chip shown in Figure 13 has a large amount of foreign material on the surface (not due to the grinding operation, since an additional coating of RTV-like material had to be removed). The metallization is shown removed in Figure 14, and a punch-through defect exists under the center emitter finger. Probes were in fact made of each finger, and the failure was electrically isolated to the middle finger. This type of failure is typically caused by high voltage breakdown from collector to emitter and a subsequent transient surge current. The energy deposited is enough to destroy the normal lattice structure and actually diffuse aluminum metallization into the lattice to cause a resistive path. Had the transistor been overheated through high power dissipation over a long period of time, much of the metallization would probably have been melted. As it is, however, the defect points to a rapid transient.

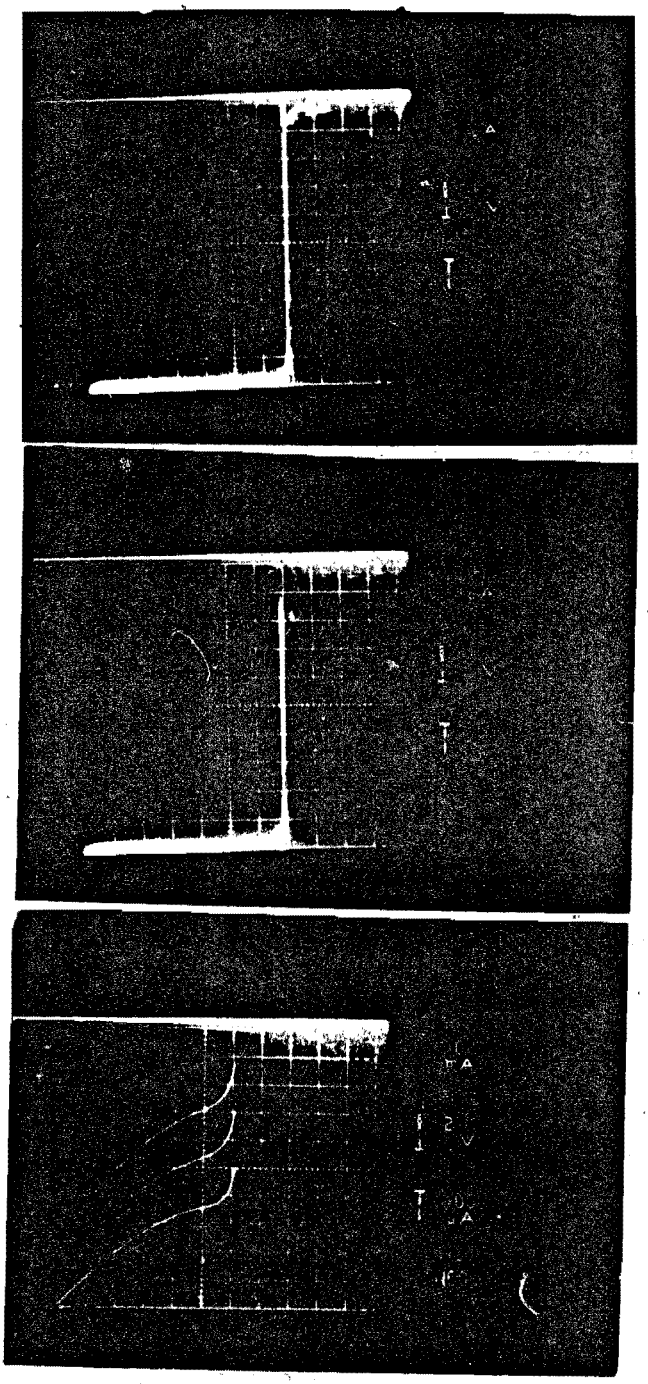

FIGURE 12. Transistor Q6 Characteristics. The top curve is BVCBO, middle curve is BVEBO and lower curve is collector current characteristics. The effect of the 163 ohm anomaly is seen as the slope of the collector current characteristics for any particular base current of the family.

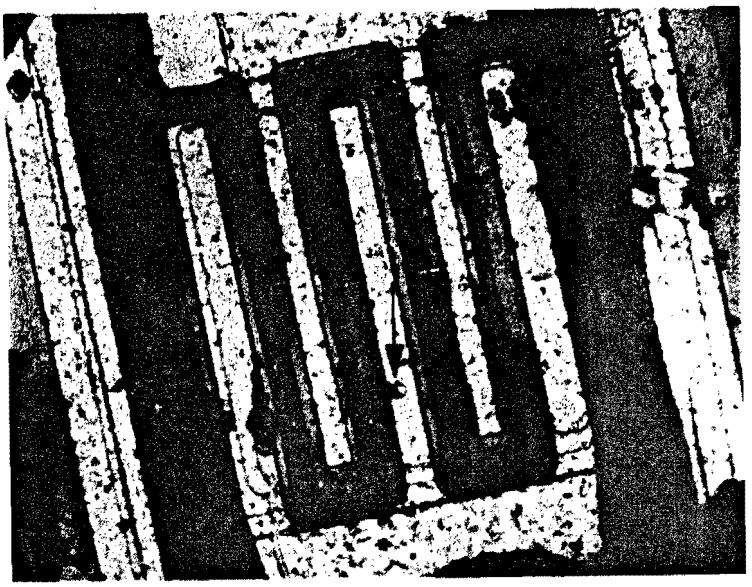

FIGURE 13. Q6 metalization. The punch through defect is apparent even through the emitter metalization (three fingers). This photograph was taken after chip probe but before the metalization was stripped. Notice the large amount of foreign material present.

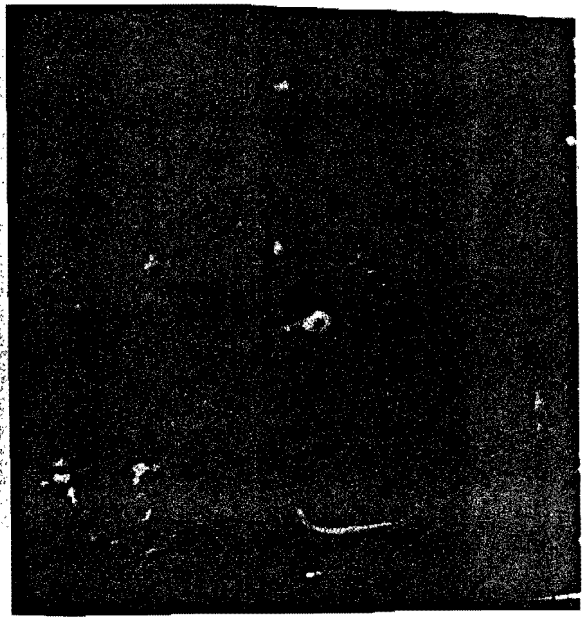

FIGURE 14. SEM Photo of Defect. The metalization was stripped, and a scanning electron microscope was used to examine the chip in detail. The punch-through is noted. Prior to complete metalization removal each emitter finger was individually tested. Only the center finger was defective.

D. Cause of Failure

While we cannot say with absolute certainty how and when transistor Q6 failed, the evidence indicates that the failure was caused either by a transient short in the detector connector backshell; from the 600 Volt GM tube supply pin to the signal output pin, or by a high voltage pulse generated elsewhere, which traveled down the cable on the signal output line. Of these two possibilities, the former appears to be much more probable.

During the removal of the detector from the containment building, the GPU technician was unable to unscrew the connector from the detector, even with the aid of channel-lock pliers. While attempting to loosen the connector, he applied downward pressure on the detector, and it broke free of the cable. The detector, connector first screw-ring assembly, and pin insert were removed as one piece. Figure 15 gives an exploded view of the connector assembly and pin connections. Later examination of the free cable end after its removal revealed the second and third connector screw-ring assemblies to be mated and encased along with the cable end in Raychem WCSF heat-shrink tubing. This tubing was tightly molded to the connector part and covered at least the lower 20 cm of cable. In fact, three layers of heat-shrink tubing were used as shown in Figure 15 to produce what appears to be a good, watertight seal between the connector and cable. Since he did not attempt to rotate the detector to unscrew it when he could not turn the connector, apparently the second screw-ring was not mated or mated by less than one thread to the threaded insert. Corrosion on the connector insert and inside the second connector screw-ring indicates exposure to steam or liquid. Scanning electron microscope (SEM) and energy dispersive spectroscopy (EDS) studies made on the insert around the solder pots were inconclusive in the search for sodium there (because of instrument limitations on the detection of low Z elements).

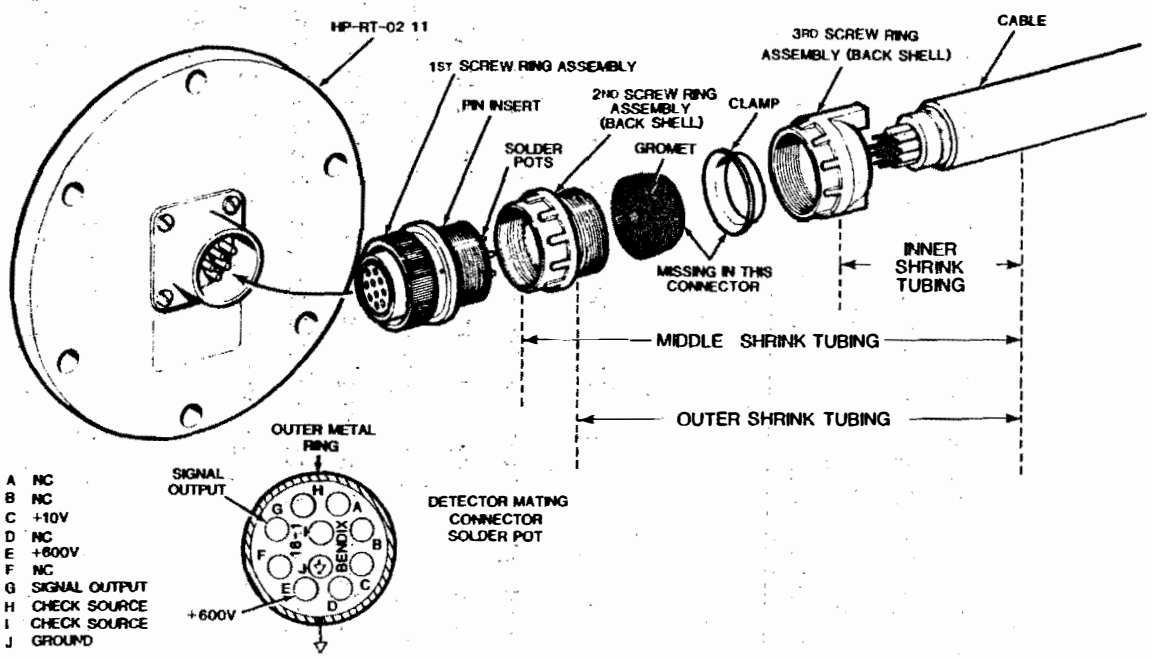

FIGURE 15. HP-R-211 Connector Assembly. The second screw-ring assembly was apparently not screwed onto the pin insert.

A chemical analysis was not performed. We believe that steam and/or NaOH/B spray entered the connector backshell through the loose-fitting insert-to-second screw-ring junction.

To investigate this postulated mode of failure, several laboratory simulations were conducted and will now be discussed. The presence of the 100 ohm current limiting resistors in the signal output line preclude Q6 from being destroyed by a short of the signal line to ground. In fact, DC shorts were made from each connector pin to the next, using the test channel, and a failure could not be induced. The 600 Volt line has a 2 Megohm current limiting resistor at the ratemeter; even though the transistor can break down, the steady-state current is limited to only 300 Microamperes. No discharge paths were found on the circuit board. Recall however, that some 152 M (500 ft.) of cable connects the detector to the power source. We found that the energy stored in the line capacitance was sufficient to cause punch-through. This was found by conducting the following experiment (refer to Figure 16): Capacitors of 0.015 μF and 0.01 μF were connected to the signal output and 600 Volt lines going to the test detector to simulate the charges stored in the 50 Ohm and 75 Ohm cable capacitances. A switch was then thrown to discharge the capacitor on the 600 Volt line into the signal output. This results in a surge current of approximately 6 amperes. The circuit diagram shows a possible current path, I.

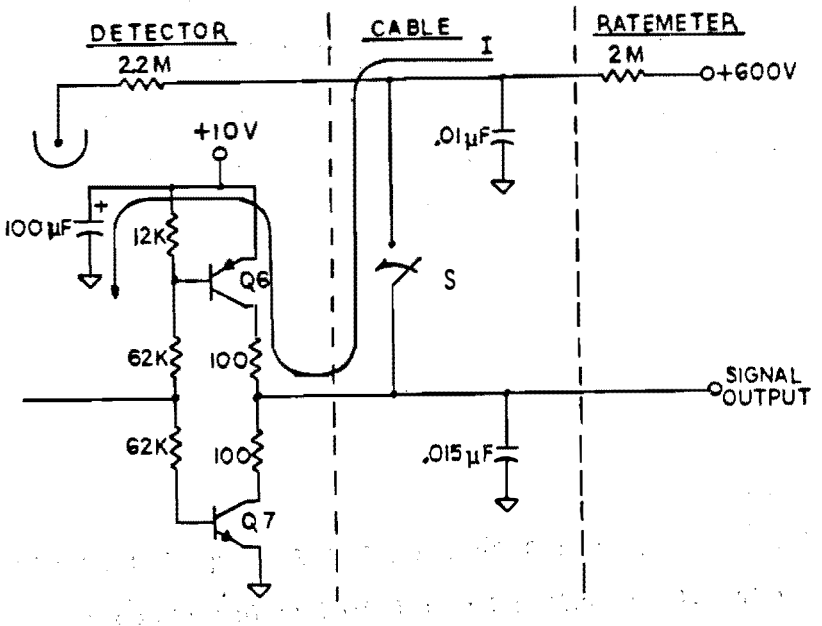

FIGURE 16. Test Circuit Showing Energy Discharge Path

We opened and closed Switch S repeatedly while constantly monitoring the signal output line. After approximately 40 closures the "O" level voltage had increased to 6.65 Volts. After 80 closures, the transistor in slot Q6 was removed, tested and found to exhibit a 96 Ohm collector-to-emitter resistive path, similar to that in the failed detector. No other circuit defects were observed. Tests have been conducted on four other 2N 3906 transistors from a different manufacturer and on two higher current 2N 2904's. All could be made to fail with a single discharge, but only if the 100 Ohm current limiting resistor was decreased. One 2N 3906 failed when the resistor was 72 Ohms, however, all others required lower resistance. The capacitive model of the cable does not simulate exactly the cable characteristic impedance of 75 Ohms and stored charge, since the cable is a transmission line and will appear to have a 75 Ohm source impedance. Since the line is not

terminated in 75 Ohms on either end, it will also ring. This will reduce the peak currents somewhat. Nevertheless, we conclude that for a weak device, one having a thin base and geometry sensitive to high current densities, a failure similar to that experienced at TMI can occur in one or more discharges. The following experiments were conducted to determine the detector response to steam and spray introduced to the connector backshell.

Steam and Spray Experiments

The HP-R-211 stripchart recording (Figures 25a and 25b) exhibits only a single observable discontinuity. This occurs at approximately 1350 hours during the time of either the hydrogen burn or five minutes of building spray. The signal first rises, drops to zero for approximately two minutes, and then steps back up abruptly to a level somewhat lower than it was prior to the transient. This five minute perturbation suggests a point in time at which the failure could have occurred.

Several simple experiments were conducted to understand in a macroscopic way the surface conductivity and electrical conduction mechanisms with regard to pin-to-pin conduction in the connector backshell. Surface conductivity and breakdown effects are discussed in some detail by Stuetzer[9] and will not be covered here. Suffice it to say that conductivity is greatly dependent on the surface material, surface contaminants, temperature, humidity and voltage potential difference. The drawing of the connector backshell pin arrangement in Figure 15 shows that the "case" is grounded, and the 600 Volt pin is separated from the signal output pin only by an unused pin. We postulate that something similar to one of the following events occurred during the transient period:

1. The rubber surface of the connector backshell was contaminated. Either steam was forced into the backshell by a pressure differential resulting from the hydrogen explosion, or the hydrogen explosion flattened water droplets which had formed on the surface due to steam condensation. In either case, the 600 volt and signal output pins were momentarily shorted; or,

2. A droplet of NaOH/B spray traveled down the cable, entered the connector backshell through the loose connector fitting and momentarily shorted the two pins.

In either case water entered the connector backshell.

In our experiments, we found the following:

1. Steam condensation on a cool connector surface, contaminated only by normal handling, tends to form constant, long duration, low resistance paths between pins. Small water droplets, initially formed, flow together until the gap between pins is bridged. Once the pins are bridged, conduction takes place until the large droplet evaporates or its ionic contamination is depleted. This could take minutes or hours to occur, and during that time the detector output would be zero. There is no evidence of this on the stripchart records.

2. Steam condensation on a heavily contaminated surface tends to "wet" the surface, resulting in short duration, low resistance conduction. Droplet formation is minimal. Resis-

tive paths between pins can form quite abruptly and disappear as fast. Interestingly, even in the presence of steam, the path can open quickly and remain open. This is illustrated in Figure 17a. Here, using the test detector and its connector, we deposited NaOH of PH 12.7 on the surface and allowed the water to evaporate. We then directed steam onto the surface, and after 100 seconds the signal output dropped to zero indicating a reduction in the 600 Volt to somewhere below 380 Volts. A minute and a half later the detector recovered and did not fail again even in the presence of steam. What happened was that the sodium ions were attracted to a more negative terminal, the surface near the 600 Volt pin was depleted, and conduction terminated. In fact, water ceased to wet this area and even to form droplets there. Figure 17b shows the 600 Volt line in the test where a large droplet of NaOH had been introduced between pins. The 600 Volts decreased abruptly then rapidly increased time-after-time (the 0.01 μF capacitor was used to supply energy). Tiny arcs could be seen around the 600 Volt pin. Each one of these delivered energy to ground or to ground through another pin.

We conclude from these tests that a large droplet of water or spray was not in the connector shell due to the absence in the stripchart recording of any long duration short or repeated signal irregularities. A highly contaminated connector, introduced abruptly to only a small puff of steam, is sufficient to produce the single drop-out noted. The presence of sodium is indicated, and it is possible that even though a single discontinuity was observed other short duration discontinuities could have occurred without being registered on the stripchart recording.

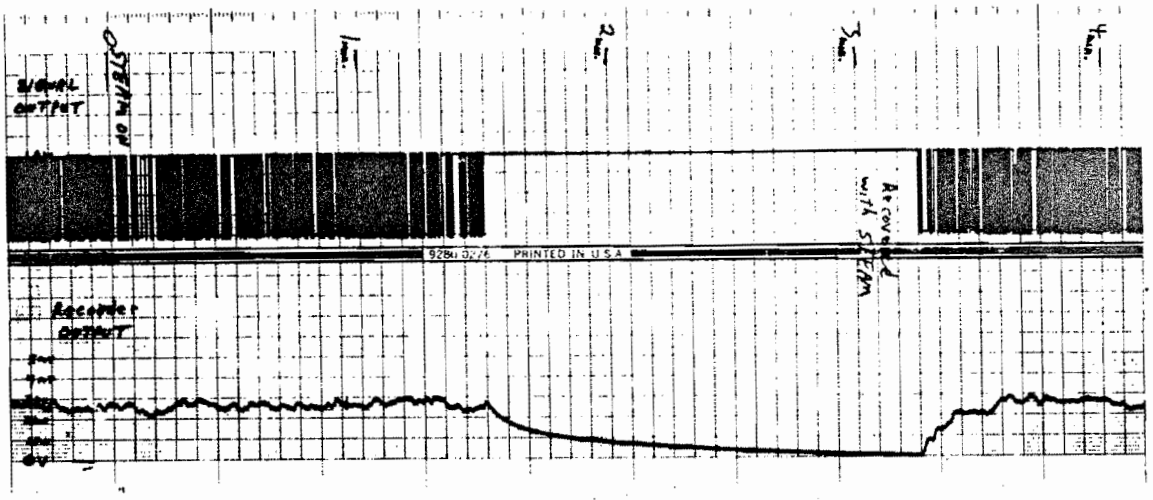

FIGURE 17a. Steam on a Contaminated Backshell. A detector connector backshell was exposed to steam after the backshell was first contaminated with NaOH. NaOH was introduced and then allowed to dry before steam was applied. The top trace is the signal output, and the lower trace is the ratemeter output. The detector failed after about 1.5 minutes of steam, but recovered even though steam was still being applied.

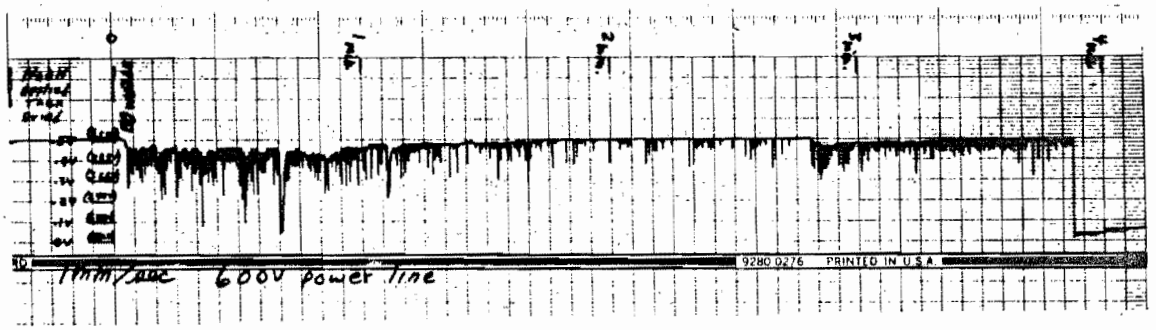

FIGURE 17b. Large Droplet Formation. A similar experiment to that shown in Figure 17a was conducted, except that here all of the detector pins are covered with a water droplet. The 600 Volt power line is plotted versus time. Repeated surges are delivered to a load during each breakdown.

E. Conclusions

The detector was found to operate properly in all respects after the defective transistor Q6 was replaced (except for the multi-valued readout discussed in the next section). The detector environmental seal was good, and no radioactive contaminants were found on the electronics inside the housing. No mechanical damage, or elastomeric material degradation was visible inside the housing or on the connector insert. The housing outside was corroded and pitted.

The failure of transistor Q6 is thought to be due to high voltage breakdown and rapid energy deposition. Although this energy could have been delivered down the cable due to EMP or some such transient, we have found no other evidence of this. Instead, we have been able to cause transistor degradation in laboratory tests where energy stored on the 600 Volt cable is rapidly discharged onto the signal output pin. This has been shown to be possible when the detector connector backshell is subjected to a steam and/or spray environment. The evidence indicates that the connector insert was apparently not properly mated to the connector second screw-ring assembly, thus providing an entryway for steam or spray to make contact with exposed connector pins. Although the manner of failure is fairly clear, the precise time of failure is not. The only stripchart discontinuity occurred at the time of the hydrogen burn, and this point represents the most likely time of failure; however, as will be discussed in the next section, further degradation of transistor Q6 must have occurred after the hydrogen burn with some degradation possibly occurring even before the burn. Our steam and spray tests indicate that a connector backshell insert with no abnormal chemical contamination, when subjected to steam only, would produce an obvious stripchart discontinuity. Once the insert is contaminated with sodium or other similar contaminant, however, it would be possible for transients to occur and not be detectable on the stripchart readout. The most

likely scenario, therefore, seems to be one in which major transistor degradation occurred at the time of the hydrogen burn and then further degradation was incurred after the backshell was contaminated with sodium. We have no direct evidence from the stripchart recording that transistor Q6 was degraded before the hydrogen burn, although the possibility exists. All other detectors recorded on the stripchart reacted in the same manner as HP-R-211 at the time of the spray initiation but all did not recover.

IV. DETECTOR CHARACTERISTICS AND RADIATION TIME HISTORY

A. Discussion

Our findings show conclusively that the only failure experienced by HP-R-211 was that of transistor Q6. When this failed transistor was replaced, the detector operated properly up to radiation levels of 500 R/H. At levels higher than this the radiation decreases as the input level is increased. This is caused by detector to cable and cable to readout module impedance mismatches. These cable mismatches cause erroneous, low radiation readings when radiation levels are in the range of 500 R/H to 10^6 R/H. This behavior is hardly noticeable on new, undegraded detectors, but becomes dramatic when transistor gains have been degraded by radiation as in HP-R-211.

Without a doubt the most difficult task has been that of attempting to reconstruct the containment gamma radiation time history as measured by HP-R-211. Of the four radiation detectors normally used to monitor containment radiation, only two, HP-R-211 and HP-R-214, have continuous stripchart outputs both during and since the accident. They, then, represent our best opportunity to supply accurate records of containment gamma radiation. The failed transistor in HP-R-211 caused erroneous, low radiation readings which possibly can be corrected with the use of the proper scale factor.

Studies[10] to date of the dome monitor (HP-R-214) record have uncovered several problems in interpreting its output. Among these is the significant difficulty of transforming radiation levels measured inside a 4 cm lead shield to radiation levels outside. Also complicating the analysis is the probable existence of a 0.3 cm diameter hole

in the lead shield. It may never be possible to unravel the HP-R-214 data.

Detector HP-R-213 failed at the time of the hydrogen burn. Unfortunately, much of the time it was pegged at its maximum reading of 10^4 mR/H. HP-R-212 was apparently not recorded until it was switched on 92 days after the accident. It functioned for 128 days thereafter until it also failed. The two fuel handling bridge detectors appear to have been off during the accident, and no records exist for them. Thus, HP-R-211 may represent our best chance to obtain a composite doserate time history.

Knowledge of the radiation environment, if only at one location, is valuable in evaluating the operation of reactor instruments and systems in the quite hostile environment to which they were exposed. Information of this type could also be valuable in assessing the validity of various reactor models relating to radionuclide dispersal following a LOCA.

This section presents measured detector characteristics using both short and long coaxial interconnection cables, stripchart data, and a brief discussion of radiation time history. Radiation time history information will be given in a separate report when this and other investigations have been completed.

B. Detector Characteristics (Short Cables)

The failed detector was mated with the test channel ratemeter using short coaxial cables and exposed at the Sandia Co-60 Vertical Range Facility. Figure 18 shows the ratemeter radiation readings vs known radiation input rates. Three curves are shown. Unfortunately,

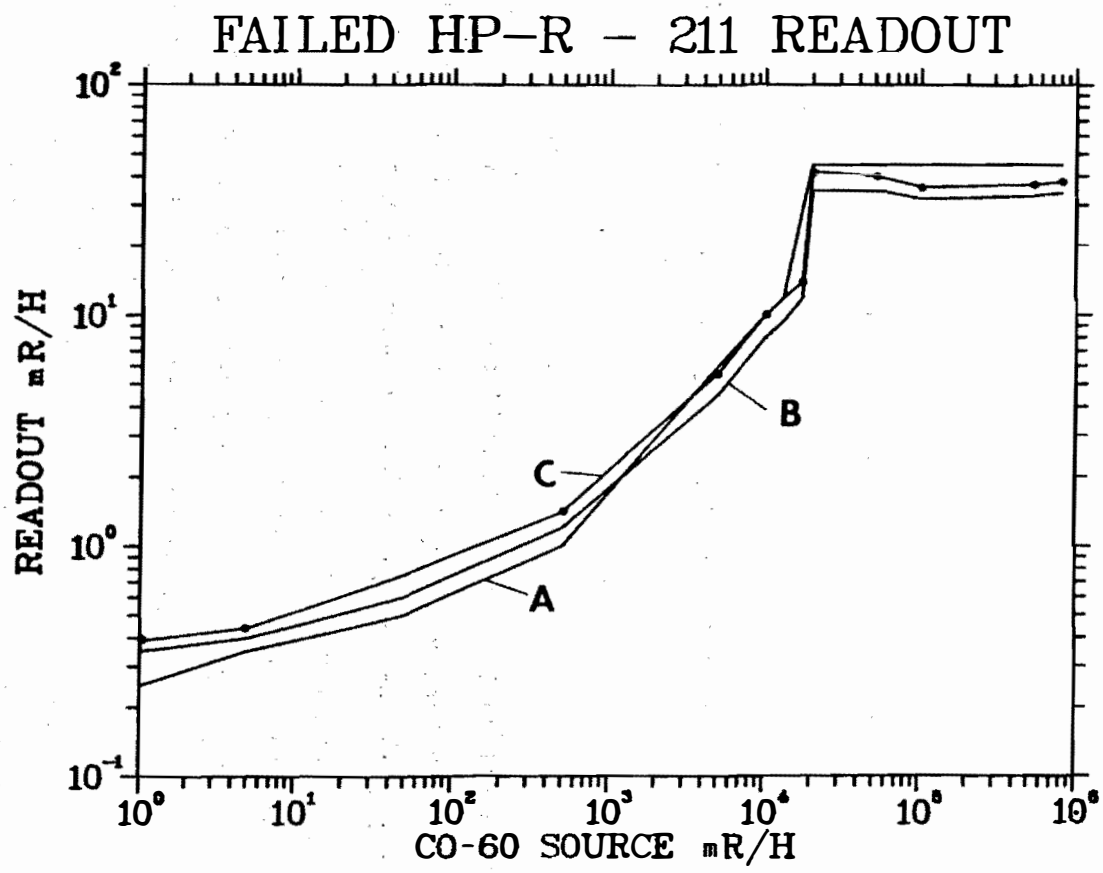

FIGURE 18. HP-R-211 Characteristics. The detector was exposed to a Co-60 source upon arrival at Sandia and produced the output shown. Curve A is for the condition of nominal detector supply voltages, Curve B is for low voltages,and Curve C is low-voltage, ratemeter corrected. These data were taken without 152 m cables or line capacitance equivalents used.

during the TEC measurements on site, we discovered that the +10 V and +22 V power supply voltages going to the detector were +9.3 V and +16 V as a result of a faulty capacitor (C1) in the TMI ratemeter. Therefore, the recorded radiation readings are in error not only because of the faulty transistor but also improper power supply voltages. The length of time this situation existed is not known. Fortunately, this low voltage condition does not have a major effect on our results. Curve A in Figure 18 shows the nominal voltage characteristic. Curve B shows the same characteristic except using the lower supply voltages as measured just prior to removal from containment. Curve C is the final result, using a ratemeter scale factor as described later. The detector level indications are seen to be below the known source levels by up to three orders of magnitude. This is due to the reduced amplitude of the detector output as a result of the failed Q6. Significantly, the anti-jam circuit is seen to cut in at about 20 R/H. Above this level, increases in source level are not followed. Transistor Q6 was replaced with an operable transistor and the detector was exposed again to the Co-60 source (at nominal voltage). Figure 19 shows the result. The detector is seen to function properly, being in error only by a voltage scale factor of 1.05. The test detector is shown for comparison. A Victoreen representative says that the slight offset between HP-R-211 and the ideal curve is normal and is caused by differences in GM tube characteristics.[15] The similarity with the test detector and the ideal curve leads us to the important conclusion that transistor Q6 was the only failure in HP-R-211 and that only minor degradation was experienced. For information, Figure 20 shows detector counts-per-minute versus input radiation level. Counts-per-minute here refers to that measured by a frequency counter which responds only to positive going signal transitions ("events", or photon/GM tube interactions, occur at twice the counter rate).

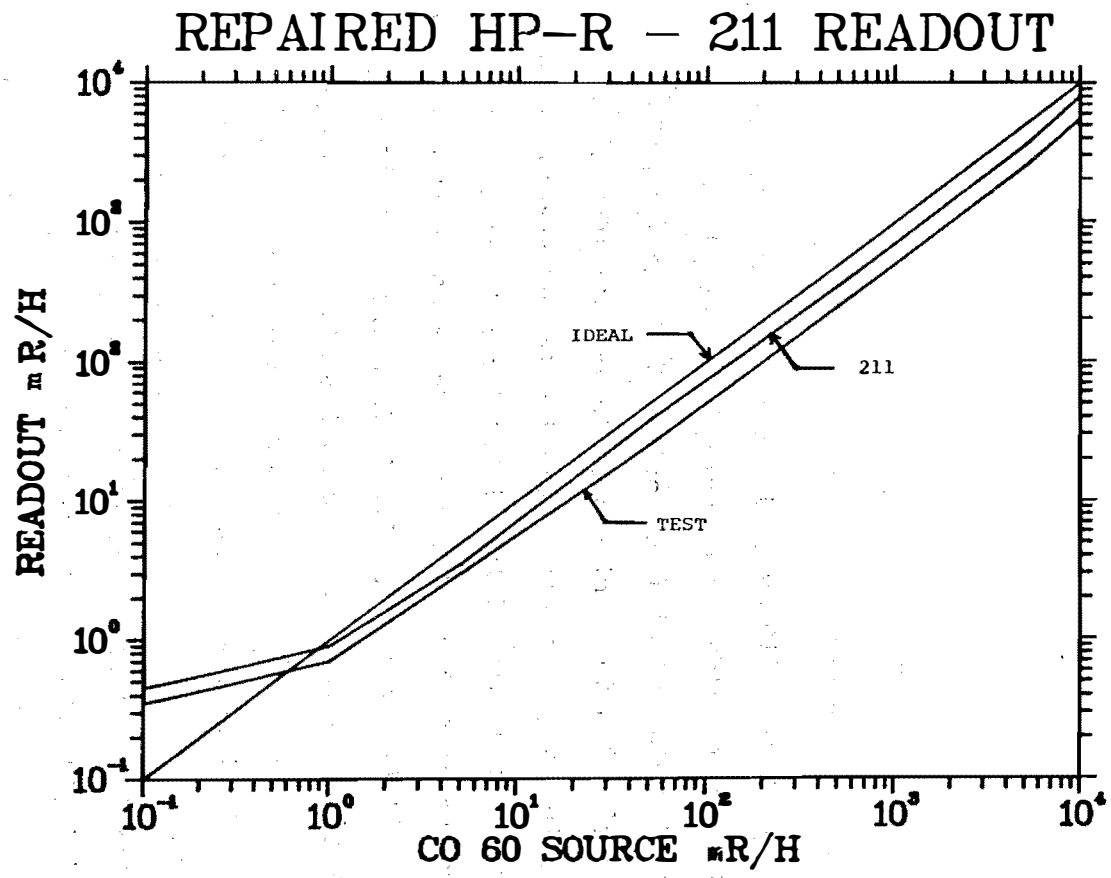

FIGURE 19. Repaired Detector Characteristics. The curve labeled 211 is a plot of the HP-R-211 readout versus Co-60 source level using the test channel ratemeter. The ideal input vs output is shown. The two curves differ by a calibration factor associated with each GM tube. So that there be no mistake that HP-R-211 is operating properly, the test detector is included for comparison. This curve also shows the need for ratemeter calibration. The changes in slope at low radiation levels are due to normal background radiation.

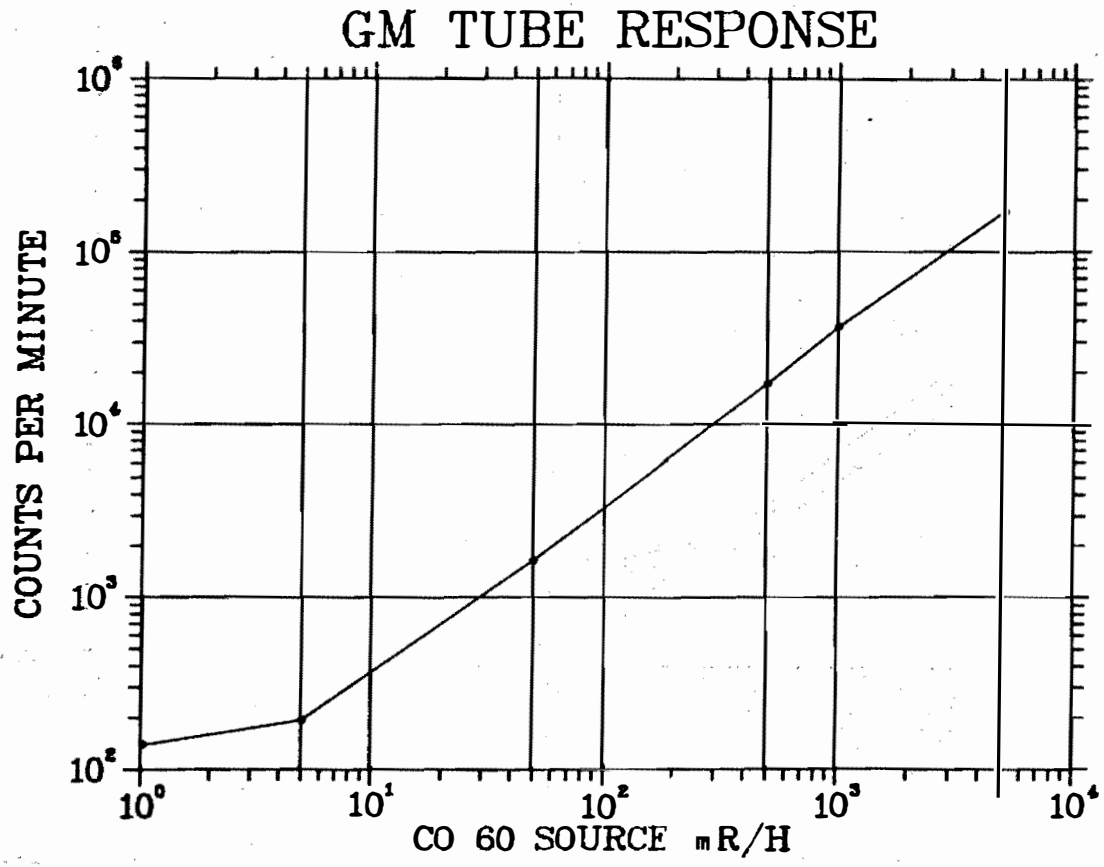

FIGURE 20. GM Tube Characteristics. The detector counts-per-minute are plotted vs gamma source level as measured with a frequency counter. Since the detector was contaminated, the lower end of the curve has a slope change.

Tests were also run to determine the temperature dependence of detector level readings. We found that for an unfailed detector temperatures as high as 60°C had negligible effects. For the failed HP-R-211 detector the readout levels at room temperature are approximately 30% lower than those at 60°C. Because of the difficulty in running tests at various temperature levels, all tests were conducted at room temperature.

C. Detector Characteristics (Long Cables)

During testing at the Sandia Co-60 Gamma Irradiation Facility (GIF), the repaired detector and its associated ratemeter radiation measurement system was observed to indicate erroneous, low radiation levels when in fact the levels were very high. These tests were being conducted to investigate stripchart anomolies, and transistor Q6 had been replaced with a functional one. Also, 152 m (500 ft.) of RG 58 and RG 59 coaxial cable were used to connect the detector Signal Output and 600 Volt lines to the ratemeter. The decrease in radiation level indication began to become noticeable at radiation levels above 500 R/H. This multivalued characteristic was found to be caused by signal reflections in the long Signal Output cable which are set up by cable impedance mismatches on the Signal Output line at both the detector and ratemeter terminations. GM tube pulse interactions above the antijam point combine with the cable reflections to accentuate the problem.

Although this detector was not designed to accurately measure radiation levels above 10 R/H, the antijam feature was added to keep the readout meter "pegged" at full-scale. Radiation degraded detector output drive transistors cause the erroneous indication to become more noticeable; and, in a LOCA induced environment, this multivalued characteristic could potentially be hazardous. The discussion which follows describes this multivalued characteristic in detail. In addi-

tion, it was discovered that the presence of the long coaxial cable changes the detector output characteristic somewhat when transistor Q6 is in its failed state at low radiation levels. This subject is also discussed.

Multivalued Output

Figure 21 shows data taken at GIF and the Sandia Vertical Range for three detector conditions. The variable measured and recorded is the ratemeter stripchart output voltage. As stated earlier, this voltage is proportional to radiation levels up to approximately 20 R/H, whereas the ratemeter meter pegs at 10 R/H. The normal, expected output is shown in Curve A. These data were generated using the test detector. The detector to ratemeter interconnection cable was made using a short, unshielded wire bundle. The radiation measurement channel output is proper up to 720,000 R/H. Curve B shows the output of the same channel except that 152 m (500 ft) of 50 ohm, RG 58 coaxial cable was used to transport the detector output signal to the ratemeter. This simulates reactor use conditions. Both the detector and cable were exposed to the source. The ratemeter output voltage begins to dip slightly above 1000 R/H; however, the readout meter is still pegged at 10 R/H. Curve C shows the result when the degraded, but repaired HP-R-211 detector is used with the long cable. Transistor Q6 was a 2N 3906 which had been degraded by exposure to 1×10^6 rads. The curve dips dramatically, reaching a minimum of 150 mR/H at a Co-60 source level of 54,000 R/H. The output recovers significantly as the radiation rate is increased. The degraded detector is seen to have a multivalued radiation indication. Exposure of the cable along with the detector was found to not be significant. Victoreen supplied us with three new detectors for testing in order to obtain some statistical data regarding this multivalued function. In each case, these detectors behaved similarly to the test detector.

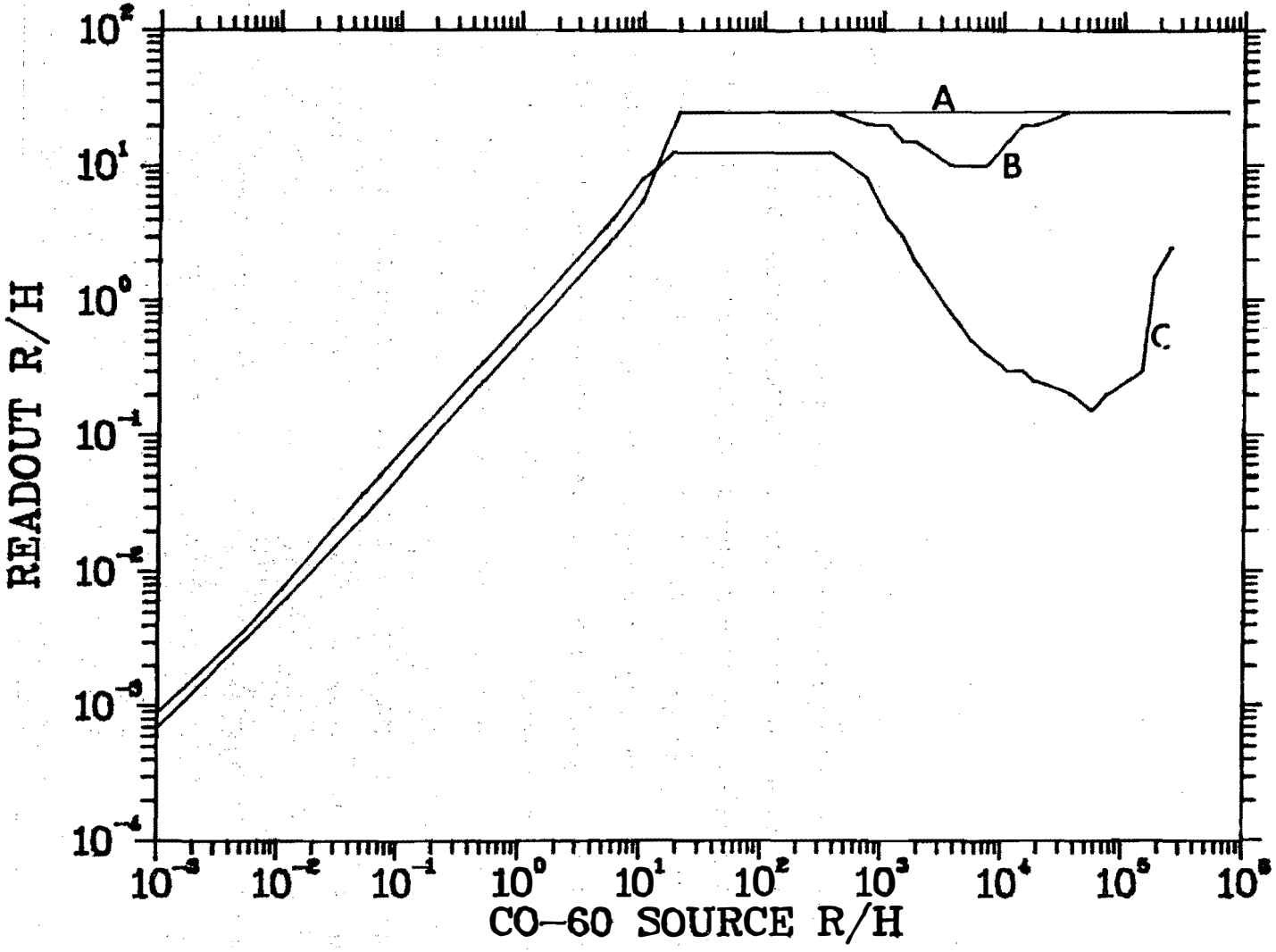

FIGURE 21. Multivalued Readout. Curve A shows the Test detector response to the Co-60 source when a short cable is used to connect the detector to the ratemeter. Curve B gives the response when 152m of coaxial interconnect cable are used. Curve C gives the HP-R-211 response using 152m interconnect cable. The response is seen to be multi-valued when long cables are used, especially for the degraded detector.

Problem Cause -- Several experiments were run in an effort to understand the cause of the detector dip in radiation indication. In order to check the majority of the detector electronics in HP-R-211, we removed the GM tube from circuit interaction. This was done by shorting across it between R1 and R2 of Figure 9. This continuously engages the antijam circuit. The readout was seen to indicate a constant, near maximum, indication regardless of source level even up to 720,000 R/H. This is the proper response for this condition. This indicates that the GM tube pulse output is interacting with the free-running multivibrator at high radiation levels.

The dip has, in fact, been determined to be due to two items: impedance mismatches between the coaxial cable and both the detector and ratemeter circuits, and GM tube circuit interactions above the antijam point. First, and probably most importantly, the detector output circuit is not designed to properly match in impedance the 50 ohm cable attached to it. The normal output impedance of the detector is approximately 100 ohms rather than 50 ohms. Further, the ratemeter input appears as an open circuit for the steady-state signal. This open circuit combined with the mismatched driver sets up reflections in the cable which have the same effect as filtering the signal. Since the ratemeter circuit is a linear log pump, both the amplitude and the frequency of the signal affect readout accuracy. Figure 22 illustrates the effects on the waveform of the mismatch. For a voltage V propagating down a coaxial cable of characteristic impedance Z_o, the voltage across the load impedance Z_L is equal to (1 + R)V, where R is the reflection constant. If Z is the termination impedance, R is given by:

$$R = \frac{Z - Z_o}{Z + Z_o}$$

A voltage of RV is reflected back down the cable. With a value of $Z_L = \infty$, R is equal to 1, and V is totally reflected. This voltage travels the

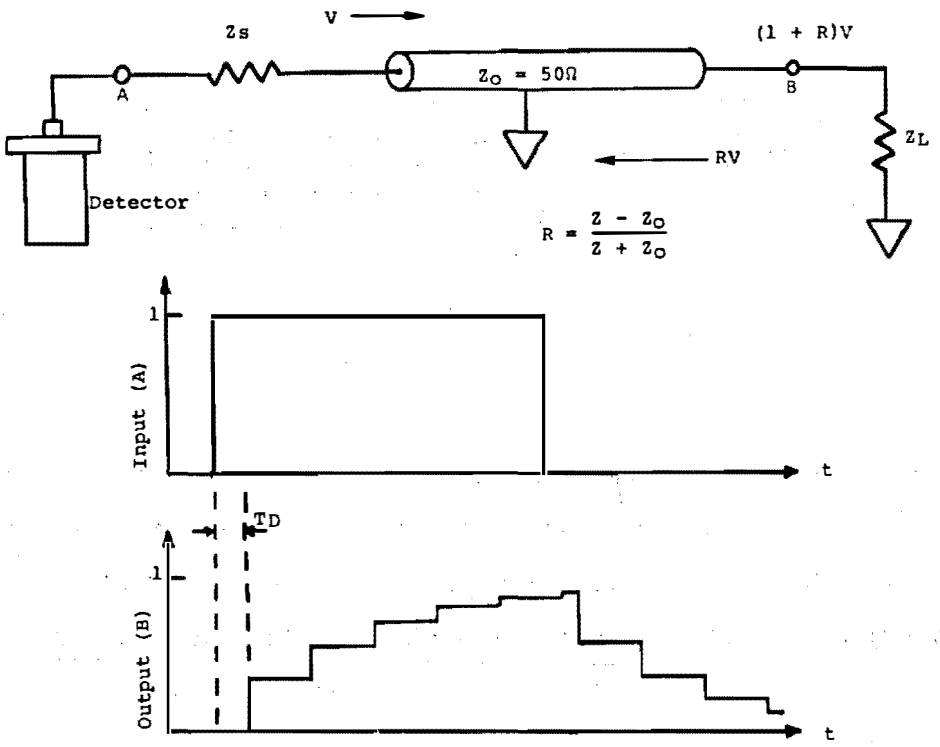

FIGURE 22. Input and Output Waveforms for a Mismatched Transmission Line (Z_S = 250Ω, Z_L = ∞)

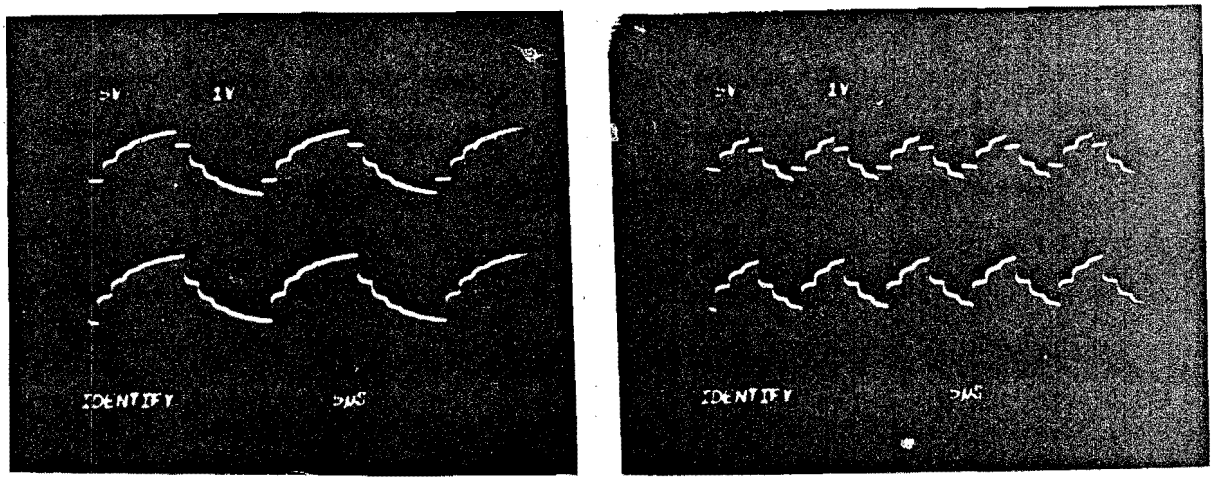

50 kHz 100 kHz

FIGURE 23. Mismatch Filtering. For both photographs Zs = 250 ohms and Z_L = ∞ . The top trace is the transmission line input voltage and the bottom trace is the output voltage. The input frequencies for left and right photographs were 50 kHz and 100 kHz respectively.

length of the cable and impinges at the detector end where it is reflected due to the improper termination. The process continues, and a voltage step at the detector end, the resultant waveform at the rate-meter shows a series of upward (or downward) steps. The width of each step is equal to $2T_D$, where T_D is the time required for the signal to propagate the length of the cable. If the detector output squarewave reaches a frequency high enough to have a period which is of the order of T_D, a substantial rolloff of the waveform will result. Figure 23 shows oscilloscope pictures of this condition.

The detector output impedance, which for a new detector is normally 100 ohms, increases as transistor gains are degraded by gamma radiation. The HP-R-211 transistor gains were degraded to the point that the equivalent source impedance was approximately 270 ohms. This has the effect of causing further impedance mismatches and more dramatic reflections. The base drive currents for transistors Q6 and Q7 are not adequate to make up for the transistor gain decreases observed.

The second major cause for the operation as described is the continued GM tube pulsing of the multivibrator circuit even after the antijam circuit has begun to control the multivibrator frequency. The antijam circuit does not disable pulse amplifier Q1. This allows GM tube output interference. This pulsing increases the detector squarewave frequency from the normal antijam frequency of 40 KHz until the reflection time T_D becomes a significant factor. More "filtering" or rounding of the signal waveform is thus produced. We attempted to monitor several of the internal circuit nodes in order to understand the GM tube interaction mechanism more clearly; however, in each case our measurement apparatus interacted with the circuit and changed its

characteristics. We did interchange GM tubes between one of the new, Victoreen-supplied detectors (SN 1344) and the HP-R-211 detector. The HP-R-211 GM tube was found to degrade the performance of SN 1344 but not too severely. Alternately, the SN 1344 GM tube improved the performance somewhat of the HP-R-211 detector. The degraded transistors and degraded GM tube both seem to influence the detector behavior. More information regarding these tests can be found in Reference 18. That the tube has changed is expected since the manufacturer introduces a quench gas in the tube to reliably halt GM discharges. This quench gas can be used up by high radiation doses.

The approach toward recovery shown above 100,000 R/H in Curve C of Figure 21 is presumably due to fewer GM tube interactions, and thus a lowering of output frequency. The frequency stabilizes at that determined by the free-running multivibrator. The cable drive is still inadequate and reflections still occur; however, the lowered frequency signal is not "filtered" as much.

Corrective Action -- The observed radiation measurement characteristic dip can be corrected by some relatively simple changes in circuit design. Specifically, any of the following changes would improve the design; by making all the changes, the detector could be made to function properly at significantly higher radiation dose levels:

1. reduce R20 and R21 to approximately 50 ohms to properly match the 50 ohm coaxial cable;
2. use more radiation tolerant transistors in the Q6 and Q7 transistor slots;
3. increase the base drives to Q6 and Q7 (if the drive was increased too much, the drive to Q5 would need to be increased also); and

4. use the antijam output to disable the GM tube pulse output to the multivibrator (a new circuit design and P.C. board layout would be required).

Although not necessary to correct this problem, two improvements in circuit design could be made in the ratemeter:

1. terminate the coaxial cable in 50 ohms to prevent reflections (this would require gain changes in the ratemeter differential amplifier); and
2. employ a zero crossing comparator circuit to reconstruct the detector squarewave and thus make the ratemeter input amplitude insensitive (a new P.C. board layout would be required).

Failed State Characteristics

When the effects of the long coaxial cable were discovered at GIF, the detector was returned to the Sandia Vertical Range for additional tests with a long cable attached. Since the failed transistor Q6 had been destructively analyzed, it was necessary to install an "equivalent" transistor in the Q6 slot. The original failed transistor exhibited a 163 ohm resistance from collector to emitter and was also degraded from exposure to radiation. We placed a resistor in parallel with an undegraded 2N 3906 and varied its value until we achieved approximately the same readout versus radiation level curve, using short cables, as we had recorded for the failed HP-R-211 detector (Curve A, Figure 18). The resistor value required to do this was 250 ohms. This produced a 3.2 V peak-to-peak output versus a 3.6 V peak-to-peak output for the original, failed detector. Figure 24 shows the data obtained using this "equivalent" transistor. Curve A shows the nominal

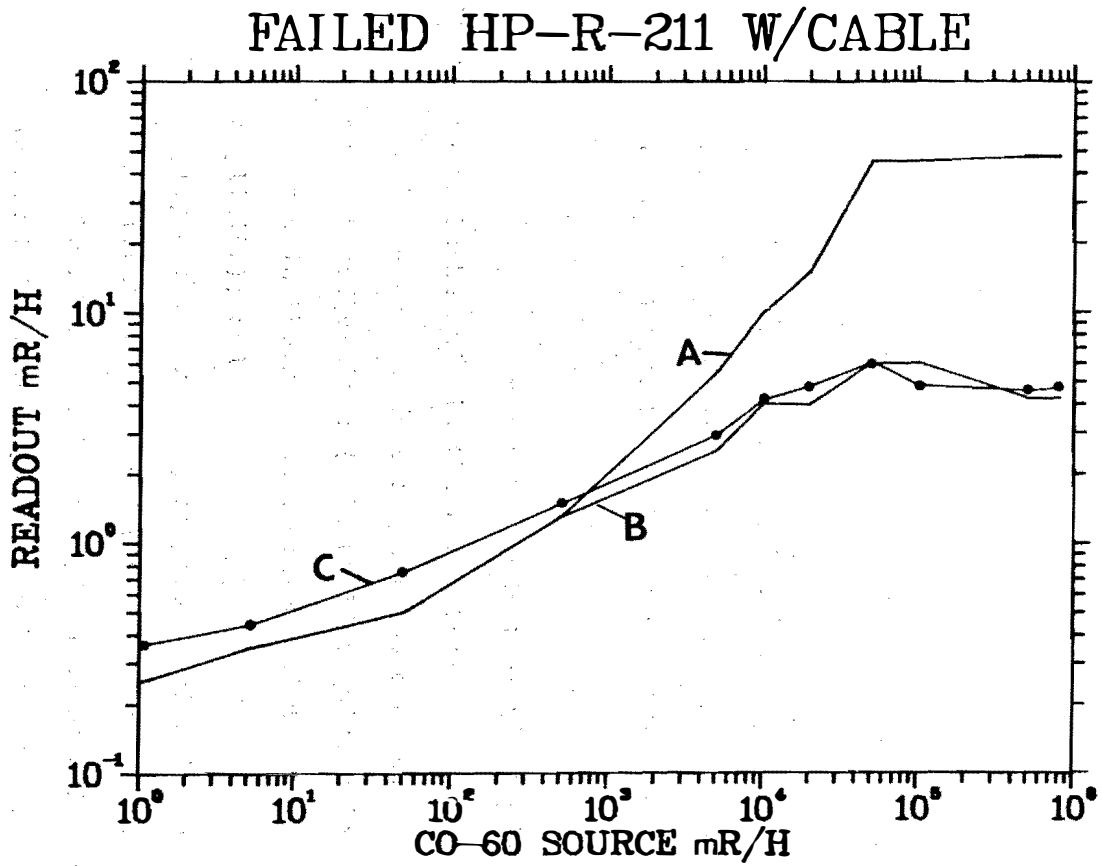

FIGURE 24. Failed HP-R-211 characteristics with 152 m of Coaxial Cable. A new 2N 3906 transistor with a parallel 250 ohm resistor was substituted in place of the failed transistor Q6. RG 58 Cable was used to connect the signal output line from the detector to the ratemeter. Curve A is the nominal-voltage characteristic with a short (3 m) coaxial cable. Curve B is the nominal-voltage characteristic using a long (152 m) coaxial cable. Curve C is the low-voltage, ratemeter corrected, characteristic, using a long cable.

voltage characteristic when a short interconnect cable is used. This compares very closely with Curve A of Figure 18, indicating a good transistor equivalent. Curve B is the nominal voltage characteristic when 152 m (500 ft) of cable are used. Curve C is the low voltage condition, corrected using the 1.05 ratemeter scale-factor. At the lower radiation rates cable effects are negligible; however, as the frequency of GM tube discharge increases at higher levels, the cable effects become apparent. The much lower "saturated" level of 4.7 mR/H makes the understanding of the HP-R-211 stripchart more difficult as will be discussed later. The validity of our "equivalent" transistor is subject to question. However, since this is the best simulation we have been able to devise, any stripchart reconstructions should use the data in Curve C of Figure 24.

D. Stripchart Recording

The HP-R-211 stripchart, as recorded on Channel 9 of multi-point recorder HP-UR-1901 and reconstructed from operator logs, is shown in Figures 25a and 25b. This record dates from March 28, 1979 through August 15, 1980.

The detector registered 0.3 mR/H, at 97% of full power, until 0400 on March 28. There, at reactor trip, it showed a slight dip, then at 0635 it shows a dramatic rise which peaks at 170 mR/H. The level decreases until at 1350, it rises for 1 minute to 52 mR/H then abruptly decreases to minimum scale. This is the approximate time of the hydrogen burn and subsequent building spray. It has not been possible for us to determine precisely which event this decrease corresponds to. Using the point of reactor trip as an accurate fiducial mark, we find that the dropout is slightly after 1350. Approximately 5 minutes after the transient began, the output recovers to 25 mR/H. Only a few data points exist before the stripchart ceased turning. Only a short burst of data was recorded over the next 14 hours. During the intermediate time the recorder printed in place. The changeover from stripchart to manual data taking is apparent on June 5, 1980 (10^4 hours). The obvious difference in readings is minor and, henceforth, the recorder level will be assumed to be the more precise indication. As described below, all the evidence we have found indicates that the HP-R-211 channel was operating properly prior to the accident and that the stripchart recorder produced accurate recordings both during the accident and up to the time it was taken out of service.

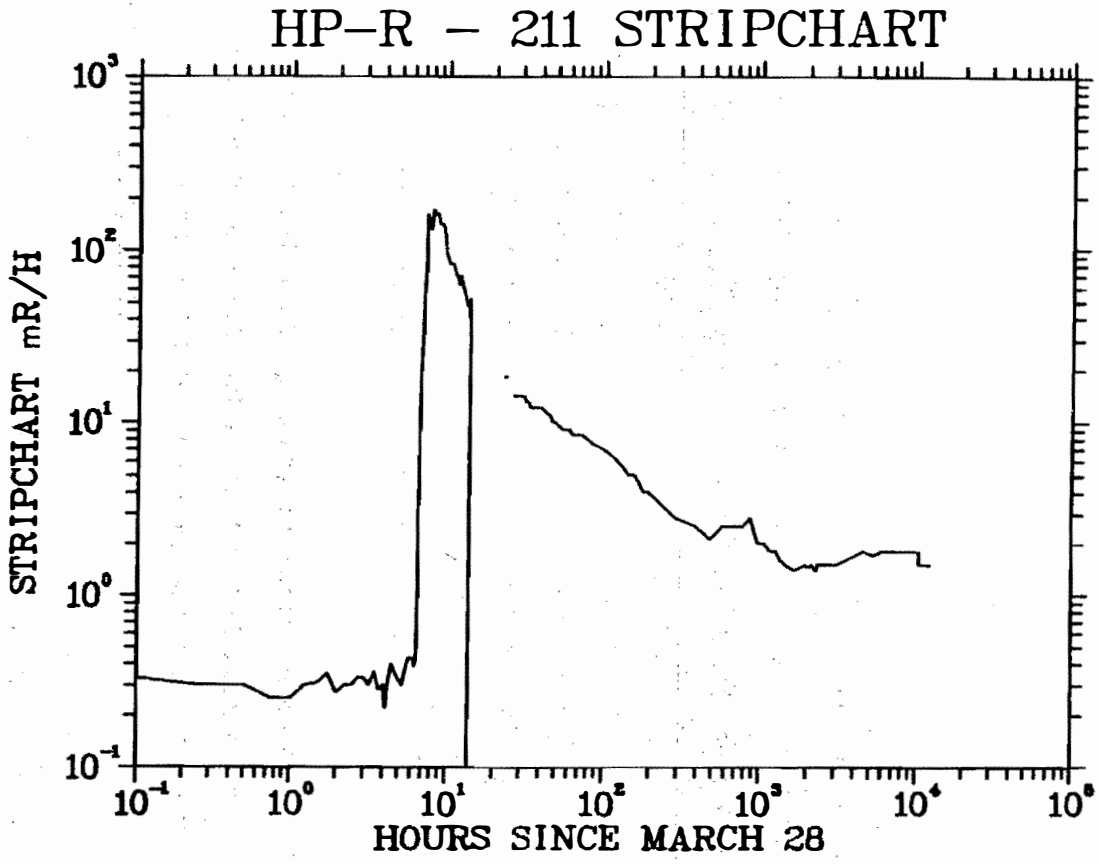

FIGURE 25a. HP-R-211 Composite Stripchart. All 506 days of stripchart and operator logs are shown. The detector output peaks at 170 mR/H at about 0800 on March 28, 1979. When removed on August 15, 1980, the detector registered only 1.5 mR/H.

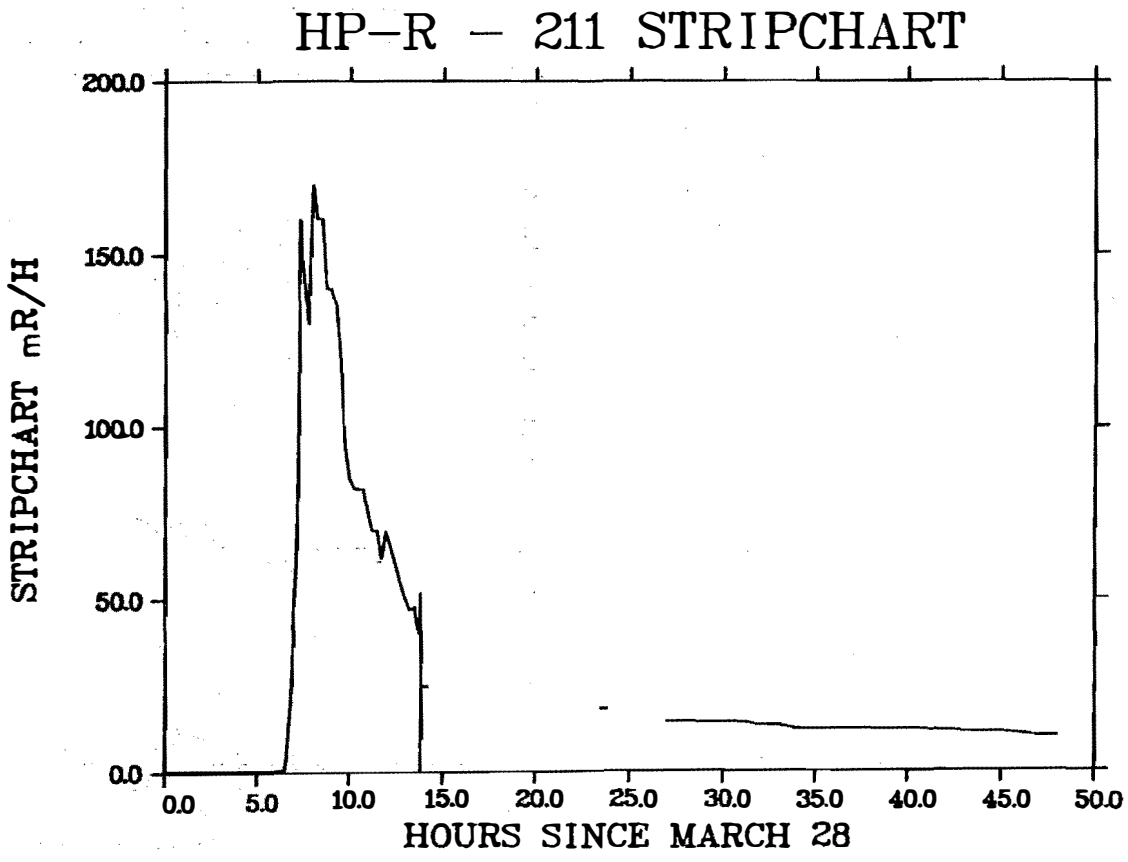

FIGURE 25b. HP-R-211 Short Term Stripchart. Only the first two days of the accident are shown on a linear scale. The ESF actuation occurred some 9 hours and 50 minutes into the accident (1350 hr). Several data points were taken just after this before the recorder printed in place. A few more points were taken at about 2400 hr.

Stripchart Notes

1. Channel 9 was occasionally labeled incorrectly on the stripchart. The recorder normally samples the signal and prints out a data point which is labeled with the channel number. In the case of HP-R-211, points obviously from the same channel are randomly labeled with 8s and 9s. This labeling has led to considerable confusion by investigators since the paper record is quite difficult to read and the presence of darker 8s has led some to the conclusion that HP-R-211, Channel 9, is not present on the stripchart. We have conclusively found that the channel labeled 8 and 9 is HP-R-211 by examining the stripchart three days before the accident when HP-R-211 was being calibrated with a Victoreen gamma source. The record clearly shows 8s and 9s being printed for the same channel (Appendix A). In addition, operator logbook readings correspond to the 8/9 channel.

2. The stripchart speed was 20.3 cm (8 in) per hour. We have examined the stripchart at various times and found the speed to be very close to this value.

3. The HP-R-211 channel was at least partially calibrated three days before the accident. The stripchart record shows that HP-R-211, HP-R-212, and HP-R-213 were calibrated at the 49 mR/H level before the accident. These stripchart data correspond to maintenance records (Appendix A) except for the two higher levels. Data taken by TEC, using a test detector in the anteroom, have been analyzed and indicate that the ratemeter gain was also approximately correct. The ratemeter is adjusted using the 49 mR/H source level.

4. The stripchart recorder calibration was checked before being taken out of service on May 30, 1980 (operator logbook data). It was found that the stripchart was accurate at that time, but that the ratemeter readout read 1.5 mR/H instead of 1.7 mR/H according to the stripchart.

5. The background reading of 0.3 mR/H, as read on the stripchart before the accident, is approximately correct. Measurements made in the vicinity of HP-R-211 by health physics personnel, with the reactor running at full power indicate that 0.3 mR/H is a reasonable reading (Appendix A). HP-R-211 was, therefore, apparently operating correctly at the time the accident began.

E. Radiation Time History

At the time HP-R-211 was removed from the containment building, it was registering a radiation level of 1.7 mR/H as shown in Figure 25a. Using the Co-60 source calibration from curve C of Figure 24, we see that this point corresponds to 740 mR/H. By using this same procedure for other data points, it should be possible to reconstruct the actual gamma radiation time history inside the containment building near the personnel hatch. Unfortunately, we have not been able to make such a reconstruction. Several factors have combined to make the analysis of the stripchart data baffling. The following discussion presents some of these difficulties.

The radiation levels measured by HP-R-211 during the time between fuel failure at approximately 0635 hours and the hydrogen burn at 1400 hours are orders of magnitude lower than we calculate them to be using radiation level measurements taken by GPU inside the anteroom. To attempt to explain this difference, we have examined the stripchart for discontinuities during that time period which would indicate the presence of a steam induced 600 Volt leakage path to ground or evidence that transistor Q6 had degraded. Although the signal is sampled and recorded only one time per minute, we have found no discontinuities in the data trace. To investigate the effects of a 600 Volt leakage path, we purposely introduced one in our Co-60 experiments and found that the GM tube either functioned with reasonable accuracy or, if the voltage was reduced below 380 Volts, failed to produce any output pulses. The absence of discontinuities and the evidence that the detector was functioning properly when the accident began both imply that transistor Q6 was not degraded. Another factor during this time period is that the stripchart does not show any long intervals of a flat or "saturated" response which should be present if the antijam

circuit were functioning. In our tests we found the antijam circuit to operate properly. Finally, we have not been able to use the detector multivalued characteristic to explain the magnitude and shape of the stripchart curve.

We cannot reconstruct the radiation history back to the time of the hydrogen burn even if we assume that transistor Q6 failed at that point. The Co-60 data of Figure 24 shows the maximum detector indication to be 4.7 mR/H with 152 m (500 ft) of cable attached. However, the stripchart indication after the burn is approximately 25 mR/H. We must conclude that either the transistor degraded further after the burn, even though no more stripchart discontinuities are present, or that the cable driving circuit was more efficient because of higher gain (less degraded) output transistors. In either case the reconstruction is somewhat imprecise. If we, nevertheless, perform this reconstruction back to April 17, 1979 where the recorded level was 5 mR/H, we find that the total integrated dose is approximately one order of magnitude lower than that estimated using transistor degradation data (see Section V). Thus, either the reconstruction is too low by an order of magnitude or, again, the stripchart indication before the hydrogen burn is orders of magnitude too low.

These inconsistencies may be resolvable after other detectors have been examined. Even now we can reconstruct a "most likely" time profile using multivalued characteristic, total dose and calibration information; however, it is premature at this time to do so. This will be done in another report.

INTENTIONALLY LEFT BLANK

V. TOTAL GAMMA DOSE

A. Summary

Equipment at TMI-2 was subjected to an actual LOCA in which large amounts of radioactive contaminants were spread around the building in varying amounts. Knowledge of the total radiation dose received by a given piece of equipment is important in understanding degradation or failure and thus evaluating the radiation hardness of the design. In short, the use of the accident at Three Mile Island as a test base for equipment survivability is of limited use if the environment is not known.

We used two indicators to determine the total gamma radiation dose received by the detector electronics: transistor gain and elastomeric material elongation. No attempt has been made to quantify beta deposition in the detector outer surface or signal cable. It is assumed that the majority of the dose received inside the aluminum case is due to gamma radiation having energies in the range of 0.5 to 3.0 MeV. Table 3 summarizes our findings.

TABLE 3. Total Gamma Radiation Dose Estimates

	TRANSISTOR GAIN[1] DEGRADATION	ELASTOMER[2]	
		TEFLON SLEEVE	BUNA NITRILE O-RING
NOMINAL RADS ($X10^5$)	2.5	2.0	10.0 [3]
ERROR BARS RADS ($X10^5$)	0.8 TO 5.1	0.7 TO 6.0 (EST.)	--

[1] Average of 6 transistors.

[2] Average of 2 teflon sleeves and 1 O-ring. O-ring included some beta dose.

[3] The O-ring appears to be very near its damage threshold of 10^6 rads.

By using the transistor data, we estimate the nominal radiation dose received by the detector electronics to be 2.5×10^5 rads. The transistor data are believed to be the most accurate, since substantial degradation did occur, and because more samples were tested. The teflon sleeving had reached a dose-level threshold where noticeable degradation had occurred; however, since only two samples of unknown pedigree were available for test, the uncertainty is larger. Although the O-ring had barely begun to degrade thereby increasing the uncertainty, the dose was almost certainly below 10^7 rads. We have not used integrated stripchart data to estimate total dose, because as described in the previous section, the stripchart data for the first day or two of the accident are not fully understood.

Although a total gamma dose of 2.5×10^5 rads is higher than the design requirement of 2×10^4 rads for most equipment at TMI-2, it is below levels required today for most new reactor equipment.

It should be understood that the use of transistor and electronic material degradation can only provide rough estimates of radiation dose. Base material parameters, processing characteristics and short and long term annealing all introduce uncertainties which are difficult to quantify. We have considered these uncertainties and present the values in Table 3 as reasonable estimates.

B. Transistor Degradation

Damage Mechanism

The permanent damage produced in semiconductors by gamma rays is of the same type as that produced by electron bombardment.[11,12] Transistor parameter changes are a result of two effects: bulk silicon damage and inducement of surface states.

For bulk silicon damage, orbital electrons are excited and scattered by energetic gamma photons, and these electrons may transfer

sufficient energy to lattice atom nuclei to displace them. This creates vacancies in the crystalline structure called Frenkel defects. For gamma radiation these are simple defects in that the amount of damage induced by a single gamma photon is limited to at most a few atoms. Much of the same is true for neutron irradiation, except that the energy transfer is orders of magnitude larger, and large defect clusters can be created. The effect of these point defects is to change carrier mobility, conductivity and lifetime.

The transistor parameters most affected are current gain and saturation voltage. Transistor gains decrease and saturation voltages increase as the dose is increased. For low-power, high gain bipolar transistors, bulk damage generally begins to become noticeable at exposure levels of greater than 10^6 rads.

Surface state phenomena primarily affect the current gain of bipolar, planar geometry transistors. Although the physics of surface states is not well understood[11,13], at least two mechanisms have been identified[19] which cause a reduction in current gain after irradiation. Gamma irradiation creates hole-electron pairs in the surface SiO_2 passivation or diffusion masks. The more mobile electrons are easily swept out of this insulating layer, leaving behind trapped positive charge in the low conductivity oxide. This positive charge, if near the SiO_2 - Si interface, may cause a depletion or inversion layer to form on the silicon surface underneath. Where this occurs over the base-to-emitter junction region, a decrease base current efficiency results. In addition, irradiation also creates new interface defects in the oxide near the SiO_2 - Si interface. This alters the surface recombination velocity. It has been observed[19] that the effects of surface states "saturate" for high dose levels. Below approximately 10^6 or 10^7 rads the gain degradation is thought to be primarily due to the formation of surface states.

Data and Interpretation

Six bipolar transistors were removed from HP-R-211 for the purpose of determining the radiation total dose. These transistors were completely characterized at room temperature with respect to parameters such as gain (HFE), leakage currents (ICBO, ICEO, IEBO), and saturation voltages (VCES, VBES).[14] Transistors, 87 in all, were procured from Fairchild (FSC), National (NAT), Texas Instruments (TI), and General Electric (GE) and exposed to a Co 60 gamma source for the purpose of comparing degradation in these devices to that in the HP-R-211 transistors. These transistors were passively exposed by Asselmeier in 7 steps until a total accumulated dose of 3×10^6 rads was achieved. The transistor parameters mentioned above were measured after each step. An examination of the change in parameters versus dose has shown the transistor current gain to be by far the most affected parameter. Saturation voltages were changed to a much lesser degree.

Appendix B contains plots of transistor gain degradation vs total dose for all the transistors tested. One of these plots is shown in Figure 26. These particular devices were National 2N 3904s. Ten units were tested, the average gain being the center curve. The maximum device had a gain characteristic corresponding to the upper curve, the minimum device the lower curve. Transistor Q7 from HP-R-211 was a Fairchild 2N 3904, and at a collector current of 100 μA had a gain of 61. This corresponds to a nominal total dose estimate of 1.6×10^5 rads (uncorrected for bias and annealing). This method was used to determine the radiation total dose absorbed by each transistor. Table 4 summarizes our dose estimates using this method (these estimates must still be modified to include bias and annealing effects). The results shown were obtained by simply weighting each transistor type equally and taking the statistical average. When curve matching was employed, where some transistor data were more heavily weighted, the result was almost the same as the statistical average.

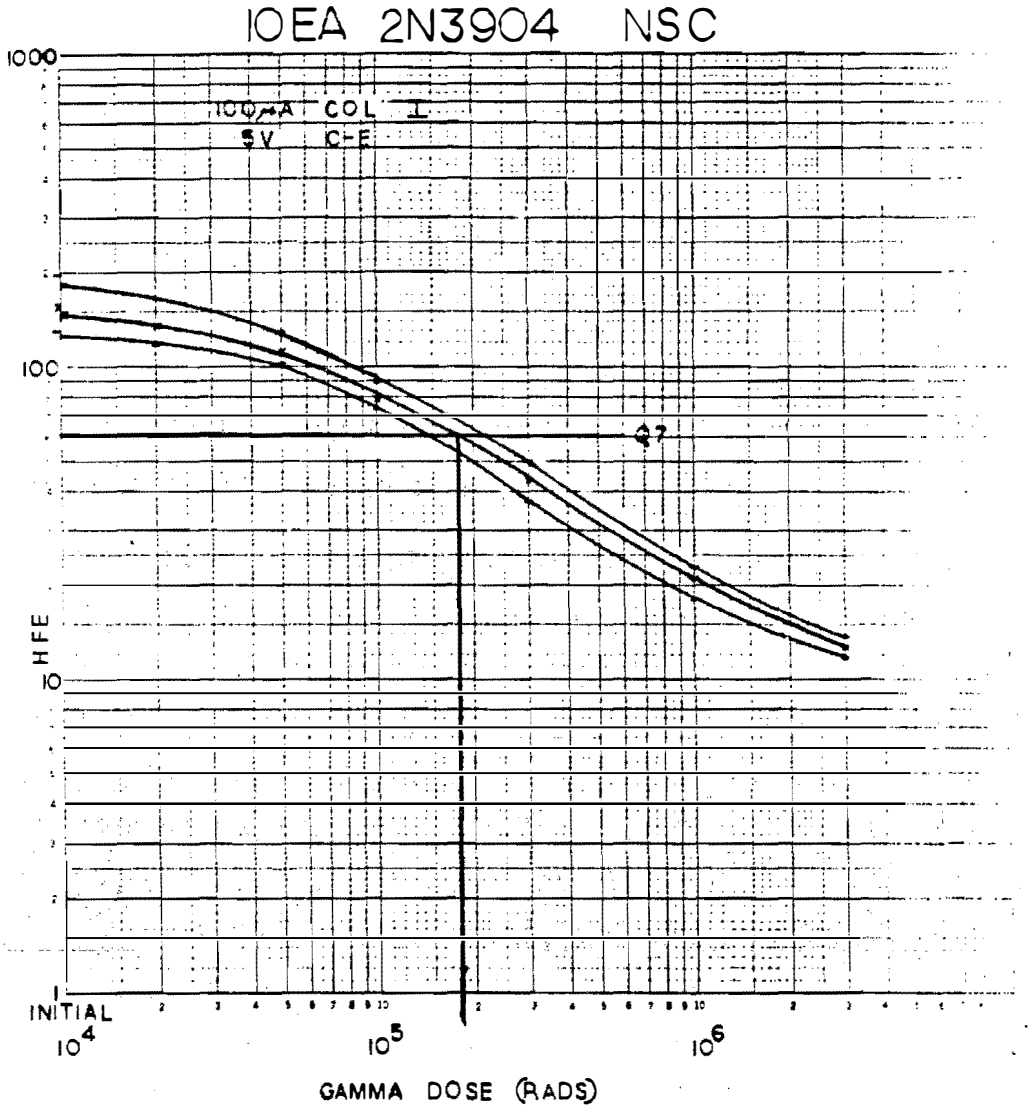

FIGURE 26. Transistor Gain Degradation. The measured gain of transistor Q7 was 61 at a collector current of 100 μa. This corresponds to a nominal gamma dose of 1.6×10^5 rads using National Semiconductor 2N 3904 data.

Table 4. Transistor Total Dose

TRANSISTOR TYPE[1]	HFE RANGE[2] (RADS) MIN	AVE	MAX	CURVE MATCH[3] I_C	V_{CES}
2N 3565 ... Q3 FSC (HFE=200)[4]					
FSC (10 ea)	1E4	3.8E4	1.1E5	P	G
NAT (10 ea)	1E4	4 E4	1.5E5	F	G
AVE	1E4	3.9E4	1.3E5		
2N 3904 ... Q7 FSC (HFE=61)					
FSC (10 ea)	3.2E4	6.5E4	9.5E4	E	F
NAT (10 ea)	1.5E5	1.8E5	2.2E5	E	E
AVE	9.1E4	1.2E5	1.6E5		
2N 3906 ... Q2 MOT (HFE=86)					
FSC (5 ea)	3.8E4	5E4	1.2E5	E	E
NAT (10 ea)	1.4E5	7E5	1.6E6	E	G
TI (10 ea)	6.5E4	1.1E5	2E5	G	E
AVE	8.1E4	2.9E5	6.4E5		
2N 3903 ... Q1 (HFE=35.5), Q4 (HFE=20), Q5(HFE=38) (HFE AVE=31), ALL FSC					
FSC (2 ea)	7E4	1.5E5	3.6E5	E	E
GE (10 ea)	1.5E5	2.5E5	4E5	G	G
NAT (10 ea)	1.5E5	2.5E5	4E5	F	E
AVE	1.2E5	2.2E5	4E5		
OVERALL AVERAGE[5]	.75E5	1.7E5	3.2E5		

NOTES:

1. The manufacturer and number of devices tested are shown. Fairchild (FSC), National (NAT), Texas Instruments (TI), General Electric (GE), Motorola (MOT).

2. The range in rads is determined by the intersection of the HP-R-211 transistor gain with the minimum, average and maximum gain vs dose plot. All data is for Ic = 100 μA. Exponential notation is used.

3. Curve match refers to the general shapes of the current gain vs collector current and saturation voltage vs collector current characteristics of HP-R-211 and the dosimetry devices. The subjective designators refer to how similar the dosimetry device characteristics were to the HP-R-211 characteristics:
E = exclient, G = good, F = fair, P = poor

4. The HP-R-211 transistor designators are listed, along with manufacturer and measured gain at 100 μA.

5. This is the "average of averages"; i.e., all transistor types were weighted equally.

The dose estimates given in Table 4 must be modified to account for transistor annealing and the fact that the Sandia transistors were unbiased during exposure. Transistor gain annealing is characterized by an initial, rapid partial recovery which is essentially complete after the first 1000 hours following irradiation[20]. Further recovery at room temperature is, for practical purposes, not accomplished. This has been confirmed by us by measuring the TMI transistor gains in November 1980 and again in July 1981. These data are presented in Appendix B, and they show the gains to be essentially unchanged at the end of this 8 month period. The transistors characterized by us, however, were practically unannealed at the time of measurement since generally, the gains were measured during the first hour or two after exposure. To determine the amount of annealing recovery, we measured the gains of these transistors in July 1981 to compare with the November 1980 gains. These data are also in Appendix B. Substantial annealing has occurred. By plotting these annealed points on the gain vs dose curves and shifting the degradation curves upwards proportionately, we find that the total dose estimates of Table 4 must be multiplied by an average annealing correction factor of 1.6.

The literature[21] suggests that gamma irradiation of NPN transistors under reverse collector-to-base bias results in substantially more damage than if they are irradiated passively. Conversely for PNP transistors passive irradiation is more damaging. To check the effects of bias Asselmeier exposed 6 NPN transistors to 1.5×10^5 rads under three conditions. One group of two devices was passively exposed, one group was exposed while saturated with 1 mA of collector current, and one group was exposed with a 10 volt collector-to-base reverse voltage. He found that the post radiation gains of the reverse-biased devices were perhaps 30% lower than those of the passive and saturated devices. The TMI transistors generally were switching between cutoff and satura-

tion at a 50% duty cycle; therefore, the effects of bias are diminished. Powered and unpowered tests reported[21] on 2N 1613 (NPN), 2N 2102 (NPN) and 2N 3799 (PNP) transistors suggest that the dose estimates of the NPN transistors should be divided by a correction factor of 3.0 assuming a 50% duty cycle, while the PNP estimates should be multiplied by 1.7.

When these annealing and bias factors are combined with the values in Table 4, our total dose estimates become 0.85×10^4, 2.5×10^5 and 5.1×10^5 rads for the lower, nominal and upper values.

Caveats

Although we feel somewhat confident about the dose estimate, several points should be made regarding this method of dosimetry.

1. Manufacturer. It was not possible for us to obtain transistors from the same lots of transistors as those used in HP-R-211. For that matter, in the time allowed to procure transistors, we were not even able to obtain devices, in some cases, from the correct manufacturer. We choose to minimize these points, however, because of the inherent variability in transistor characteristics regardless of manufacturer. Statistical averages become more important than the manufacturer.

2. Current level. The collector current level of 100 μA selected for comparison was not at the HFE peak point; however, several comparisons were made at the HFE peak point, and the results were similar.

3. Energy dependence. The majority of the gamma emission occurs in the range of 0.5 to 3.0 MeV. Since transistor parameters are affected primarily by the total energy deposited as measured in rads, the energy spectrum of the source has a negligible effect (except for very low energies). Therefore, in this allowed region, the Co-60 source (1.25 MeV) is an excellent simulator.

4. Bias. Transistor gains begin to drop off significantly at relatively low radiation levels. This, and the fact that saturation resistance is relatively unaffected, indicate that surface states are responsible for the majority of the damage. Bias effects therefore must be considered. As stated, we have very little data regarding what correction factors should be used. The 50% duty factor introduces another variable. The bias correction factors of 3 and 1.7 are only estimates. They are, however, in line with our limited test data and test data of others.

5. Annealing. Annealing has occurred in both the TMI transistors and transistors characterized by us. We have assumed that the effects of annealing can be linearly extrapolated to lower doses from the dose of 3×10^6 rads where annealing changes were measured. We have assumed that essentially all annealing occurs during the first 1000 hours, but that none occurred during the 1 to 3 hours between measurement and test. The annealing correction factor of 1.6 is an average applied to all transistor types equally.

C. Elastomeric Degradation

A polymer is a highly ordered chain of molecules with very little degree for freedom of atoms. Radiation acts to destroy these molecular bonds. This has the effect of altering electrical insulating properties, weight (because of outgassing), and strength. By measuring the tensile strength and elongation at the time of rupture and comparing with properties of unirradiated material, we can estimate the total gamma radiation dose received.

Teflon and BUNA-N rubber were analyzed for degradation. The teflon samples were used as wire insulators on the check source assembly, which is mounted on the printed wiring board. These two 30 gage teflon sleeves were 38 mm long and had 0.292 mm and 0.229 mm ID and nominal wall thickness respectively. The type of teflon was not determined (FEP or PTFE); however, the difference in post-irradiation properties is small. The other material was the detector lid O-ring. We determined through gas chromotography on an O-ring from a new detector that the material was BUNA-N (Nitrile) rubber. This was independently confirmed with Victoreen. The results of data taken on an Instron Model 1020 tensile testing machine are listed in Table 5. In each case new, unirradiated samples from a new detector were compared with those from HP-R-211.

Table 5. Elastomeric Degradation

	HP-R-211		NEW DETECTOR	
	ELONGATION	FORCE AT BREAK	ELONGATION	FORCE AT BREAK
TEFLON SLEEVES				
Sample 1	80%	28.0N (6.3 Lb)	310%	40.0N (9.0 Lb)
Sample 2	75%	28.5N (6.4 Lb)	340%	36.5N (8.2 Lb)
Avg.	78%	28.5N (6.4 Lb)	325%	38.3N (8.6 Lb)
O-RINGS (BUNA-N)				
Sample 1	245%	32.5N (7.3 Lb)	245%	45.4N (10.2 Lb)
Sample 2	290%	36.5N (8.2 Lb)	205%	38.3N (8.6 Lb)
Sample 3	310%	37.4N (8.4 Lb)	205%	41.4N (9.3 Lb)
Avg.	281%	35.6N (8.0 Lb)	218%	41.8N (9.4 Lb)

These data show that neither the teflon or the O-ring experienced much degradation. In fact, the elongation properties for the irradiated O-ring are better than those of a new sample. This is easily explained because of lot to lot variations in material. Teflon data is sparse because it is not widely used in radiation environments, since it undergoes property changes sooner than other polymers. We were fortunate, however, that the teflon was used in this case, because radiation levels were just above the damage threshold. Based on information from Etherington's Nuclear Engineering Handbook and CERN - European Organization for Nuclear Research's Selection Guide to Organic Materials for Nuclear Engineering - 1972, the absorbed dose was nominally 2×10^5 rads. We estimate the dose to lie between 0.7 and 6.0×10^5 rads. The O-ring appears to be near its damage threshold of 10^6 rads. Substantial degradation should have been observed had the dose been as high as 10^7 rads.

INTENTIONALLY LEFT BLANK

VI. CONTAMINATION

A. Summary

As part of the overall investigation of the instrument, we made an effort to identify the contaminants on the detector housing and measure their concentrations. Since an electronic failure had occurred inside, we were also concerned about preserving any of the contaminating elements that may have leaked inside and caused the failure. Table 6 summarizes the results of the investigation. Our major findings were:

1. Cesium-134 and 137 and strontium 90 were the principal contaminants. No plutonium or uranium were detected.
2. Top horizontal surfaces contained a factor of 10 more cesium than the sides and bottom.
3. Reported swipe surveys in the containment building are over a factor of 10 lower than the activity on the detector.
4. Swipe surveys in the reactor building see about the same factor of 10 difference between horizontal and vertical surfaces.
5. No contamination or signs of moisture were found inside the detector housing, indicating that the seals held.
6. The cesium-137 activity on receipt at Sandia was about 125 μCi for 128 cm^2 for the lid and about 73 μCi for 709 cm^2 for the body.
7. The ratio of cesium-137/134 was about 6.3/1 during the months of November and December, 1980.
8. Large quantities of sodium and boron were found on the detector lid, indicating the unit had been exposed to the building spray.

The approach[16] used to identify contaminants simply stated was:

A. Get the unit to Sandia packaged in such a way as to prevent surface contamination from changing location.

B. Evaluate the innermost plastic bag that contained the unit during shipment for any material that may have fallen off or rubbed off.

C. Determine if the contamination levels and types occur as hotspots or are evenly distributed on the top, bottom, and sides.

D. Conduct a complete evaluation of the outside before opening the unit.

E. Remove a sample of the inside environment before opening the lid in the event a gas was still present from the building overpressurization.

F. Determine if any containment building spray chemicals had reached the detector.

G. Archive the detector lid in a condition where it is close to its in situ condition.

TABLE 6.

RADIOACTIVE ANALYSIS HP-R-211 AREA MONITOR HOUSING

CONDITION	AREA	CS-137 TOTAL	CS-137 PER AREA	CS-134 Δ TOTAL	CS-134 Δ PER AREA	OTHER TOTAL	OTHER ISOTOPE
	cm^2	µCi	µCi/cm^2	µCi	µCi/cm^2	µCi	
AS RECEIVED							
LID (w/o label, ring, 1 in^2 of Paint)	128.3	~86.0	0.670				
* VICTOREEN ALUM. LABEL	11.89	28.8	2.422				
* CONNECTOR THREADED RING	65.85	4.46	0.068	0.567	.0086	0.11 Not Det. <0.002 Not Det. (<10 ppm)	Sr-90 Tellurium Plutonium Uranium
PAINT REMOVED (est.)	6.45	5.67	0.879				
TOTAL LID	128.3	~124.9	0.973				
BODY (est.)	708.5	65 to 75	0.099 ave				
PLASTIC ID LABEL (est.)	15.94	1.64	0.103				
PAINT REMOVED (est.)	12.91	1.28	0.099				
TOTAL BODY	708.5	68 to 78	0.103 ave				
TOTAL LID & BODY	836.8	193 to 203					
AFTER HANDLING FOR FILM & CIRCUIT WORK							
LID (with label, Ring, etc.)	128.3	118.2	0.921				
BODY (with labels & no paint removed)	708.5	42.2	0.060				
BEFORE DECON (w/o labels, etc.)							
LID	128.3	79.3	0.618				
BODY	708.5	39.3	0.055				

Δ Ratio Cesium 137/134 = 6.3/1 (range 5.8 to 6.8) except on connector ring.

* Evaluated by Los Alamos National Lab - CMB-1

B. Shipment to Sandia

A major concern was that of transporting the unit from TMI to Sandia. We felt that rough handling could alter the state of the circuits and devices inside as well as tend to redistribute or remove the contaminants. The unit was packed as shown in Figures 27 and 28. A wood cage was fabricated to hold the detector inside to prevent its rubbing the cage. This was accomplished by using standoff screws that were modified to remove the sharp points. Where the screws contacted the unit outer bag, tape was applied. Nine screws contacted the sides, and three each were used on the bottom and top. The bottom cover had five shock indicators attached. They were threshold accelerometers that trip when the threshold has been exceeded. We attached 40g, 60g, 80g, 100g and 150g indicators. (A 50g indicator attached to the inner box of a double-boxed 27.2 kg [60 lb.] piece of equipment with hard foam corners for its inner carton support, will be tripped when the total package is dropped from a height of 45.7 cm [18 inches] onto a concrete floor.) At the time the unit was packaged it was thought that lead would be used around the inner box. The entire structure was put in plastic bags and then into a cardboard box padded with paper towels and "popcorn" packing material. The cardboard box was put in a 55-gallon drum and insulated with more "popcorn" and styrofoam. However, no lead shielding was used. On removal at Sandia none of the shock indicators had tripped and no detectable contamination had breached the innermost plastic bag.

C. Inner Bag Evaluation

Another indication of the influence that the transfer had on the unit was the innermost plastic bag contamination levels. The bag was evaluated for gamma radiation using gamma spectroscopy. The principle contaminates were cesium-134 and cesium-137, which totaled 0.67 and 4.0

FIGURE 27. Detector Shipping Cage. The wooden cage was used to transport 211 from TMI to Sandia. It reduced the redistribution of the contamination.

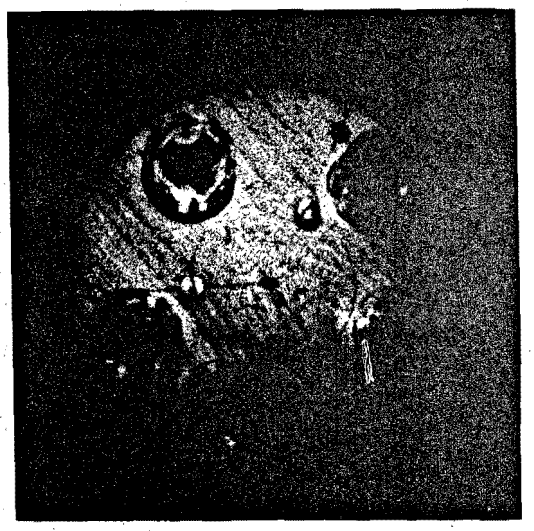

FIGURE 28. Shipping Shock Indicators. Five shock indicators were attached to observe whether there were shipping and handling abuses.

microcuries respectively. This represented about 1 percent of the total activity that was remaining on the detector.

D. Contamination Hotspot Identification

Before proceeding with the gamma spectrum analysis and the electrical investigation, film exposures were conducted on the entire detector housing. The purpose of conducting the exposures was to determine whether the activity was from uniform plateout or whether the contaminants puddled and dried. The film indicates the latter case took place. There were no efforts made to quantify these hotspot differences through photodensitometer measurements. The pictures in Figures 29 and 30 illustrate these variations. The negative with the hole in the center is that of the lid while the other is that of the bottom. Figure 30 illustrates how the film was placed. Type M film was used on the lid and "AA" on the bottom. Type M film is four times slower than "AA" film; and, consequently, the dark spots, although they may appear to be from about equal source activities, indicate at least four times more activity on the lid. The lid picture (Figure 29) illustrates that the activity in the region of the aluminum Victoreen label is higher. Pictures of the sides and bottom illustrated that the activity was mostly uniform. There were spots on the bottom that indicate water may have run down the sides and formed a drip release point. As it dried it became a point for concentrating radioactive isotopes. For all film work, the detector was wrapped in a single poly bag. This prevented contaminating the film. The bag was 0.00445 cm (0.00175 inch) thick and represented a beta particle "range" of 4.8 mg/cm^2 (Figure 31). All film used was Kodak types AA, M, and single coated R with 0.0267 cm (0.0105 inch) of orange paper with a black poly coating sandwiching the film. The black poly coating was about 0.00635 cm (0.0025 inch) thick and represented a beta particle "range" of 7.1 mg/cm^2. Dark spots on the film were primarily from beta exposure. To demonstrate the contribution from gamma, a set of exposures were made using 0.159 cm

FIGURE 29. Film Negative of Detector Lid.
Illustration of the variation in beta activity.
Dark area was over the Victoreen label and light
rectangular area was a position tag.

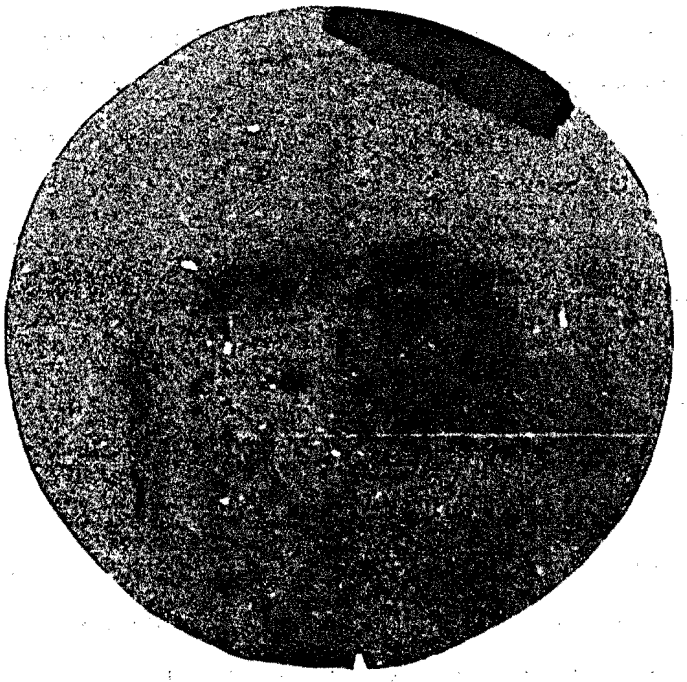

FIGURE 30. Film Negative of Detector Bottom.
The dark spots identify areas where contaminated
liquids probably concentrated and dried.

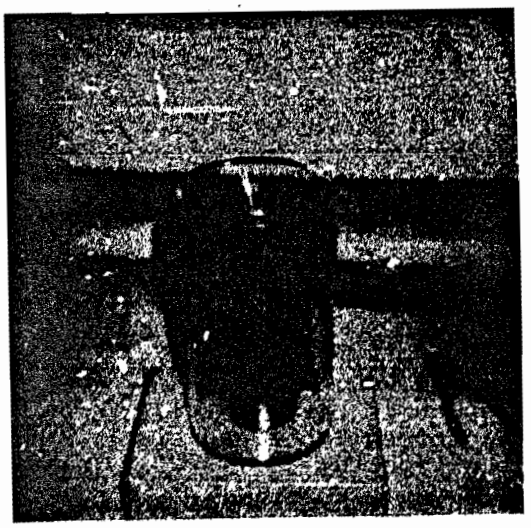

FIGURE 31. Film Located on Detector. Typical arrangement of film location on top.

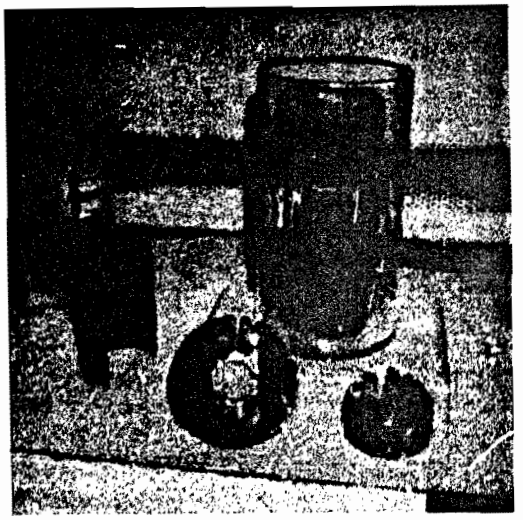

FIGURE 32. Lead Shield for Beta and Gamma Discrimination. Lead, 0.159 cm (1/16 inch) thick, was used to determine whether hotspots were beta or gamma radiation.

(1/16 inch) of lead between the detector and film (Figure 32). Film exposure fogging (background) was about the same with or without lead when using the same type films and exposure times. There were no noticeable shaded areas. This indicates that the film "hot spots" were primarily caused from beta radiation.

It was evident from the film work that horizontal surfaces (the lid, the mounting bracket ledges that were facing up during the accident, and the gussets between the mounting bracket legs) were the chief contributors. These ledges served to trap the contaminated liquids that later dried and plated out. Close observation of the original film negatives showed that in the areas where the plastic bags had several folds the increased thickness was enough to further attenuate the beta particles.

E. Contamination Levels and Type Identification

After completing two sets of film exposures, we examined the detector to determine the gamma emitting isotopes and their concentrations. The detector housing was studied at Sandia Laboratories using a gamma spectrometer, while radiochemical analyses of an aluminum label and connector were made at Los Alamos National Laboratories. Table 6 summarizes our findings.

Using a solid-state Ge (Li) detector to survey the housing, we were able to detect only cesium-134 and cesium-137 isotopes. To quantify the activity levels the detector was rotated through six different positions (top, bottom, and four side positions 90 degrees apart and measurements were made at each position. The physical size of the detector also introduced some geometry problems in counting. The uncertainties in counting shown in Table 6 are a result of some shielding by the apparatus that supported the unit above the detector. The labels, a 6.4 cm^2 square of paint, and the connector shell were removed before determining that this problem existed. We have,

nevertheless, been able to determine within some limits the original activity on the unit.

In order to expedite our effort, the labels on the detector were removed along with the mating connector pieces at the top. These were sent to Los Alamos for analysis. Figure 33 shows the detector with the labels removed. The top label was an aluminum Victoreen label held in place by an adhesive. The side label was a plastic TMI identification label held in place by two screws. Figure 34 shows the major items removed. The analysis of the Victoreen label supported the film work results. Its cesium activity was about three times higher than the rest of the lid. A reason for this may be that some of the contaminants were held in the adhesive beneath the label. The hand probe measurements verify this to some extent. The connector ring was the hottest gamma-emitting item sent to Los Alamos (7 mR/hr vs 3.6 mR/hr for the Victoreen label), but it had a much lower cesium activity than the label (4.46 vs 28.8 μCi). Costs limited identification of all the isotopes present, but for our purposes in determining an approximate total activity, cesium-134 and 137, as well as strontium 90 were found as the principle contaminants. No plutonium or uranium were detected.

Perhaps the most significant findings were the relationship between horizontal and vertical surfaces. The lid had a cesium activity a factor of 10 higher than the sides per unit area. The top had a esium-137 activity of 0.973 $\mu Ci/cm^2$ vs 0.103 $\mu Ci/cm^2$ on the sides. Table 7 gives the published results[17] of swipes in the area where HP-R-211 was located for comparison.

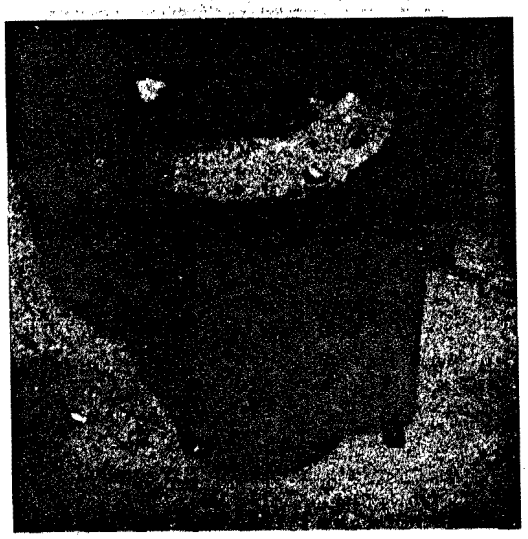

FIGURE 33. Detector with Labels Removed.
A picture of the detector showing how the labels were attached and the overall condition of the detector.

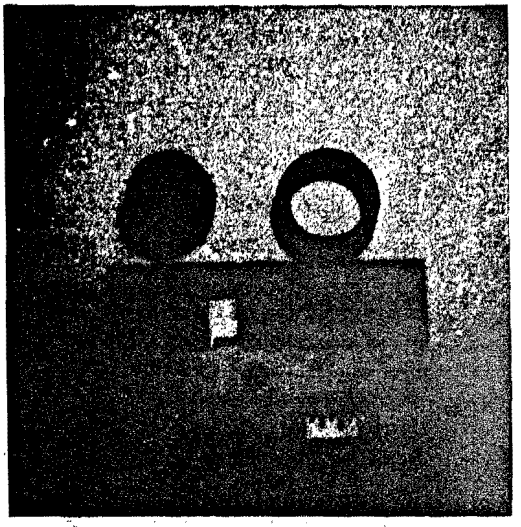

FIGURE 34. Labels and Connector Parts.
Parts that were removed for isotope and chemical contaminant evaluation.

TABLE 7

Results of Swipes, HP-R-211 and Surroundings

	Sr-90 ($\mu Ci/cm^2$)	Cs-134 ($\mu Ci/cm^2$)	Cs-137 ($\mu Ci/cm^2$)
JULY 23, 1980 ENTRY			
Floor in front of HP-211		0.030	0.100
Wall by HP-211		1.5×10^{-5}	9.8×10^{-5}
AUGUST 15, 1980 ENTRY			
Floor under HP-211		0.066	0.407
Swipe of HP-211 itself	3.1×10^{-5}	2.2×10^{-4}	1.6×10^{-3}

These values indicate that the swipe surveys are low by over a factor of 10. This is to be expected because of the difficulty we had in decontaminating the unit. These swipe surveys and others also reflect the ratio of 10:1 or higher between vertical and horizontal surfaces.

F. Internal Sampling and Findings

Following the initial evaluation of the unit exterior and the electronic investigation and calibration, the detector was prepared for opening. A 3.81 cm (1.5 in.), 18 gage syringe was inserted through the rubber in the connector to remove a sample of contaminants that may have leaked into the unit when the containment building underwent its pressure excursion(s). Figure 35 shows the operation. There was no internal pressure, as it would have been apparent with the ejection of the syringe plunger. Likewise, there was no obvious vacuum because the syringe withdrew with no undue force. Three gas samples were removed in this manner and immediately inserted in 10 cc serum-separator tubes. No measureable levels of radiation were detectable through the glass serum tubes (< 0.01 mR/hr). The screws were then removed from the lid and the unit opened. Swipes were immediately taken on the circuit board and the housing interior walls. Beta radiation levels were slightly above background and considered to be from the opening operation. An inspection of the circuit board and interiors showed no sign of moisture, rust,

FIGURE 35. Internal Detector Sample Removal. Actual photograph of the first sample being removed from inside the detector prior to removing the lid.

oxidation, or mildew. We did have a problem in separating the lid from the unit body. A crust had formed almost all the way around in the region of the O-ring seal. The O-ring was highly contaminated.

G. Non-radioactive Analysis

In the process of developing a scenario for the radiation time history plot, it became obvious that during the time period the containment building sprays came on, all the radiation monitors in the building reacted. The reaction could have been caused by the high temperature or the building pressure that preceded the spray. However, because all detectors (located in different areas and floor levels) reacted at the same time it is not very probable that the drastic upturns followed by some failures were caused by temperature, since the hydrogen burn did not evidence itself throughout the building. The highest temperature was at the 353 foot level and was approximately 85^{o}C (185^{o}F). Building pressure did not affect the 211 detector as described above since no contamination was found inside the unit. To determine for sure whether the detector had been sprayed, analyses were run to determine if there were any traces of sodium or boron. Scanning electron microscopy (SEM), energy dispersive spectroscopy (EDS), and X-ray diffraction (XRD) analyses were done at Sandia on the electrical connector. Because of the predominance of other elements, neither sodium nor boron could be found, however, the presence of calcium indicated that hard water had contacted the connector. The aluminum Victoreen label, which had been removed from the detector lid and sent to Los Alamos along with other items, was analyzed for sodium and boron. This was done by leaching a sample with purified water and chemically analyzing the results. This proved conclusively that the detector had been sprayed. The results are shown in Table 8.

Table 8

Aluminum Victoreen Label Analysis

NaOH	1.25 microgram
Na_2S_3ON	$\leq$ 1 microgram
Boron	0.25 milligram
Sodium	1.56 milligrams
Cs-137	28.8 microcuries

Appendix C contains the complete documentation concerning these analyses.

H. Archiving

As part of our original objectives, we determined that some items should be archived in the event that some questions may arise regarding activity, decontamination, etc. The entire detector lid, less its aluminum Victoreen label and one square inch of paint, were stored. None of the paint scrapings, connector parts, the internal atmosphere samples, or the plastic label plate from the detector body side have been analyzed. Lack of funds and time have prevented these analyses as well as a complete investigation of the films exposed to characterize the hotspots.

INTENTIONALLY LEFT BLANK

VII. DECONTAMINATION

All the decontamination (decon) work was done on the detector body. As previously stated, the lid was preserved for future information. The information that exists at this time indicates that the contamination and consequent radiation levels prevent sending teams of people in to scrub and wipe down the building and its equipment. Our approach, therefore, was to analyze decon methods by simply applying a solution, rinsing it, and determining its effectiveness. There are some limitations that must be applied to properly interpret the results. Some results are tabulated as "percent decrease"; this is a comparison to the previous activity and not to the starting activity. The more contamination that is removed the harder it gets to remove the remainder. Because of this, a heavier weight should be applied to the methods used at the end. This is the first painted item that was removed from containment and represented the most relevant surface to decontaminate. It has a gray paint on a rough cast aluminum surface.

Table 9 summarizes the efficiencies of the various decon steps. Handling was considered to be the first step. It is significant that about 44 percent was lost through the handling required to conduct the film exposures and to make electronic measurements. Throughout these exercises care was taken to reduce rubbing, but a significant quantity came off easily.

Five different decontamination methods/steps were performed and, in four out of the five steps, it was a liquid lightly sprayed onto the detector body. A 500 mL squirt (wash) bottle was used to apply the solutions and to rinse them off in the manner shown in Figure 36. The nozzle pressure was controlled by hand squeezing and was limited to

TABLE 9
DECONTAMINATION
HP-R-211 AREA MONITOR

NOTES: (1) Decontamination was conducted only on the detector body.
(2) Approach: No scrubbing, low velocity spraying only.
(3) Ratio of Cs-137 to Cs-134 was about 6.3/1 in Oct. thru Dec. 1980.
(4) Calculated, based on relative position measurements

	DECONTAMINATION STEP						
	AS RECEIVED	(BEFORE DECON) HANDLING	WATER SPRAY	DETERGENT SPRAY	LOW PRESS STEAM	TURCO 4512A 1/2 HR. SOAK	TURCO 4512A 1 HR SOAK
GAMMA SPEC. ANALYSIS							
Activity (4) (Cs-137) µC: measured / calcul.	No Data / ~70	No Data / 39.3	No Data / 33.6	25.3 / 30.1	14.7 / 18.9	No Data	No Data / 10.1
Percent Decrease per Step		~44	14.5	10.5	37.3	No Data	46.2 Total
Accum. Reduction-Percent		-	14.5	23.4	52.0	No Data	74.2 Total
Wash & Rinse Solution Act. (Cs-137 µCi)		-	3.63	2.69	-	-	-
BETA - GAMMA PROBE							
mRad/hr After Decon Step (Avg)							
Beta		20.5	17.1	16.4	9.6	5.6	4.4
Gamma		3.3	2.8	2.5	1.5	0.98	0.76
Ratio (Beta to Gamma)		6.2	6.1	6.6	6.4	5.7	5.8
mRad/hr After Decon Step (hotspot)							
Beta		98.2	80.0	71.0	46.2	26.4	15.7
Gamma		7.9	6.6	5.9	3.4	2.2	1.5
Ratio (Beta to Gamma)		12.4	12.1	12.0	13.6	12.0	10.5
Percent Decrease per Step							
Beta/Gamma (Avg)		-	17/15	4/11	41/40	42/35	21/22
Beta/Gamma (hotspot)		-	19/16	11/11	35/42	43/35	41/32
Accum. Reduction-Percent							
Beta/Gamma (Avg)		0/0	17/15	20/24	53/55	73/70	79/77
Beta/Gamma (hotspot)		0/0	19/16	28/25	53/57	73/72	84/81
Peak to Avg Ratio							
Beta/Gamma		4.8/2.4	4.7/2.4	4.3/2.4	4.8/2.3	4.7/2.2	3.6/2.0
LID mRad/hr-(no label)- Avg							
Beta/Gamma		254/19					

VII. DECONTAMINATION

All the decontamination (decon) work was done on the detector body. As previously stated, the lid was preserved for future information. The information that exists at this time indicates that the contamination and consequent radiation levels prevent sending teams of people in to scrub and wipe down the building and its equipment. Our approach, therefore, was to analyze decon methods by simply applying a solution, rinsing it, and determining its effectiveness. There are some limitations that must be applied to properly interpret the results. Some results are tabulated as "percent decrease"; this is a comparison to the previous activity and not to the starting activity. The more contamination that is removed the harder it gets to remove the remainder. Because of this, a heavier weight should be applied to the methods used at the end. This is the first painted item that was removed from containment and represented the most relevant surface to decontaminate. It has a gray paint on a rough cast aluminum surface.

Table 9 summarizes the efficiencies of the various decon steps. Handling was considered to be the first step. It is significant that about 44 percent was lost through the handling required to conduct the film exposures and to make electronic measurements. Throughout these exercises care was taken to reduce rubbing, but a significant quantity came off easily.

Five different decontamination methods/steps were performed and, in four out of the five steps, it was a liquid lightly sprayed onto the detector body. A 500 mL squirt (wash) bottle was used to apply the solutions and to rinse them off in the manner shown in Figure 36. The nozzle pressure was controlled by hand squeezing and was limited to

TABLE 9
DECONTAMINATION
HP-R-211 AREA MONITOR

NOTES: (1) Decontamination was conducted only on the detector body.
(2) Approach: No scrubbing, low velocity spraying only.
(3) Ratio of Cs-137 to Cs-134 was about 6.3/1 in Oct. thru Dec. 1980.
(4) Calculated, based on relative position measurements

	DECONTAMINATION STEP						
	AS RECEIVED	(BEFORE DECON) HANDLING	WATER SPRAY	DETERGENT SPRAY	LOW PRESS STEAM	TURCO 4512A 1/2 HR. SOAK	TURCO 4512A 1 HR SOAK
GAMMA SPEC. ANALYSIS							
Activity (Cs-137) μC: measured / calcul.(4)	No Data / ~70	No Data / 39.3	No Data / 33.6	25.3 / 30.1	14.7 / 18.9	No Data	No Data / 10.1
Percent Decrease per Step		~44	14.5	10.5	37.3	No Data	46.2 Total
Accum. Reduction-Percent		-	14.5	23.4	52.0	No Data	74.2 Total
Wash & Rinse Solution Act. (Cs-137 μCi)		-	3.63	2.69	-	-	-
BETA - GAMMA PROBE							
mRad/hr After Decon Step (Avg)							
Beta		20.5	17.1	16.4	9.6	5.6	4.4
Gamma		3.3	2.8	2.5	1.5	0.98	0.76
Ratio (Beta to Gamma)		6.2	6.1	6.6	6.4	5.7	5.8
mRad/hr After Decon Step (hotspot)							
Beta		98.2	80.0	71.0	46.2	26.4	15.7
Gamma		7.9	6.6	5.9	3.4	2.2	1.5
Ratio (Beta to Gamma)		12.4	12.1	12.0	13.6	12.0	10.5
Percent Decrease per Step							
Beta/Gamma (Avg)		-	17/15	4/11	41/40	42/35	21/22
Beta/Gamma (hotspot)		-	19/16	11/11	35/42	43/35	41/32
Accum. Reduction-Percent							
Beta/Gamma (Avg)		0/0	17/15	20/24	53/55	73/70	79/77
Beta/Gamma (hotspot)		0/0	19/16	28/25	53/57	73/72	84/81
Peak to Avg Ratio							
Beta/Gamma		4.8/2.4	4.7/2.4	4.3/2.4	4.8/2.3	4.7/2.2	3.6/2.0
LID mRad/hr-(no label)- Avg							
Beta/Gamma		254/19					

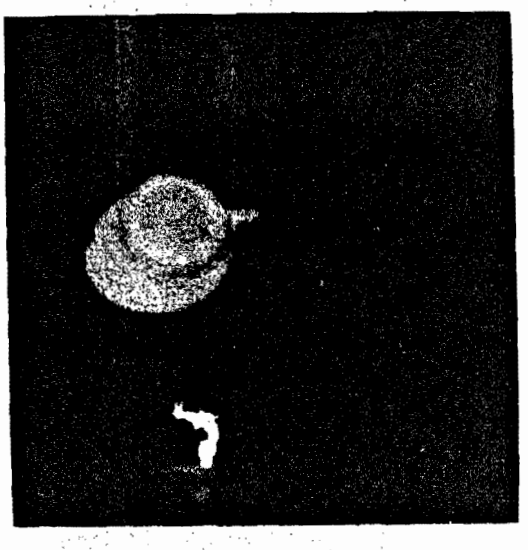

FIGURE 36. Typical Decon Wash and Rinse Operation. Demonstration of the method used to apply the wash solutions or rinse water.

prevent splashing the contaminants beyond the catch beaker rim. The third decon step was low pressure steam. It was an attractive choice because it appeared that after the first two washes, the activity was imbedded in the paint and higher temperatures might liberate the contaminants. The objective was to apply the steam at a low temperature and pressure and at the same time keep the nozzle velocity to a minimum. An advantage to the use of steam is that it keeps the quantity of liquids to a minimum thus reducing handling problems.

An extension of the loss due to handling was the first decontamination step using a 500 mL potable water rinse. It was felt that the loosely-held contaminants would come off with this small assistance and would indicate a separation between the more easily removable from the tenacious. About 50 percent of the initial activity remained after this step. The table, however, illustrates this as the first decon step with a 14.5 percent reduction. The water was later reduced to 450 mL and put in a "Marinelli Beaker" for measurement. The gamma spec analysis showed that 3.63 µCi of Cs 137 was removed.

A commercial laundry detergent (Tide™) was used next, mixed at the ratio of 2 teaspoons per 500 mL of warm water. After the spray wash the surface was drip dried for 5 minutes and then rinsed with 500 mL of cold tap water. A surprisingly small 10.5 percent reduction was accomplished with this method. Both the wash and rinse waters were collected and concentrated (by boiling) to 450 mL each for measuring. The total Cs 137 removed was 2.69 µCi and the reduction closely coincided with other measurements. No further solutions were evaluated following this step, since our instrumentation methods closely agreed with the solution measurements.

The detergent spray step indicated that the remaining activity was firmly embedded in the paint and possibly in the aluminum. Liberation of this activity by elevating the temperature,using steam, was the next step. A commercial engine cleaning and degreasing steam

system was used. A number of problems were encountered in getting the steam temperature and matching pressure low enough to use. We estimate the pressure to range from zero to 5 psig. The steam was puffing from the end of the nozzle and had no significant velocity. A 37 percent drop in the activity level from the preceding step was accomplished. As stated earlier, steam has some advantages in that it requires less fluid. An alternative method may be to elevate the temperature through the use of an oven followed by a warm water rinse. For the in situ case, where the reactor containment building is too radioactive to permit adequate time for personnel to enter and decon, another possibility exists. Allow the building temperature to rise to around 93°C (200°F) and turn on the building spray system for some short period of time. Although this appears drastic, it would probably reduce the levels to the point where "stay times" allow other decontamination methods to be used.

Contact with TMI and Bechtel personnel about our results suggested the final two decon methods used. At the request of R. C. Rudolph and D. Giefer, both from Bechtel, we sprayed the detector with a commercial product they supplied. It was a phosphoric acid chemical (both chloride and fluoride free) identified as TURCO 4512A. The instructions were to spray a 10% by volume solution and let set for 15 minutes. The solution temperatures were to be 60° to 66°C (140° to 150°F). Two tests were conducted using the TURCO solution but with some modifications to the method recommended. Following the wash of the first test it was allowed to set for 30 minutes before being rinsed. In the second test the soak time was 1 hour. Both were approved by Giefer. The total wash solution in each case was 500 mL and a rinse with 750 mL and 500 mL. All solution and rinse temperatures were at 57°C (135°F) at the start and about 52°C (128°F) at the end of spraying. The first TURCO decon step reduced the average activity about 40 percent and the second another

20 percent. At this point the levels on the detector were so low (average beta 4.4 and gamma 0.76 mRad/hr) that any further testing would not be warranted.

In conclusion, it can be stated that the contamination has migrated into the paint and will require repeated applications of a selected decon method. About half of the contamination is loosely tied, and hotspot zones do not tend to decon faster as a result of blending but drop at the same rate as the average.

Decon Measurements

Two methods were used to determine the effectiveness of the decon step. Gamma spectroscopy was used to keep track of the relative drop in activity as well as an intermittent check of the actual changes in activity. The solutions used to wash and rinse for each step were collected but only in the first two steps were they evaluated. They were also used as a check on the measuring systems. The second method used to evaluate the decon effectiveness was a portable beta-gamma instrument. The purpose for this was to determine whether the "hotspot" areas on the detector dropped faster (easier and faster to decon) or whether the hotspot and average areas dropped by the same percentage. We found that the latter case is what took place from beginning to end. The gamma-spec analysis gave an overall point-source presentation of relative changes and total activity differences, while the hand probe was able to follow relative changes of hot spots and general area as well as present a true contact dose-rate in millrad per hour for both the beta and gamma source activities. The principle contaminates were cesium-134 and 137 emitting beta and gamma, and strontium 90 emitting only beta.

A swipe was taken from a bag that had contained the detector in order to generate a calibrated "absorption curve" for our probe against the type of activity it was to see. The calibration also considered the fact that all readings were to be done through a single plastic bag having a "range" or "absorber thickness" of 4.8 mg/cm^2. This combined with a probe thickness of 30 mg/cm^2 for a total thickness of about 35 mg/cm^2 and translates to a "transmission" of 30% or a beta correction factor of 3.3. A calibration of the Eberline HP-270 probe connected to an Eberline "Rascal" ratemeter-scaler model PRS-1 and an NBS certified Cesium 137 source produced a conversion of 1400 CPM (counts per minute) per millirad/hr. To determine the dose rates the following equations were applied:

$$\text{mRad/hr (Beta)} = \frac{\text{Open Window (CPM)} - \text{Closed Window (CPM)}}{1400} \times 3.3$$

$$\text{mRad/hr (Gamma)} = \frac{\text{Closed Window (CPM)}}{1400}$$

Appendix D contains some of the actual data sheets from the hand probe measurements. A total of 44 locations were selected for measurement initially. This was later changed to 28 positions with little effect on the average values. Table 9 is a condensation of all the work done in decontaminating the detector body. The bottom line of the table provides hand probe measurements made on the detector lid only for comparison, since it was not decontaminated. The hotspot contact beta dose rate was on the aluminum label and read about 1 rad/hr when received at Sandia.

INTENTIONALLY LEFT BLANK

APPENDIX A

Stripchart Information

Appendix A contains miscellaneous documentation used to understand the HP-R-211 stripchart recording.

Contents

1. Channel 8 vs Channel 9 discrepancy and HP-R-211 calibration prior to accident.
2. Maintenance record; HP-R-211 calibration prior to the accident.
3. Health physics gamma rate measurements at full reactor power.
4. Gamma rate maps as measured during manned entries 1, 2 and 3.
5. HP-R-211 stripchart near the time of the hydrogen burn and sodium hydroxide spray.

1.

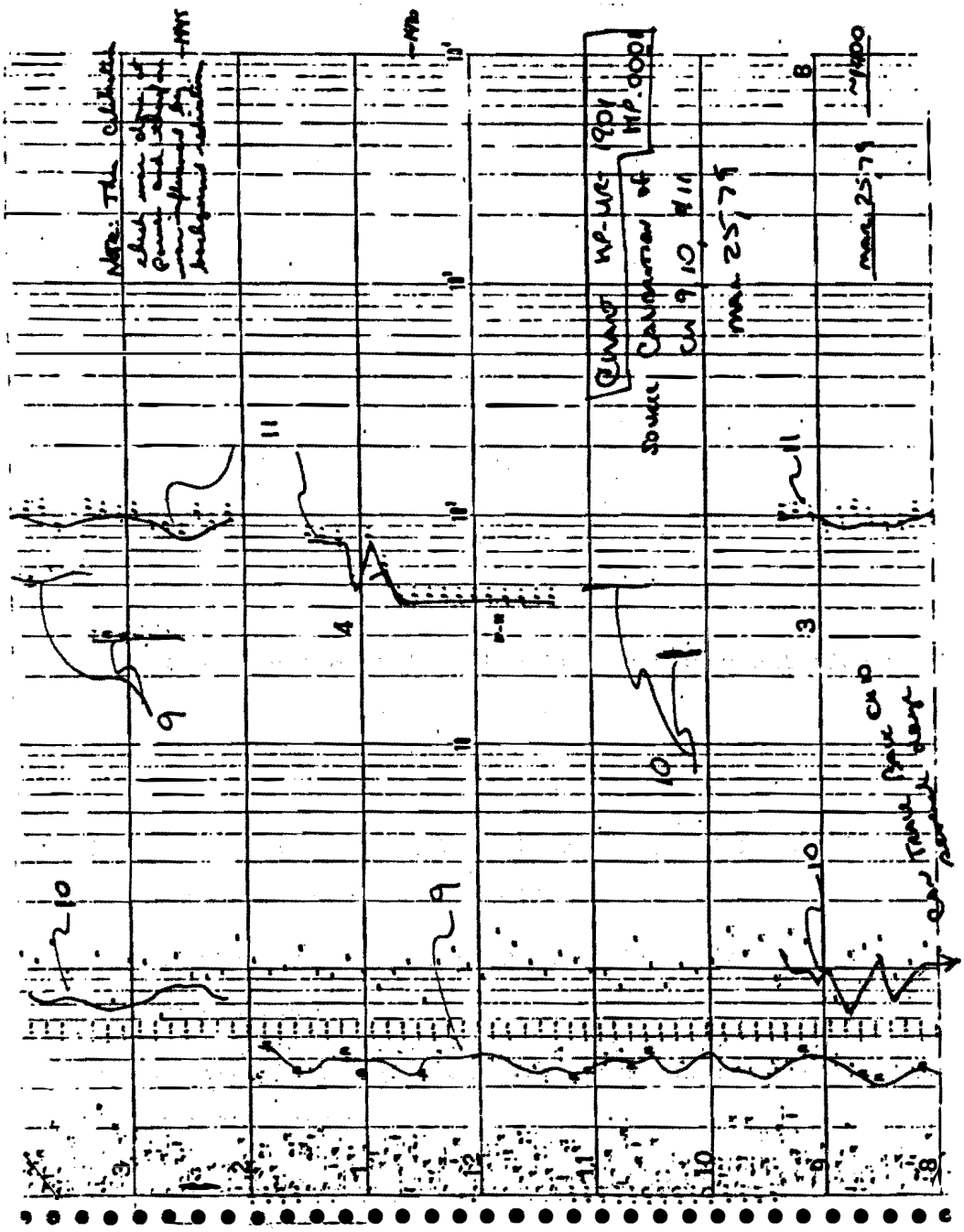

2. Pre Accident Data

DATA SHEET 1
RADIATION MONITORING SYSTEM

Revised 07/19/78

Procedure Step											
6.1.1.2	MONITOR HP-R-211	LOCAL METER	AS FOUND	(AS LEFT)	RECORDER TRACE MARKED YES/NO						
		FCK SOURCE KNOB POSITION									
		CLOSED			INTERMEDIATE			OP			
	DESCRIPTION	RATEMETER	INT	RECORDER	INT	RATEMETER	INT	RECORDER	INT	RATEMETER	IN
6.1.2.3											
6.1.2.4											
6.1.2.5	Source	48 MR/hr	MR/hr			350 MR/hr	MR/hr			1800 MR/hr	
6.1.3.3	Background	1- MR/hr	- MR/hr			1- MR/hr	- MR/hr			1- MR/hr	
6.1.3.1	Actual Source Readings	47 MR/hr	MR/hr			349 MR/hr	MR/hr			1799 MR/hr	
6.1.4.1	Original Reading	54	MR/hr			400	MR/hr			2000	
6.1.4.2	Original Reading Date	1975									
6.1.4.3	Expected Reading	48	MR/hr			352	MR/hr			1762	
6.1.4.4	+15% of Expected Reading	55	MR/hr			409	MR/hr			2026	
6.1.4.5	-15% of Expected Reading	41	MR/hr			299	MR/hr			1498	
6.1.5.1	Actual Source Reading within 15% of Expected? Yes/No	YES	*			YES	*			YES	*
	Setpoint Data										
		ALERT				INT				HIGH	
6.1.6.1	Required Setpoint										
AL 6.1.6.3	Indicated "As Found"										
Hi 6.1.6.4	Setpoint					MR/hr					MR/h
AL 6.1.6.7	"Tripped" Observed										
Hi 6.1.6.8	Setpoint					MR/hr					MR/h
6.1.6.9	Observed Setpoint within One Minor Division of Required Yes/No		*				*				
	Check Source, Recorder, Acceptance Criteria, Sign-Off										
6.1.7	Observed Increase in Reading Due to Check Source					2 MR/hr				INT	
6.1.7.2	Recorder Trace Marked Yes/No									INIT.	

* Acceptance Criteria: All Yes/No Blanks Indicate "Yes".
** Record "Pegged" if Meter Pegs High Due to Background.
New Calibration Sticker Attached Yes/No

DATA SHEET 1
RADIATION MONITORING SYSTEM

07/19/78

Procedure Step											
6.1.1.2	MONITOR HP-R-211	LOCAL METER	(AS FOUND)	AS LEFT	RECORDER TRACE MARKED YES/NO						
		FCK SOURCE KNOB POSITION									
		CLOSED			INTERMEDIATE			OP			
	DESCRIPTION	RATEMETER	INT	RECORDER	INT	RATEMETER	INT	RECORDER	INT	RATEMETER	I
6.1.2.3											
6.1.2.4											
6.1.2.5	Source	30 MR/hr	MR/hr			250 MR/hr	MR/hr			1300 MR/hr	
6.1.3.3	Background	-1 MR/hr	- MR/hr			- MR/hr	- MR/hr			- MR/hr	
6.1.3.1	Actual Source Readings	29 MR/hr	MR/hr			249 MR/hr	MR/hr			1299 MR/hr	
6.1.4.1	Original Reading	54	MR/hr			400	MR/hr			2000	
6.1.4.2	Original Reading Date	1975									
6.1.4.3	Expected Reading	48	MR/hr			352	MR/hr			1762	
6.1.4.4	+15% of Expected Reading	55	MR/hr			409	MR/hr			2026	
6.1.4.5	-15% of Expected Reading	41	MR/hr			299	MR/hr			1498	
6.1.5.1	Actual Source Reading within 15% of Expected? Yes/No	NO	*			NO	*			NO	*
	Setpoint Data										
		ALERT				INT				HIGH	
6.1.6.1	Required Setpoint										
AL 6.1.6.3	Indicated "As Found"										
Hi 6.1.6.4	Setpoint					MR/hr					MR/
AL 6.1.6.7	"Tripped" Observed										
Hi 6.1.6.8	Setpoint					MR/hr					MR/
6.1.6.9	Observed Setpoint within One Minor Division of Required Yes/No		*				*				
	Check Source, Recorder, Acceptance Criteria, Sign-Off										
6.1.7	Observed Increase in Reading Due to Check Source					0 MR/hr				INT	
6.1.7.2	Recorder Trace Marked Yes/No									INIT.	

* Acceptance Criteria: All Yes/No Blanks Indicate "Yes".
** Record "Pegged" if Meter Pegs High Due to Background.
New Calibration Sticker Attached Yes/No

3.1

Met-Ed / GPU

Metropolitan Edison Company
Post Office Box 480
Middletown, Pennsylvania 17057
717 944-4041

22 October 1980

I-80-242

Mr. Frank Thome
Division 4445
Sandia National Laboratory
P. O. Box 5800
Albuquerque, NM 87185

Dear Mr. Thome:

A copy of the Three Mile Island Unit 2 Biological Shield Survey (TP 800/3) test results are attached per your request. Also attached are a complete set of marked-up drawings indicating the approximate location where the radiation readings were taken.

As discussed in the phone conversation between yourself and John Flint, problems with water evaporation from the movable shield tanks around the reactor vessel flange area effected the measured neutron dose rate. A small effect on the gamma dose rate would also be expected. The data recorded at 40% full power indicates the relative magnitude of the problem when compared to the data obtained at 100% full power. This problem still existed on 28 March 1979.

If we can be of any further assistance, please feel free to contact us.

Sincerely Yours,

T. M. Hawkins
Superintendent, Startup and Test

TMH/JHF/slo

Attachments

cc: J. A. Brummer, without attachment
C. P. Miller, without attachment
Correspondence File
Central File

3.2

POS. 19,20,23,24 ARE
ON OUTSIDE OF D-RING
WALL ACROSS FROM DETECTORS.

BIOLOGICAL SHIELD SURVEY

Ref. Step 9.2.1

REACTOR POWER: 0%

E-2

POSITION NUMBER	DOSE MEASUREMENT γ mREM/hr	DOSE MEASUREMENT n, mREM/hr	INSTRUMENT NUMBERS	TIME	DATE	DATA TAKER INITIALS
19	<.2	<.5	RNR-4 #3554	0700-1400	4-9-78	KLM+DWE
20	<.2	<.5	RO-2 #483	"	"	"
21	<.2	<.5	"	"	"	"
22	<.2	<.5	"	"	"	"
23	<.2	<.5	"	"	"	"
24	<.2	<.5	"	"	"	"
25	<.2	<.5	"	"	"	"
26	<.2	<.5	"	"	"	"
27	<.2	<.5	"	"	"	"
28	<.2	<.5	"	"	"	"
29	<.2	<.5	"	"	"	"
30	<.2	<.5	"	"	"	"
31	<.2	<.5	"	"	"	"
32	<.2	<.5	"	"	"	"
33	<.2	<.5	"	"	"	"
34	<.2	<.5	"	"	"	"
35	<.2	<.5	"	"	"	"
36	<.2	<.5	"	"	"	"

OFFICIAL FIELD COPY

Duplicate Page 0

3.3

BIOLOGICAL SHIELD SURVEY

Ref. Step 9.3.1

REACTOR POWER: 40%

POSITION NUMBER	DOSE MEASUREMENT γ MRH MR/HR	DOSE MEASUREMENT n, MREM/hr mrem²/hr cm.	INSTRUMENT NUMBERS	TIME	DATE	DATA TAKER INITIALS
E-2						
19	0.6	1.5	R Pack = 3554 RO2 = 478	0930	10-2-78	MLL - KLM
HP-211 → 20	< 0.1	1.0				
21	0.1	1.0				
22	< 0.1	0.5				
HP 212 → 23	0.2	0.1 1.0				
24	0.4	2.0				
E-3 25	9.0	5.0				
26	7.0	25				
27	17	100				
28	13	100				
29	7	25				
30	8	30				
E-3 31	11	75				
32	< 0.1	< 1				
33	< 0.1	< 1				
34	< 0.1	< 1				
35	< 0.1	< 1				
36	< 0.1	< 1	✓	✓	✓	✓

OFFICIAL FIELD COPY

DATA SHEET 2
Page 2 of 3

TMI UNIT II
TP 800/3
Effective Page 0
Page 20

Duplicate Page 0

BIOLOGICAL SHIELD SURVEY

Ref. Step 9.4.1

REACTOR POWER: 100%

POSITION NUMBER	DOSE MEASUREMENT γ ~~REM~~ MR/HR	n, MREM/HR ~~n/cm² sec.~~	INSTRUMENT NUMBERS	TIME	DATE	DATA TAKER INITIALS
19	1.2	2.5	[illegible]	[illegible]	[illegible]	[illegible]
20	.5	1.2				[illegible]
21	.5	1.3				[illegible]
22	.3	.2				[illegible]
23	.3	.7				[illegible]
24	.7	3.2				[illegible]
25	12	40				[illegible]
26	7	22				[illegible]
27	19	60				[illegible]
28	20	75				[illegible]
29	7	20				[illegible]
30	8	31				[illegible]
31	13	50				[illegible]
32	<.1	0				[illegible]
33	<.1	0				[illegible]
34	<.10	0				[illegible]
35	<.1	0				[illegible]
36	<.1	0	[illegible]	[illegible]	[illegible]	[illegible]

OFFICIAL FIELD COPY

DATA SHEET 3
Page 2 of 3

TMI UNIT II
TP 800/3
Effective Page 0
Page 23

Duplicate Page 0

4.

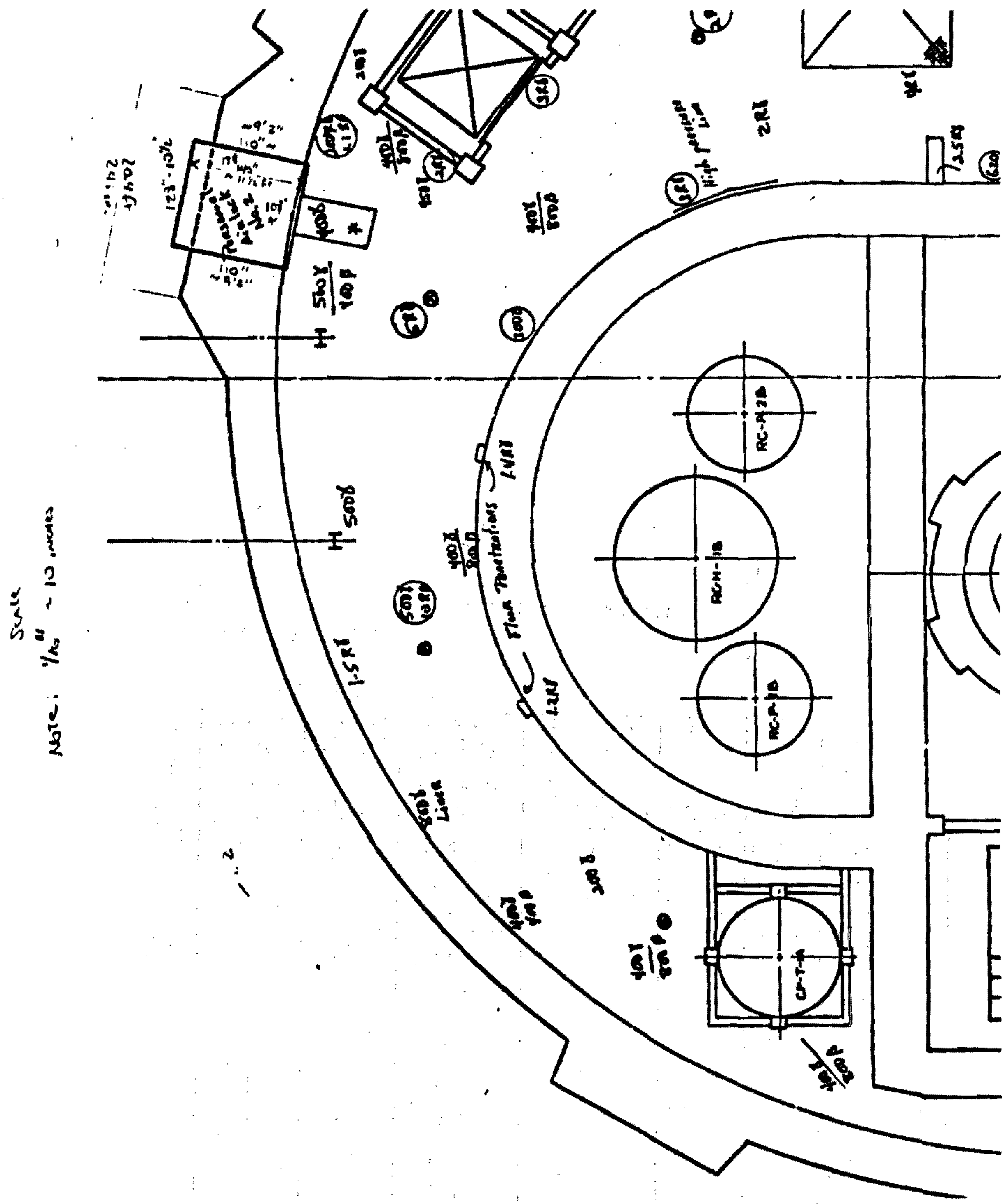
Note: Scale 1/16" ~ 10 inches
RC-P-2B
RCH-1B
RC-P-1B
CF-T-1A
Floor Penetrations
500 δ Liner
High pressure line

5.

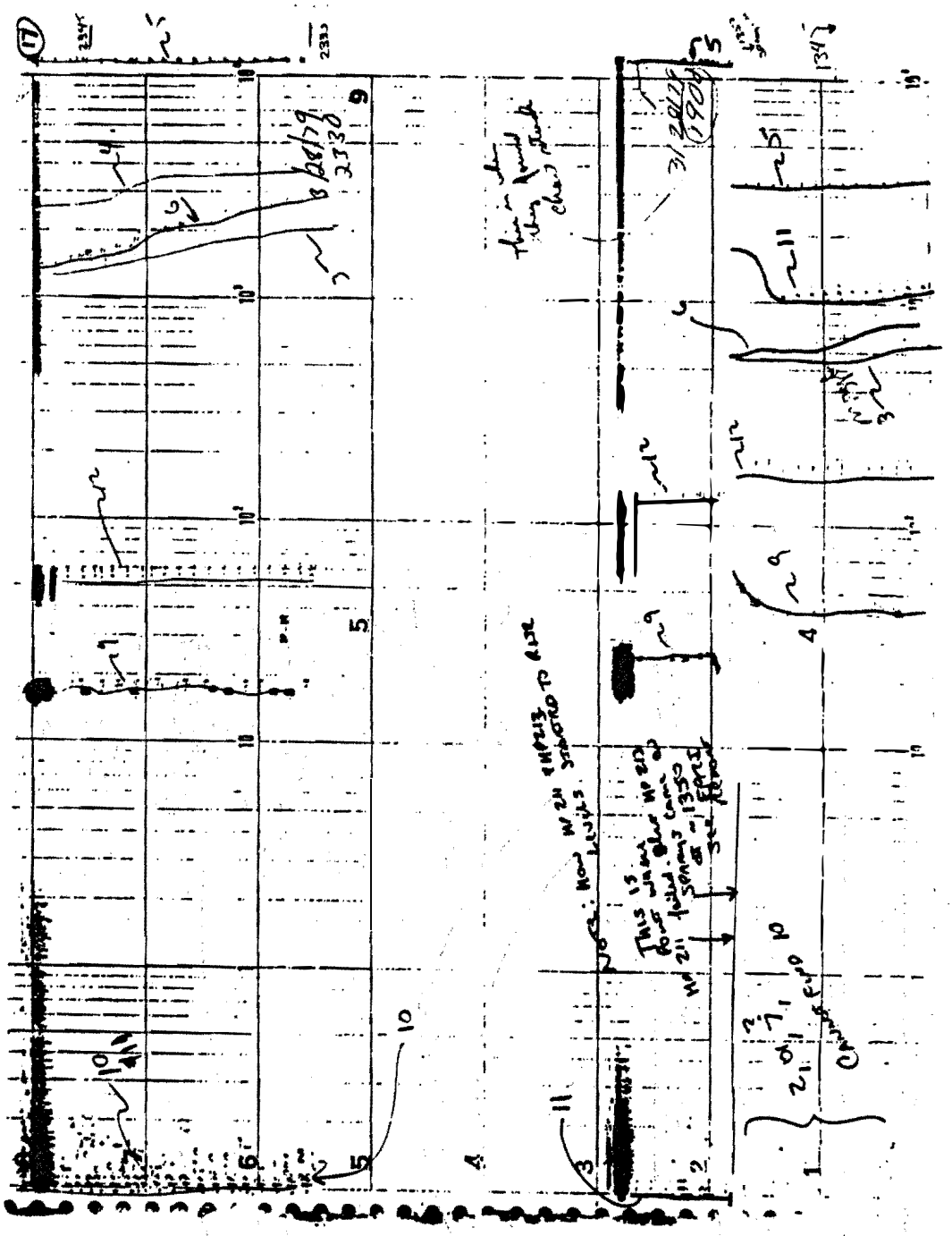

INTENTIONALLY LEFT BLANK

APPENDIX B

Transistor Characteristics

Transistor current gain, HFE, degradation is plotted in the curves given here versus cumulative gamma radiation dose. Eighty-seven devices from four manufacturers were passively exposed to a Co 60 source in progressive steps, and the characteristics were measured after each step. Transistor HFE's are plotted for collector currents of 100 microamperes. The three curves shown for each device type represent HFE characteristics from the minimum device, the maximum device and the average of all the devices of that manufacturer. Also shown are the intersections of these curves with the HFE values measured for the devices removed from HP-R-211. The number of devices of each type as well as the manufacturer is listed on each graph.

Contents

2.

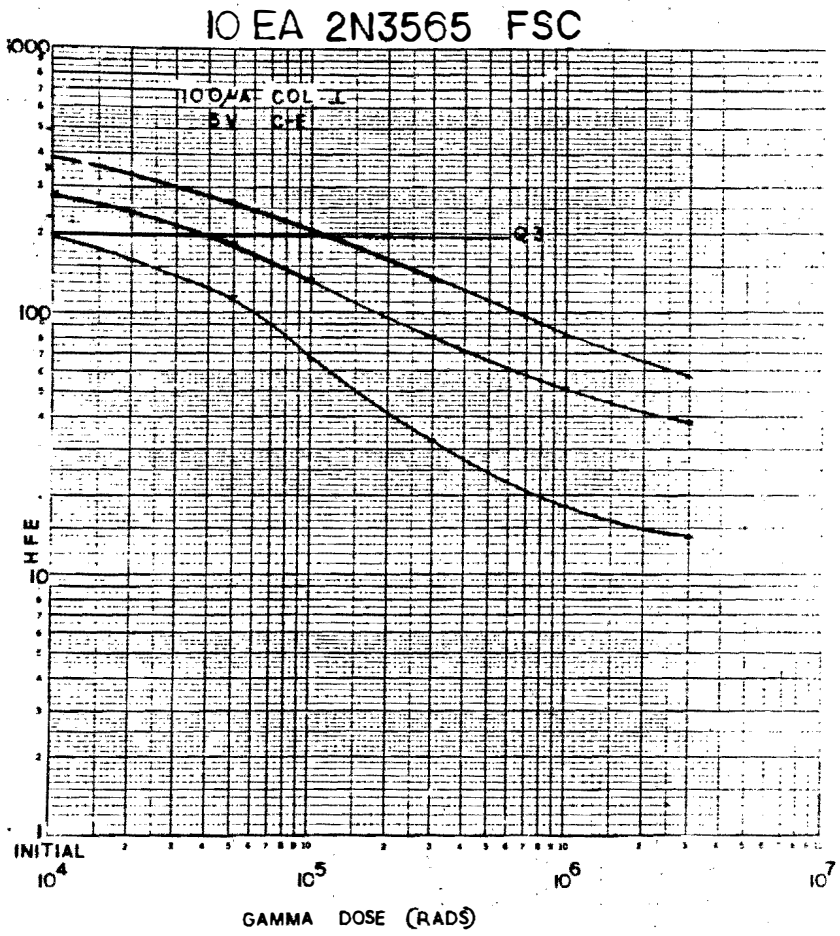
10 EA 2N3565 FSC
100MA COL I
5V C-E
Q3
HFE
INITIAL
10^4
10^5
10^6
10^7
GAMMA DOSE (RADS)

1.

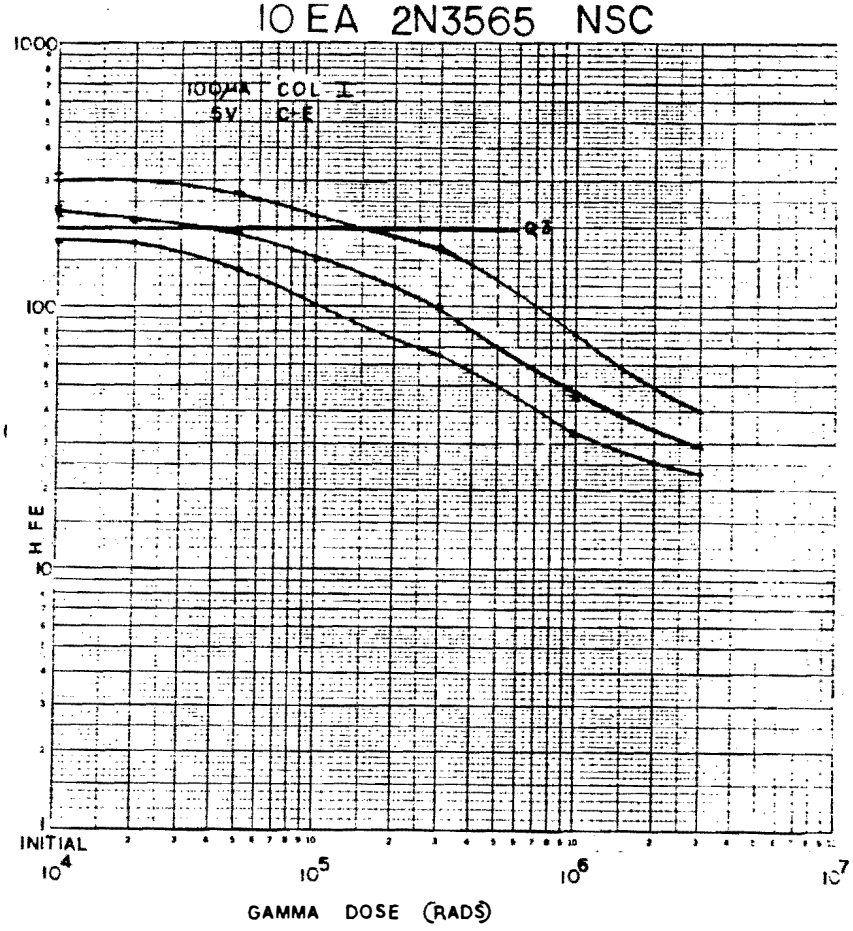
10 EA 2N3565 NSC
100MA COL I
5V C-E
Q3
HFE
INITIAL
10^4
10^5
10^6
10^7
GAMMA DOSE (RADS)

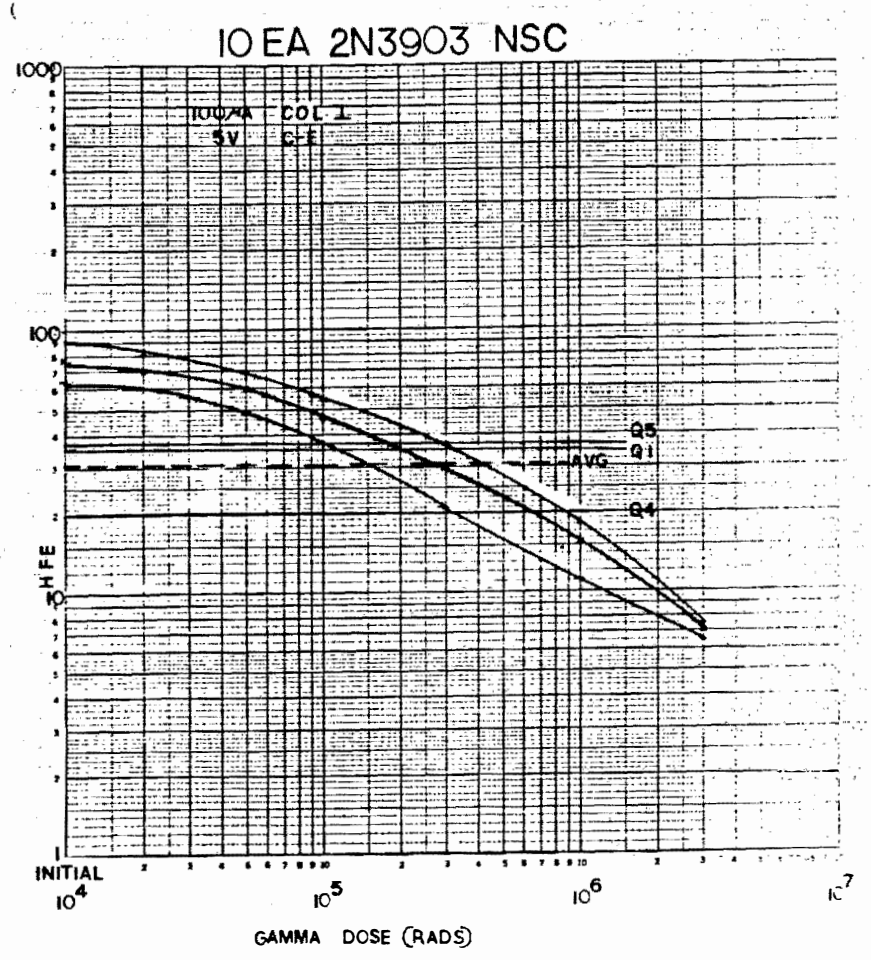
10 EA 2N3903 NSC
100 MA COL I
5V C-E
1000
100
10
1
HFE
Q5
Q1
AVG
Q4
INITIAL
10^4
10^5
10^6
10^7
GAMMA DOSE (RADS)

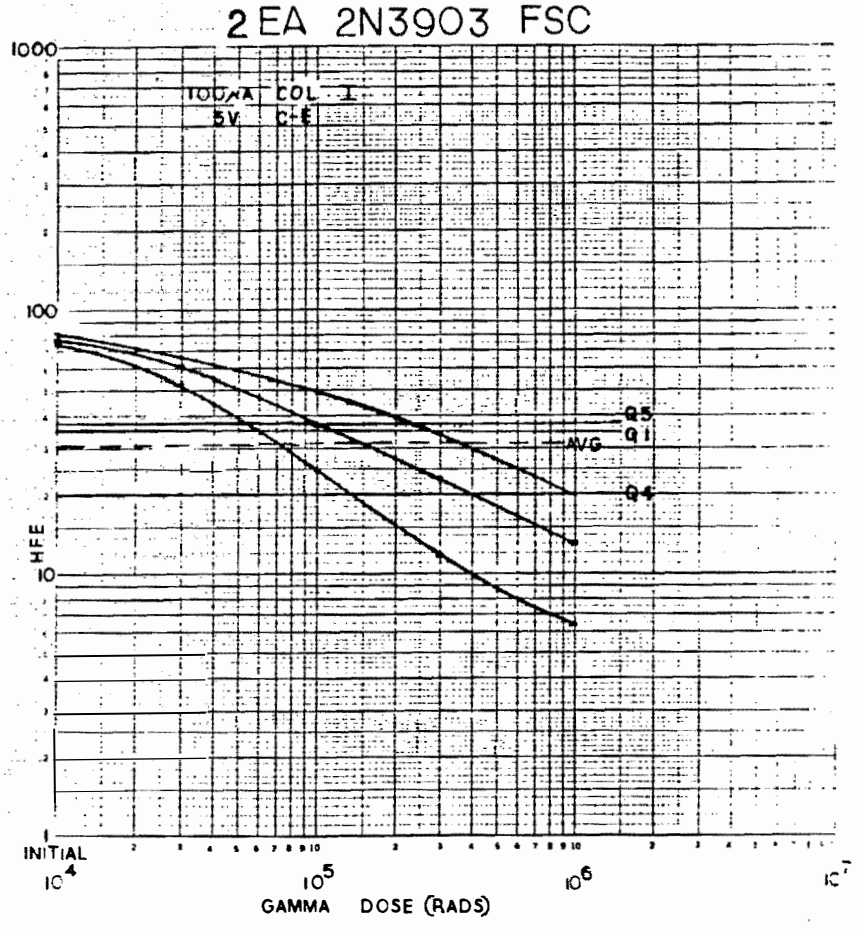
2 EA 2N3903 FSC
100 MA COL I
5V C-E
1000
100
10
1
HFE
Q5
Q1
AVG
Q4
INITIAL
10^4
10^5
10^6
10^7
GAMMA DOSE (RADS)

5.

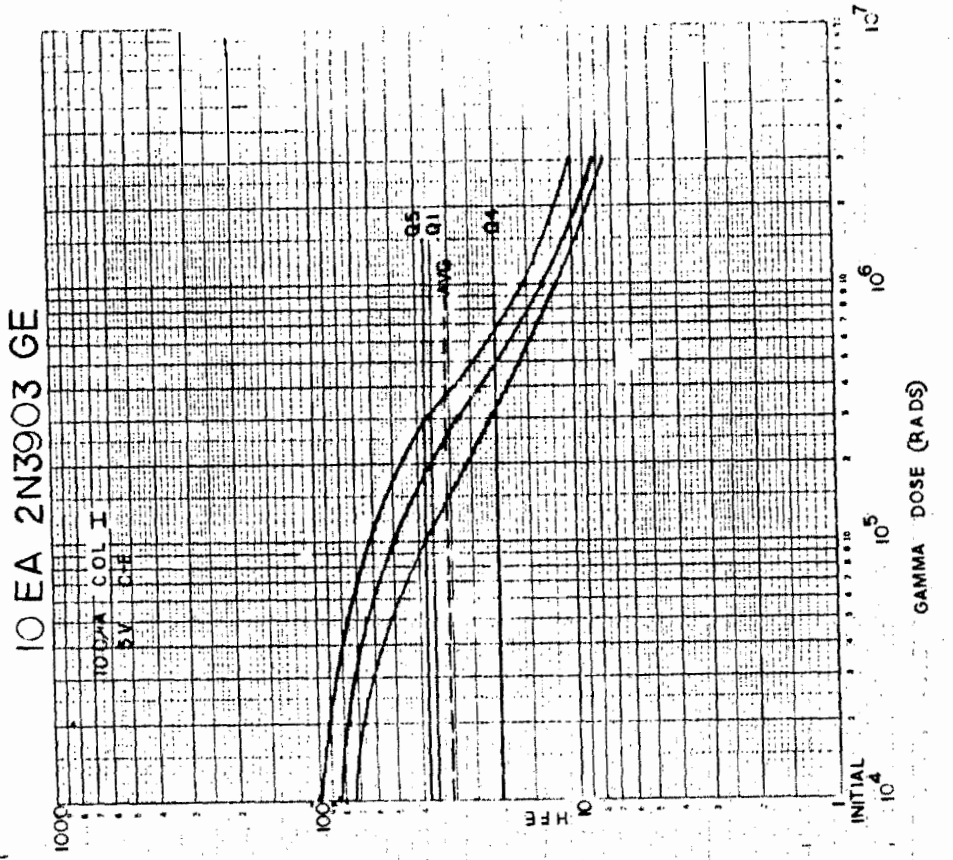
10 EA 2N3903 GE
Q5
Q1
Q4
INITIAL
GAMMA DOSE (RADS)

6.

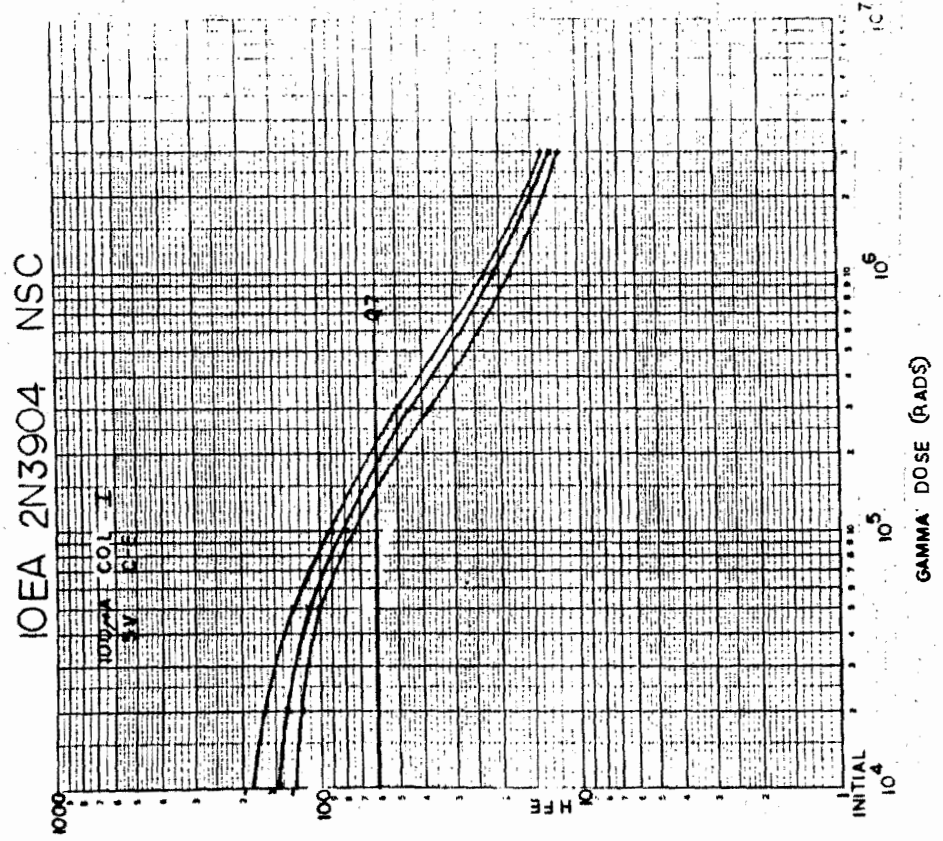
10EA 2N3904 NSC
Q7
INITIAL
GAMMA DOSE (RADS)

8.

5EA 2N3906 FSC

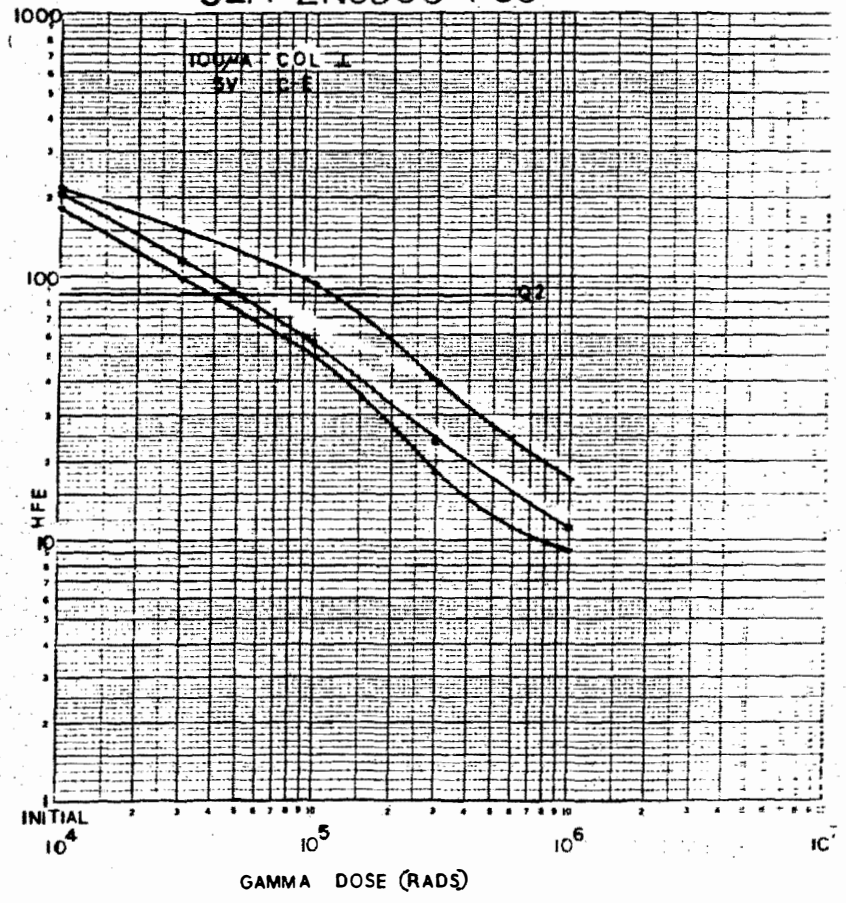

7.

10 EA 2N3904 FSC

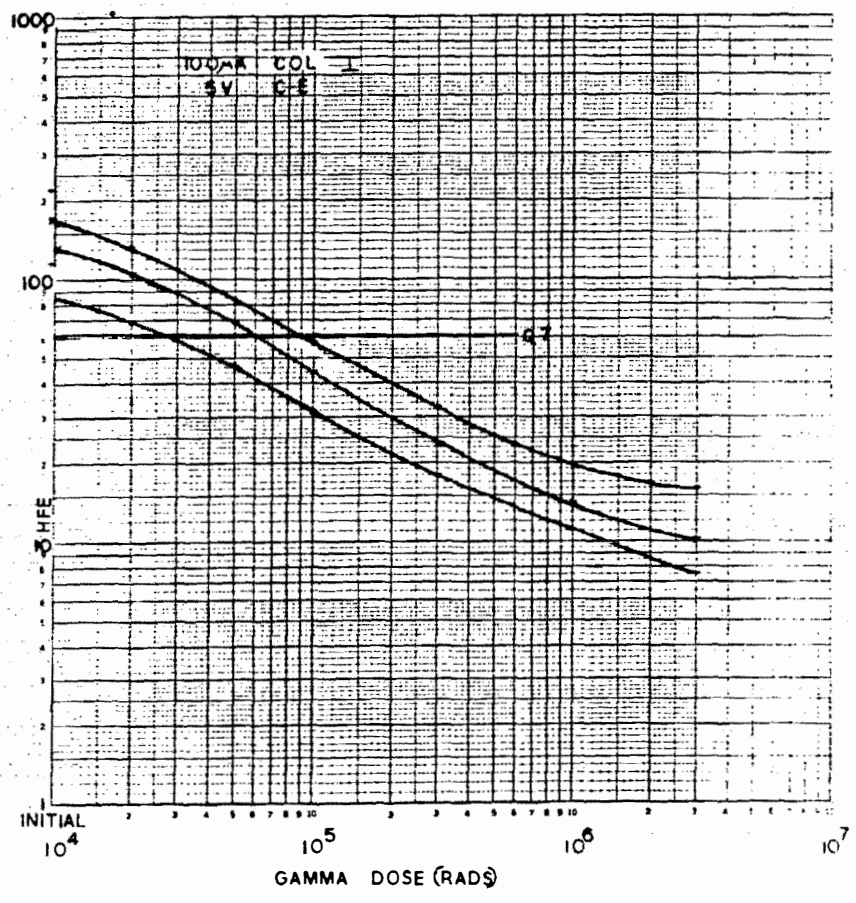

9.

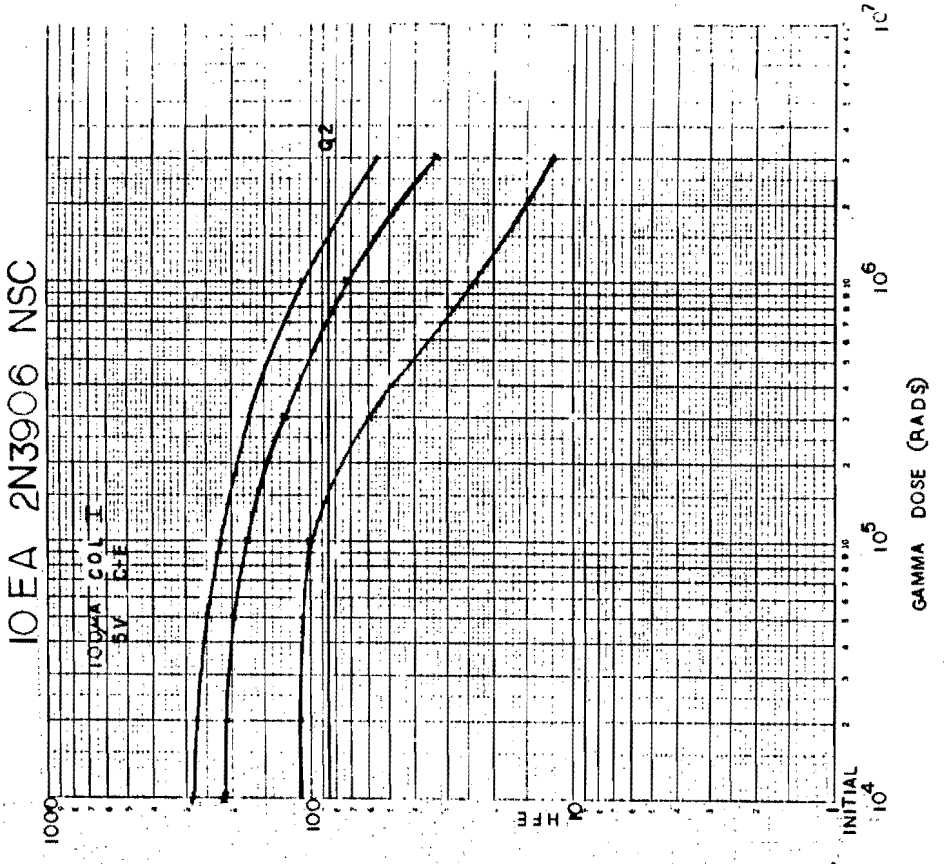
10 EA 2N3906 NSC
10 μA COL I
5V
G.E
Q2
HFE
INITIAL
GAMMA DOSE (RADS)

10.

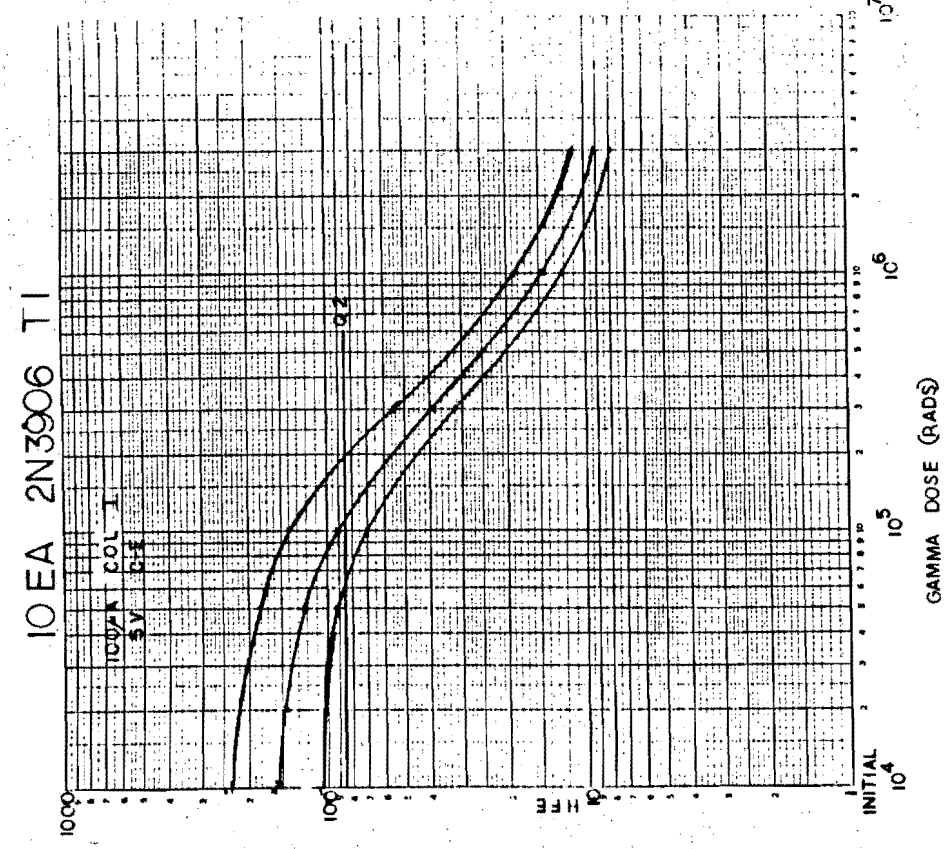
10 EA 2N3906 TI
10 μA COL I
5V
G.E
Q2
HFE
INITIAL
GAMMA DOSE (RADS)

11.

Anneal Data

TRANSISTOR TYPE	MFR	INITIAL HFE	NOV 1980 HFE [1]	JULY 1981 HFE [1]	CORRECTION FACTOR [2]
2N 3965	FSC	350	38	55	1.3
NPN	NAT	240	29	71	1.25
2N 3903	NAT	90	7	14	2.0
NPN	GE	78	9	18	1.6
	FSC	-	-	-	-
2N 3904	NAT	160	13	28	1.8
NPN	FSC	170	11	16	2.0
2N 3906	NAT	230	33	53	1.85
PNP	TI	-	-	-	-
	FSC	-	-	-	-
				Average	1.6
TMI Q1			35.5	40.0	
Q2			86.0	88.0	
Q3			200.0	-	
Q4			20.0	18.7	
Q5			38.0	34.0	
Q7			61.0	52.0	

[1] Measured at Ic = 100 μa

[2] Obtained from gain vs dose graphs. Anneal data measured after exposure to 3 x 10^6 rads. Multiply dose estimates by this factor.

12.

Bias Data

Transistor type 2N 3903 NPN FSC
Exposure level 1.5×10^5 rads
Gain measurement at 100 μA collector current

TRANSISTOR SERIAL NUMBER	INITIAL[1] HFE	POST RAD HFE	NORMALIZED[2] HFE	BIAS CONDITION DURING RADIATION
1	55.0	25.0	45.4	V_{CB} = +10V
2	49.6	21.0	42.3	V_{CB} = +10V
3	59.0	33.0	55.9	Isat = 1 mA
4	29.7	22.0	74.1	Isat = 1 mA
5	46.4	27.0	58.2	Passive
6	24.71	19.0	76.9	Passive

[1] It is unclear why the initial device gains are so low.

[2] This refers to normalizing all gains assuming the initial gains were equal to 100.

APPENDIX C

Contamination Information

Appendix C contains some of the documentation from analyzing the contaminants.

Contents

1. LANL radiochemical and gamma spectrum results.
2. Sandia investigation of the connector surface for building spray analysis.
3. LANL tests of the Victoreen label for sodium and boron spray residue.

UNIVERSITY OF CALIFORNIA
LOS ALAMOS SCIENTIFIC LABORATORY
(CONTRACT W-7405-ENG-36)
P. O. BOX 1663
Los Alamos, New Mexico 87544

IN REPLY REFER TO: CMB-1
740

December 2, 1980

Mr. Frank V. Thome
Systems Safety Information
Division 4445
Sandia Laboratories
Albuquerque, NM 87115

Dear Mr. Thome:

Enclosed are copies of the requested radiochemical analyses of the samples received recently from you. The "connector ring" also was analyzed spectrophotometrically for uranium which was not detected (< 10 ppm).

If there are questions or further analyses needed, please contact me.

Very truly yours,

G. R. Waterbury
Group Leader, Analytical Chemistry

GRW/vmw
Encl: a/s
cc: T. Gardiner, ADEP, MS-178, w/o enc.
CRMO (2), w/o enc.
File, w/enc.

CMB-1 RADIOANALYSIS REPORT

SAMPLE NUMBER	SUBMITTED BY	CODE	RECEIVED
CMB-1-CONNECTOR PING	WATERBURY	S299	11-14-80

BETA GAMMA DOSE RATE=7.0 MR/HR AT 5 CM.
CS-137=4.46 MICROCURIES, CS-134=0.567 MICROCURIES
SR-90=0.11 MICROCURIES, TELLURIUM ACTIVITY NOT DETECTED
PU LESS THAN 2E-03 MICROCURIES

CMB-1-HP-R-211-HATCH PLATE	WATERBURY	S299	11-14-80

GAMMA SPECTRUM SHOWED CS-134 AND CS-137
BETA GAMMA DOSE RATE=0.2 MR/HR AT 5 CM.

CMB-1-PLASTIC BAG	WATERBURY	S299	11-14-80

GAMMA SPECTRUM SHOWED CS-134 AND CS-137
BETA GAMMA DOSE RATE=0.5 MR/HR AT 5 CM.

CMB-1-VICTOREEN DECAL	WATERBURY	S299	11-14-80

GAMMA SPECTRUM SHOWED CS-134 AND CS-137
BETA GAMMA DOSE RATE = 3.6 MR/HR AT 5 CM.

CMB-1-FILTER PAPER	WATERBURY	S299	11-14-80

GAMMA SPECTRUM SHOWED CS-134 AND CS-137
BETA GAMMA DOSE RATE=0.1 MR/HR AT 5 CM.

PRINTED AND COMPUTED NOVEMBER 25, 1980

Sandia Laboratories

Albuquerque, New Mexico
Livermore, California

date: February 19, 1981

to: F. V. Thome - 4445

from: S. F. Duliere and S. J. Caldwell - 5822

subject: Analysis of Three Mile Island Electrical Connector Surface

Scanning electron microscopy (SEM), energy dispersive spectroscopy (EDS), and x-ray diffraction (XRD) analyses were done on an electrical connector from the Three Mile Island nuclear power plant to: 1) characterize the surface condition of the connector, 2) to identify the chemical composition of the surface material, and 3) to determine if steam from the reactor malfunction or water from a sprinkler system was responsible for the connector's present condition.

SEM observations indicated that the threaded area of the connector was corroded and contained material deposited on its surface. EDS of various areas on the connector showed the presence of Cd, Fe, Cu, Al, Ti, Si, and Pb. Samples for XRD analysis were taken of surface material from the top of the connector and from the threads, and $CdCO_3$ and $CaCO_3$ were definitely present in the area of the threads, and $CdCO_3$ and $CaCO_3$ were identified from the top material. A data reduction program indicated a low probability that the following compounds were also present in the surface material: 1) for the top of the connector, $CaSO_4$, $Na_2CS \cdot 3H_2O$, (Al_7Cu_2Fe), CuO, Cu_2SiS_3, and $(alCu_4)$ and 2) for the threads, $Ca_2Al_3Si_3O_{12}(OH)$, $NaNO_3$, $CaH_4Si_2O_7$, and $Ca_3Al_6Si_2O_{16}$.

The Three Mile Island connector appeared to exhibit both corrosion and material deposition on its surface. Cd (cadmium), $CdCO_3$ (cadmium carbonate), and $CaCO_3$ (calcium carbonate) were definitely identified as constituents of the surface material. For a cadmium plated connector, the presence of cadmium carbonate indicated corrosion, and the deposition of silica and calcium carbonate, constituents in hard water, indicated that the water from a sprinkler system was probably its source.

SFD/SJC:5822:jg

4445 L. O. Cropp
4453 W. J. Whitfield
5822 K. H. Eckelmeyer
5822 S. F. Duliere
5822 S. J. Caldwell
5822 File (2)

University of California
LOS ALAMOS SCIENTIFIC LABORATORY
Post Office Box 1663 Los Alamos, New Mexico 87545

In reply refer to:
Mail stop: CMB-1, MS-740

February 19, 1981

Mr. Frank V. Thome
Systems Safety Information
Division 4445
Sandia Laboratories
Albuquerque, NM 87115

Reference: Program S299

Dear Mr. Thome:

Analyses of the Victoreen Name Plate from TMO have been completed. The entire sample was radiochemically analyzed using a non-destructive method for ^{137}Cs. The sample surface was then leached with purified water to remove surface contamination, and the leach solution was analyzed for basicity, sodium, thiosulfate, and boron. The results follow:

	^{137}Cs	- 28.8 microcuries
Basicity, calculated as NaOH		- 1.25 micrograms of NaOH
	$Na_2S_2O_3$	- $\leq$ 1 microgram
	Boron	- 0.25 milligram
	Sodium	- 1.56 milligrams

Following leaching, the name plate was measured for physical dimensions. The average values were as follows:

Thickness with backing	- 0.0232 to 0.037 inch - ave. 0.0257 in. or 0.065 cm
Thickness without backing	- 0.0173 inch or 0.044 cm
Width	- 1.735 inches or 4.41 cm
Height	- 1.062 inches or 2.70 cm

All remaining samples will be returned to you under separate cover. If there are questions, please contact me.

Very truly yours,

Glenn R. Waterbury

G. R. Waterbury
CMB-1 Group Leader
Chemical and Instrumental Analysis

INTENTIONALLY LEFT BLANK

APPENDIX D

Decontamination Data

Appendix D contains data taken during various stages of decontamination.

Contents

1. Detector layouts showing the four positions and the location where measurements were taken with the hand probe.

2. Data taken with hand probe of the detector lid after the Victoreen label had been removed and with the detector body disconnected.

NOV. 11,80

HAND HELD PROBE MEASURING LOCATIONS (B & Y)
TAKEN DURING DECON WORK

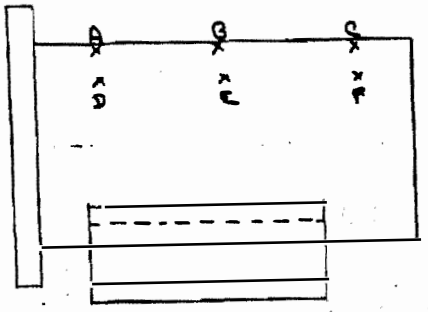

POSITION 1

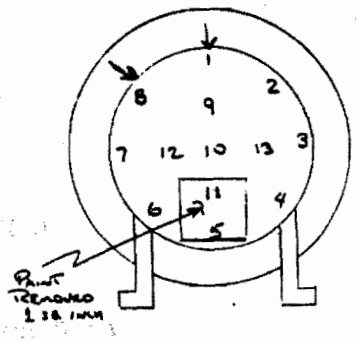

BOTTOM VIEW

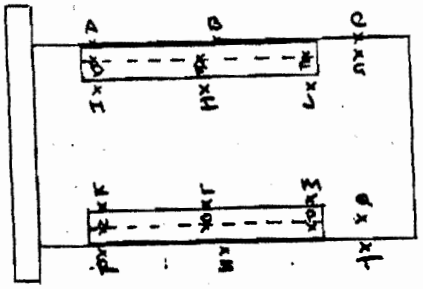

POSITION 2

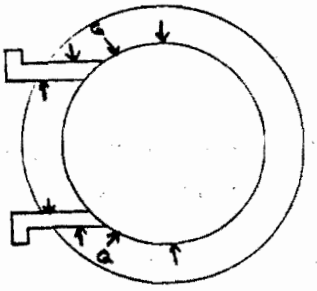

BOTTOM VIEW

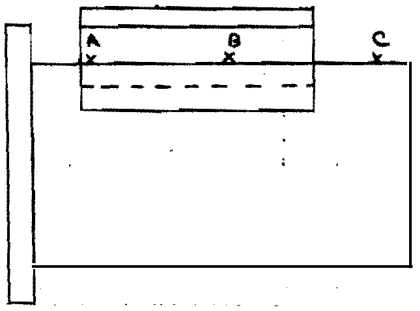

POSITION 3

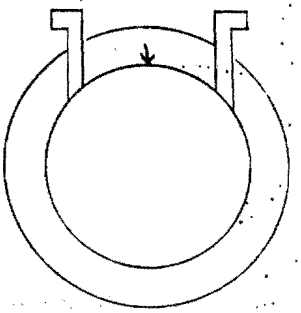

BOTTOM VIEW

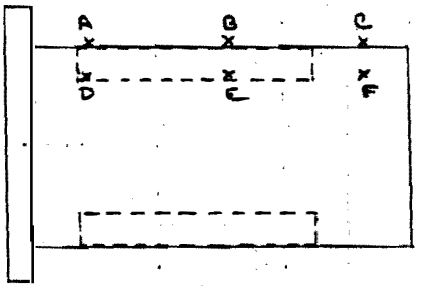

POSITION 4

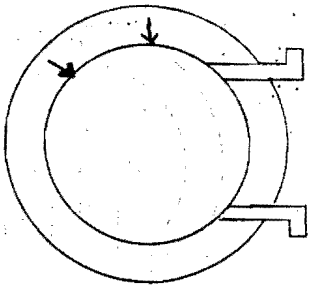

BOTTOM VIEW

2.

NOV 18, 80

Took HP 211 lid to Billy O'Neal
(It had the Alumin Victoreen label removed &
90° away had 1 sq inch of paint removed.

WO = Window open
WC = Window closed

NOTE:
- Bottom of detector removed for measurements

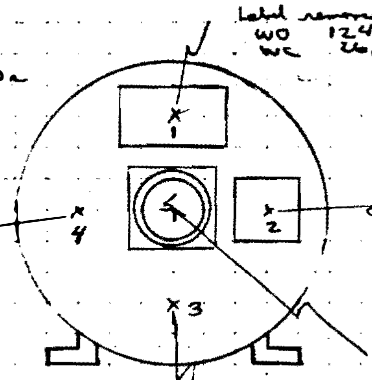

Measurement made with pancake Eberline model PRJ-1 Serial 165

WO - Window Open
WC - Window Closed

Beta $\left(\frac{WO_{5cm} - WC_{5cm}}{1400}\right) \times 3.3$ = mRad/hr

γ : $\frac{WC}{1400}$ = mRad/hr

		Beta mRad/hr	γ	β/γ
Point	1	231	19.1	12.1/1
	2	117	17.8	6.6/1
	3	285	20.7	13.8/1
	4	247	18.4	13.4/1
	~~5~~	~~36~~	~~11.5~~	Data bad. on top connector
	ave	254	19	13.4/1

ave 220 mR/h with paint removed data
ave 254 mR/h without paint

APPENDIX E

Examination Steps and Archive Storage

The examination of HP-R-211 was conducted in such a way to prevent the loss of information as the various steps were taken. The list below highlights in approximate chronoligical sequence the steps that were taken:

1. perform electrical methods and calibration checks with spare detector and ratemeter (test channel)
2. unpack 211
3. unpowered electrical tests
4. point source radioisotope analysis
5. radiation sensitive film contaminant mapping
6. gamma range test channel measurements
7. gamma range 211 measurements (powered) with and without buffer
8. temperature and low voltage tests of test channel using gamma source
9. temperature and low voltage tests of 0211 using gamma source
10. gamma range 211 measurements at low voltage
11. detector 211 gas sample removed
12. detector 211 opened and examined
13. insert test detector electronics into 211 housing for background level check
14. high impedance measurements on 211 connector backshell
15. powered circuit board troubleshooting on 211
16. nametags and connector sent to Los Alamos for radioisotope analysis.
17. repair 211 by replacing Q6 and again test at gamma range
18. failed transistor sent for analysis

19. teflon sleeve and O-ri[illegible]longation tests

20. decontamination tests

21. failure inducement tests on test detector

22. gamma range tests to determine spatial or incident angle veriability on 211

23. detector/ratemeter calibration experiments

24. steam/spray experiments

25. extremely high gamma source range tests on test and 211 detectors

The undisturbed detector housing top assembly, connector, backshell 1 in.^{2} paint scraping, plastic label, and gas sample are being held in archive storage in an undisturbed state. All the components are being stored.

REFERENCES

1. J. Jones, Technology for Energy Report on cable room measurements on HP-RT-0211, unpublished 1981.

2. Sandia Laboratory Notebook, ENG-F-730, Michael B. Murphy, 1980.

3. Sandia Laboratory Notebook, B-1257, Frank V. Thome, 1980.

4. International Seminar, Held November 21, 22, 1980 in Washington, D.C., TMI-2 Information and Examination Program", sponsored by U. S. Department of Energy.

5. "Instruction Manual for G-M Area Monitoring Systems, Model 855 Series", Victoreen, Inc. 10101 Woodland Ave., Cleveland, Ohio.

6. Analysis of Three Mile Island - Unit 2 Accident, NSAC-1, Oct. 1979.

7. U. S. Nuclear Regulatory Commission Investigative Report No. 50-320/79-10, Investigation into the March 28, 1979 Three Mile Island Accident by Office of Inspection and Enforcement.

8. Los Alamos Scientific Laboratory memo, dtd. February 19, 1981, G. R. Waterbury to F. V. Thome, Subject: Radiochemical Analysis of TMI Components.

9. Sandia Laboratories Report, SAND80-1957, O. M. Stuetzer, January 1981, "Electrical Insulators in a Reactor Accident Environment".

10. Metropolitan Edison Memo, Donald Nitti to J. B. Logan, B. C. Rusche, June 27, 1979, Subject: Containment Dome Radiation Monitor.

11. Radiation Effects in Semiconductor Devices, Frank Larin, John Wiley and Sons, Inc.

12. Microwave Semiconductor Devices: Fundamentals and Radiation Effects, R. J. Chaffin, 1973, John Wiley and Sons. pp 92, 95

13. Sandia Data File, A. Asselmier, Division 2117, Three Mile Island HP-RT-0211 Detector Transistor Data.

14. Floyd Coppage, Sandia Laboratories, Personal Communication.

15. Dave Smotzer, Victoreen, Personal Communication.

16. Meeting to define objectives held September 3, 1980; L. Bonzon, M. Murphy, B. O'Niel, A. Stanley, F. Thome, D. Thompson, C. Tucker, P. Yarrington.

17. "TMI Update" by EG&G Idaho, October 28, 1980, Issue and Preliminary data from Entry No. 2 August 15, 1980.

18. Sandia Laboratory Notebook, ENG-F-777 Geoffrey M. Mueller, 1980.

19. W. Poch and A. G. Holmes-Siedle, "A Prediction and Selection System for Radiation Effects in Planar Transistors", IEEE Trans. Nuclear Science, Vol NS-15, December 1968.

20. Rudie, N. J., "Principles and Techniques of Radiation Hardening", Western Periodicals, N. Hollywood.

21. P. R. Measel and R. R. Brown, "Low Dose Ionization-Induced Failures in Active Bipolar Transistors", IEEE Trans. Nuclear Science, Vol NS-15, December 1968.